NASw-4435

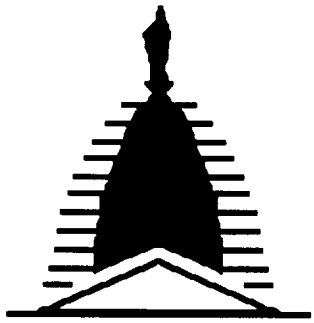

UNIVERSITY of
NOTRE DAME

NASA/USRA UNIVERSITY ADVANCED DESIGN PROGRAM 1993-1994

PROJECT CENTER MENTOR:
NASA-AMES DRYDEN FLIGHT RESEARCH FACILITY

FINAL DESIGN PROPOSAL

The Elite

A HIGH SPEED, LOW-COST GENERAL AVIATION AIRCRAFT FOR "AEROWORLD"

April 1994

Department of Aerospace and Mechanical Engineering
University of Notre Dame
Notre Dame. IN 46556

Rueter's Raiders Aeronautics

Presents

The Elite

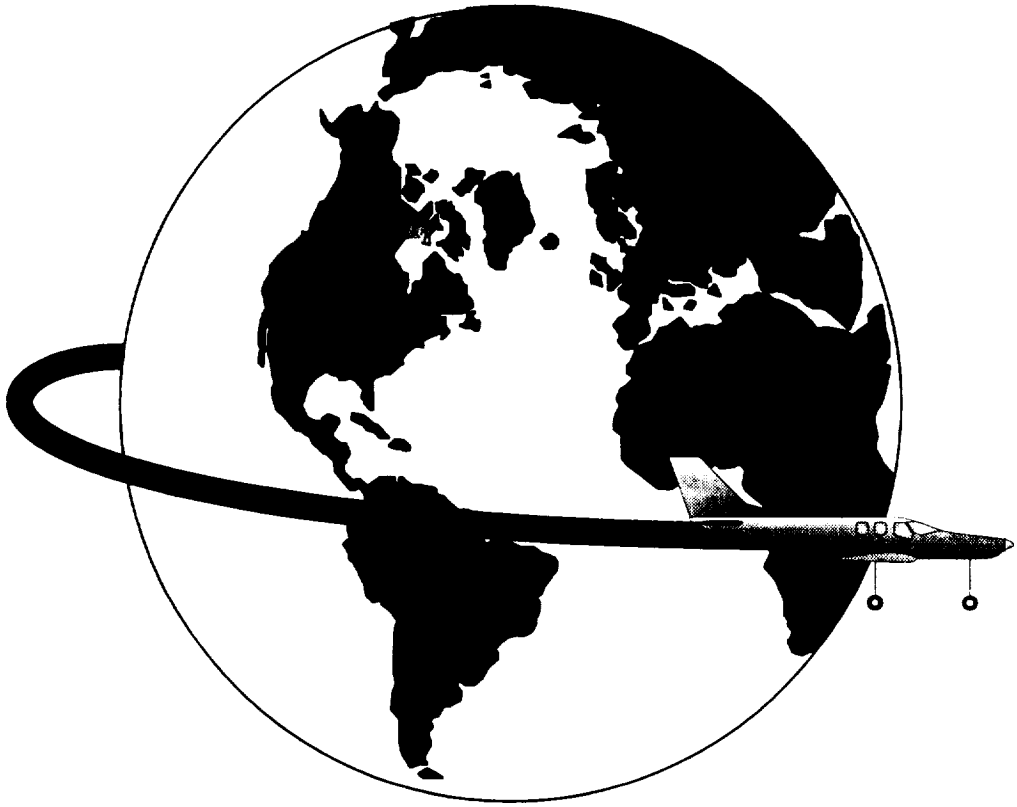

Design Group Members

Amy Rueter

Jonathan Fay

Douglas Staudmeister

Daniel Avis

Tuan Le

Steven Stem

Table of Contents

Table of Contents .....
List of Figures .....
List of Tables .....
EXECUTIVE SUMMARY 1
2 DESIGN REQUIREMENTS AND OBJECTIVES 9
2.1 Mission Statement 9
2.2 Marketing and Economics 9
2.3 Manufacturing 10
2.4 Performance 10
2.5 Exceptions to Original DR&O 11
2.6 References 12
3 CONCEPT SELECTION 13
3.1 High Wing Conventional - Aileron Control 13
3.2 Rectangular Fuselage - Polyhedral Wing 15
3.3 The "Backward" Airplane 15
3.4 Low Wing - "T" Tail 15
3.5 Low Wing - Winglets 18
3.6 Low Wing - Stabilator Control 18
3.7 The Elite 18
4 AERODYNAMIC DESIGN DETAIL 24
4.1 Main Wing Basic Concept 24
4.2 Main Wing Airfoil Selection 24
4.3 Airfoil Characteristics 27
4.4 Wing Sizing and Aspect Ratio 27
4.5 Empennage Planform and Airfoil Selection 30
4.6 Drag Breakdown 30
4.7 Aircraft Aerodynamic Summary 34
4.8 References 35
5 PROPULSION SYSTEM DESIGN DETAIL 36
5.1 Requirements and Objectives 36
5.2 System Selection 36
5.3 Motor Selection 36
5.4 Propeller Design 39
5.5 Engine Control & Battery Selection 44
5.6 Installation 46
5.7 Propulsion System and Performance Summary 47
5.8 References 48
6 WEIGHT ESTIMATE DETAIL 49
6.1 Level Zero Weight Estimate 49
6.2 Improved Weight and C.G. Estimate 50
7 STABILITY AND CONTROL 54
7.1 Requirements and Objectives 54
7.2 Longitudinal Stability 54
7.3 Longitudinal Control: 60
7.4 Directional and Lateral Stability: 62
7.5 Lateral Control 63
7.6 Directional Control: 65
7.7 Control Mechanisms: 67
7.8 References: 68
8 AIRCRAFT PERFORMANCE 69
8.1 Requirements and Objectives 69

8.2 Summary of Performance 69
8.3 Take-Off Performance 70
8.4 Range and Endurance 71
8.5 Power Required and Power Available 73
8.6 Climb and Gliding Performance 74
8.7 Turn Performance 75
8.8 References 76
9 STRUCTURAL DETAIL DESIGN 77
9.1 Requirements and Objectives 77
9.2 Main Wing Spar Design 77
9.3 Main Wing Rib Spacing 80
9.4 Fuselage Structural Design 81
9.5 Wing Carry-Through and Fuselage Mating Design 87
9.6 Empennage Design 89
9.7 Aircraft Loading 92
9.8 Landing Gear Design 93
9.9 References 95
10 ECONOMIC ANALYSIS 96
10.1 Requirements and Objectives 96
10.2 Cost Breakdown 96
10.3 Economic Performance 99
APPENDIX A: CRITICAL DESIGN SUMMARY
APPENDIX B: INITIAL WEIGHT DATA BASE
APPENDIX C: COMPUTER CODES
APPENDIX D: ZINGALI PROPELLER DATA
APPENDIX E: MANUFACTURING PLAN

List of Figures

Figure 1.1.1: Top View 4
Figure 1.1.2: SideView 5
Figure 1.1.2: 2-View Internal 6
Figure 3.1.1: High Wing Conventional - Aileron Control Concept 14
Figure 3.2.1: Rectangular Fuselage - Polyhedral Wing 16
Figure 3.3.1: The "Backward" Airplane 17
Figure 3.4.1: Low Wing - "T" Tail Concept 20
Figure 3.5.1: Low Wing - Winglets Concept 21
Figure 3.6.1: Low Wing - Stabilator Control 22
Figure 4.2.1: Airfoil Comparison of Resulting Wing Weights and Drag 26
Figure 4.3.1: Aerodynamic Data for the DF101 (reprint from ref. 1) 27
Figure 4.4.1: Airfoil Model Incorporated into the Lifting Line Code 28
Figure 4.4.2: Wing CL Distribution at Stall 29
Figure 4.6.1: Aircraft Drag Polar 32
Figure 4.6.2: L/D Curves -- a) vs. Angle of Attack b) vs. Level Flight Velocity 33
Figure 4.7.1: CL vs a of Aircraft 34
Figure 5.3.1: Motor Torque and Battery Constants 38
Figure 5.4.1: Thrust Coefficient as a Function of Propeller 39
Figure 5.4.2: Power Coefficient as a Function of Propeller 40
Figure 5.4.3: Propeller Efficiency as a Function of Propeller 41
Figure 5.4.4: Propeller Maximum Power Available verses Velocity 42
Figure 5.4.5: Zingali Propeller Efficiency as a Function of Advance Ratio 43
Figure 5.5.1: Effect of Throttle Setting on Power Available 44
Figure 5.5.2: Range and Endurance Versus Velocity at WMTO 45
Figure 6.2.1: Weight & Balance Diagram 53
Figure 7.2.1: Lt vs. Tail Area for Rotation at Take-off 55
Figure 7.2.2: Variation of Static Margin and Cma 57
Figure 7.2.3: Pitching Moment Coefficient vs. a 59
Figure 7.2.4: Pitching Moment Coefficient for Aft and Forward C.G. 60
Figure 7.3.1: Effect of Tail Deflection on Pitching Moment 61
Figure 7.5.1: Inboard and Outboard Location vs. Roll Rate 64
Figure 7.6.1: Control Surface Area Ratio vs. Control Power 66
Figure 8.3.1: Effect of Manufacturing Imperfections upon Take-Off Performance 71
Figure 8.4.1: Variation of Range and Endurance with Velocity 72
Figure 8.4.2: Dependence of Range and Endurance Upon Payload 73
Figure 8.5.1: Power Required and Power Available Curves 74
Figure 9.2.1: Limit Loading of Wing a) shear b) moment 78
Figure 9.2.2: Idealized Cross-Section 78
Figure 9.2.3: Comparison of Tested Cross-Sections 79
Figure 9.3.1: Webbing Between Main Spars (Wing Front View) 81
Figure 9.4.1: Fuselage Model for Stress Analysis 82
Figure 9.4.2: Idealized Cross-Section 82
Figure 9.4.3: Fuselage Ground Loading a) shear b) bending moment 83
Figure 9.4.4: Fuselage Loading at Cruise a) shear b) bending moment 83
Figure 9.4.5: Fuselage Structure 85
Figure 9.4.6: Bulkhead Model for Shear Analysis 86
Figure 9.4.7: Balsa Sheet versus 3-Ply Balsa 87
Figure 9.5.1: Wing Mounting System 89
Figure 9.6.1: Vertical Tail Structure 90
Figure 9.6.2: Stabilator Structure 91
Figure 9.6.3: Stabilator Mounting System 91

Figure 9.7.1: V-n diagram for Elite Aircraft 92
Figure 9.7.2: Angle of Attack and Velocity Envelope for Elite Aircraft 93
Figure 9.8.1: Main Gear Mounting System 94
Figure 10.2.1: Breakdown of Total Aircraft Cost 98
Figure 10.2.2: Breakdown of Manufacturing Costs 98
Figure 10.2.3: Influence of Waste Disposal and Production Hours on Cost 99

List of Tables

Table 1.1 Data Summary 7
Table 3.7.1: Summary of Concept Selection 23
Table 4.2.1: Listing of Considered Airfoils 25
Table 4.4.1: Summary of Wing Characteristics 30
Table 4.6.1: Drag Breakdown Components for Two Different Sets of Data 31
Table 4.7.1: Summary of Aircraft Aerodynamics 34
Table 5.2.1: Aircraft Data 36
Table 5.3.1: Comparison of Astro 15 motor with Astro 25 motor 37
Table 5.3.2: Other Astro 15 Characteristics 38
Table 5.4.1: Propeller Performance Comparison 42
Table 5.5.1: Throttle Setting for Desired Flight Condition 45
Table 5.5.2: Battery Specifications 46
Table 6.1.1: Zero Level Weight Component Breakdown 49
Table 6.1.1: Improved Weight Component and C.G. Breakdown 50
Table 7.2.1: Longitudinal Stability Parameters 58
Table 7.3.1: Characteristics of Stabilator 62
Table 7.4.1: Directional and Lateral Stability Parameters 63
Table 7.5.1: Lateral Control Parameters 65
Table 7.6.1: Directional Control Characteristics 67
Table 8.2.1: Performance Specifications for The Elite Aircraft 70
Table 9.2.1: Idealized Cross-Section Coordinates and Dimensions 79
Table 9.4.1: Idealized Cross-Section Coordinates and Dimensions 82
Table 9.4.2: Longeron Stress Analysis Results 84
Table 9.4.3: Bulkhead Shear Analysis Results 86
Table 9.8.1: Summary of Landing Gear Properties 94
Table 10.2.1: Cost Breakdown of The Elite 97
Table 10.3.1: Economic Figures of Merit for The Elite 100

NOMENCLATURE

AR, AR_W	Aspect Ratio of Wing
$C_{l_{max}}$	Maximum Coefficient of Lift
$C_{l_{\alpha_v}}$	Lift Curve Slope of Vertical Tail
C_n	Yaw Moment Coefficient
C_{n_β}	Change in Yaw Moment Coefficient With Respect to Yaw Angle
$C_{n_{\beta_{wf}}}$	Change in Yaw Moment Coefficient With Respect to Yaw Angle for Wing and Fuselage
$C_{n_{\beta_v}}$	Change in Yaw Moment Coefficient With Respect to Yaw Angle for Vertical
$C_{l_{\delta_a}}$	Change in Roll Moment Coefficient with Aileron Deflection Angle
C_{l_p}	Change in Roll Moment Coefficient with Roll Rate
C_m	Pitching Moment
C_{m_0}	Pitching Moment Coefficient at Zero Angle of Attack
C_{m_α}	Change in Pitching Moment Coefficient Due to Angle of Attack
$C_{m_{\delta_e}}$	Change in Pitching Moment Coefficient Due to Elevator Deflection
β	Yaw Angle
δ_a	Aileron Deflection
δ_e	Elevator/Stabilator Deflection
δ_r	Rudder Deflection
Γ	Dihedral Angle
p	Roll Rate about x-axis
$\dot{p}$	Time Rate of Change of the Roll Rate
L_{δ_a}	Change in Roll Moment with Aileron Deflection Angle
L_p	Change in Roll Moment with Roll Rate
SM	Static Margin
X_{NP}	Position of neutral point relative to the wing's leading edge
X_{CG}	Position of center of gravity relative to the wing''s leading edge
S	Wing Planform Area
b	Wing Span
c	Chord
d	Maximum Fuselage Depth
i_W	Incidence Angle of the Wing
i_t	Incidence Angle of the Tail
S_e	Elevator Planform Area

S_t	Horizontal Tail Planform Area
S_v	Vertical Tail Planform Area
V_v	Vertical Volume Ratio
l_t	x-Distance from Center of Gravity to Mean Aerodynamic Chord of the Horizontal Tail
l_v	x-Distance from Center of Gravity to Mean Aerodynamic Chord of the Vertical Tail
x	Coordinate Along Length of Aircraft (Positive Forward)
y	Coordinate Along Span of Aircraft (Positive Out Right Wing)
z	Vertical Coordinate of Aircraft (Positive Down)
CPF	Cost Per Flight
CPFM	Cost Per Flight Minute
DR&O	Design Requirements and Objectives (Section 2.0 of this document)
RFP	Request for Proposals
RPV	Remotely Piloted Vehicle
WMTO	Aircraft Maximum Take-Off Weight
Z_w Fuselage	Distance Parallel to z-Axis Between Wing Root 1/4 Chord and Centerline
$\Lambda_{1/4c}$	Sweep of 1/4 Chord of Vertical Tail
η_v	Ratio of Dynamic Pressures at the Vertical Tail and the Wing
σ	Side Wash

EXECUTIVE SUMMARY

The Elite is a six passenger, general aviation aircraft targeted at the upper middle class private pilot. *The Elite* is a low wing, conventional monoplane utilizing rudder, ailerons and a stabilator. *The Elite* will create a new class of aircraft in Aeroworld. This class of aircraft will demonstrate a substantial improvement in cruise speed over the current existing commercial fleet of aircraft in Aeroworld. This new class will be capable of servicing all existing airstrips in Aeroworld, including rough and short runways.

The drivers of this design were aesthetics, a high cruise speed, and take-off distance. Aesthetic requirements are difficult to quantify in terms of whether or not an aircraft meets those requirements. *The Elite* attempts to appeal to the upper-middle class private pilot by employing a rounded fuselage, smooth and curving nose, and a swept empennage. These decisions were made early in the design and thus drove much of the aerodynamic detailed design. Aesthetics influenced other aspects of the design as well. One aspect of the design includes the use of an all-movable tail. The implementation of this technology will reduce the tail area needed by increasing the control effectiveness of the horizontal tail. This increased effectiveness will increase the moment generated by the horizontal stabilizer, thus decreasing the necessary fuselage length. Another aspect of the design influenced by the desire for aesthetics was the choice of a low wing configuration for the aircraft.

A high cruise speed was pursued to increase the marketability of the aircraft. One of the main drivers for the selection of the propulsion system was the desire to cruise at speeds substantially higher than existing designs. *The Elite* cruises at a velocity of 60 ft/s, a large improvement over recent designs which cruised at speeds of 30 ft/s. Higher cruise speeds could have been attained by decreasing the wing area. However, decreased wing area has an adverse effect upon aircraft take-off performance.

Another marketable aspect of *The Elite* is the ability to service all airports in Aeroworld. This drove the selection of the propulsion system, wing area and landing gear. The short and rough field take-off requirements placed limitations upon the performance of the aircraft. Aircraft maximum speed, range, and weight were all directly affected by take-off objectives.

The Aerodynamics of *The Elite* consist of a DF101 airfoil section for the wing, a symmetric airfoil for the horizontal tail and a flat plate for the vertical tail. Although the incorporation of a flat plate for the vertical tail goes against the design driver of aesthetics, a flat plate was chosen to offset the time-consuming construction of the stabilator and fuselage. Of all the airfoils considered, the DF101 provided the best combination of small area to minimize drag and weight while still providing sufficient lift at a take-off speed of 25 ft/s. The wing area was chosen as 6.5 ft^2 to minimize the area

while keeping the wing slightly below stall at take-off. A high aspect ratio of 9 was chosen to increase the lift-curve slope while decreasing the induced drag. The symmetrical SD8020 airfoil was selected for the horizontal tail because this airfoil had the most consistent lift-curve response in the zero angle of attack regime and possessed the best drag characteristics.

The propulsion system was chosen based upon the requirement for a high cruise speed. The system consists of the Astro 15 Cobalt motor, a Zingali 10-8 three-blade propeller and 13 Panasonic 1300 mah batteries. The Zingali 10-8 propeller was chosen based upon the drivers of aesthetic appearance and maximum velocity. The Panasonic 1300 mah batteries were chosen based upon the desire for the aircraft to have adequate range to service all airports in Aeroworld.

The landing gear of *The Elite* provides ground control through the use of tricycle landing gear with a steerable nose wheel. This configuration provides good stability on the rough airstrips and prevents the occurrence of ground loops.

The horizontal tail is a stabilator, or all-moving tail. It was sized based on rotation for takeoff and trim at all portions of the flight regime. The aileron sizing was based upon the slow turning speed turn requirement. The ailerons were designed to create a roll rate of 20.5 deg/s at a speed of 28 ft/s. The rudder was designed to counteract the adverse yaw created by the ailerons, thus allowing for a "coordinated turn".

A major selling point of this aircraft is its performance. At the cruise speed of 60 ft/s, *The Elite* is capable of servicing 94.3% of all routes flown in Aeroworld. The maximum range of 32900 ft allows the aircraft to service all airports in Aeroworld. *The Elite* satisfies the take-off requirement by lifting off within 26 ft. The high lift-to-drag ratio for this airplane yields a minimum glide slope of 3.87 degrees. This is important with respect to power-off landing conditions. The maximum velocity for *The Elite* is 71.7 ft/s. This velocity ensures that the aircraft will be able to adequately maneuver at cruise.

Cost was not an issue that limited most of our design decisions. The total cost of the aircraft is $4410.13, 64% of which is comprised of personnel costs. The total number of man-hours to complete the manufacturing of *The Elite* was conservatively estimated at 180 hours. This amount of time is significantly higher than the construction times for previous Aeroworld aircraft because of the complexity of building the circular fuselage and of connecting the stabilator to the fuselage. The cost per flight (CPF) was $8.38/flight.

The trademark of *The Elite* is its aesthetically appealing circular fuselage, as well as its swept empennage. *The Elite* also has many strengths in its design. Incorporation of a stabilator reduces the size of the horizontal tail, thus reducing empennage weight. The

placement of the horizontal tail minimizes the downwash, reducing the pitching moment that the aircraft must overcome at cruise. Also, *The Elite*'s performance is superior to that of any existing aircraft in Aeroworld.

The primary weakness of *The Elite* is the difficulty in manufacturing this design. In particular, manufacturing the curved fuselage and the fuselage-stabilator interface requires a large amount of tooling and man-hours. Another weakness in *The Elite*'s design is that the low-wing necessitates that the aircraft be inverted to access the avionics. Furthermore, the cost of *The Elite* is fairly high compared to the cost of competing designs. Only after the technology demonstrator has been constructed and the final cost has been tallied will the worthiness of pursuing aesthetics instead of low cost be determined.

Figure 1.1.1: Top View

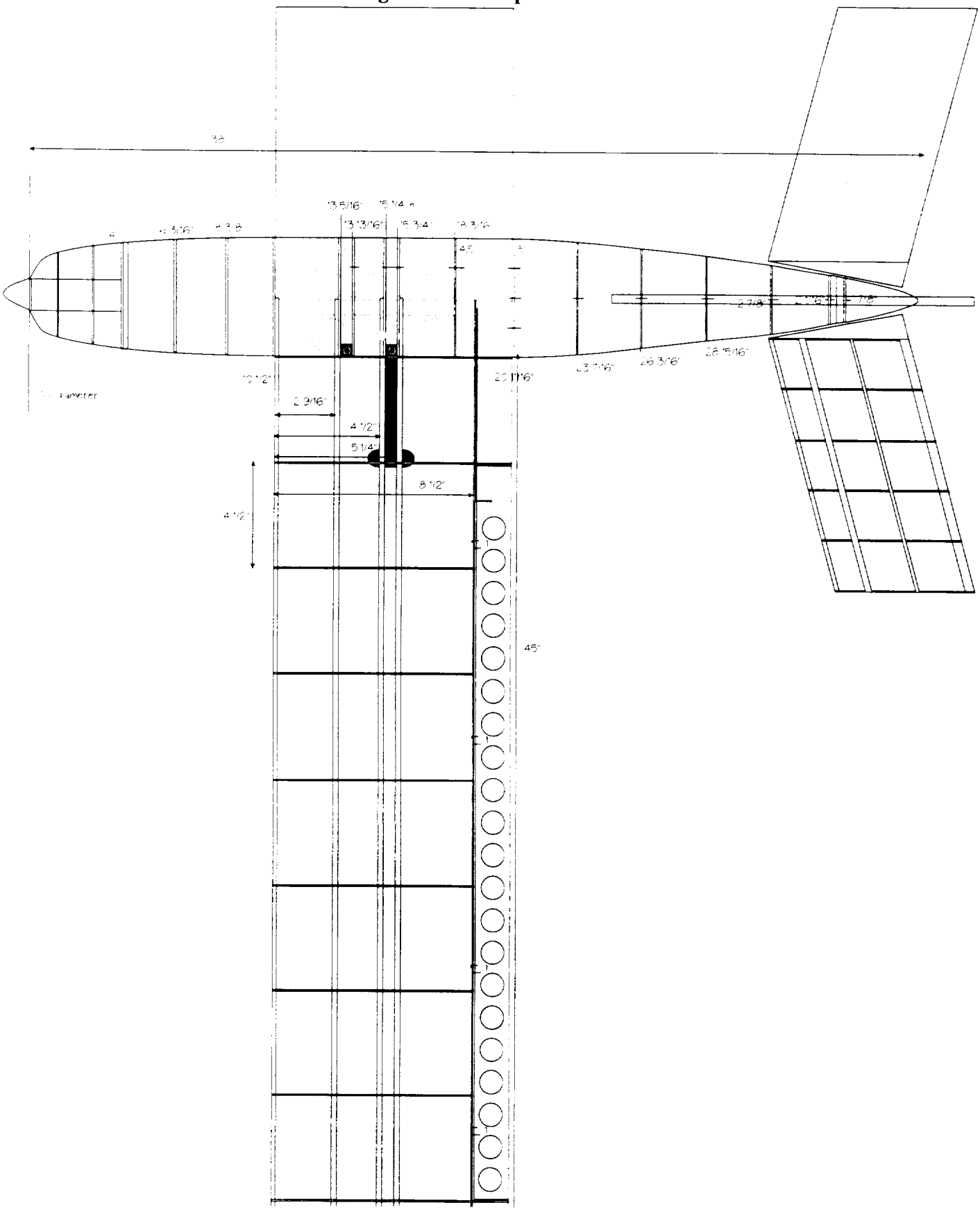

Figure 1.1.2: SideView

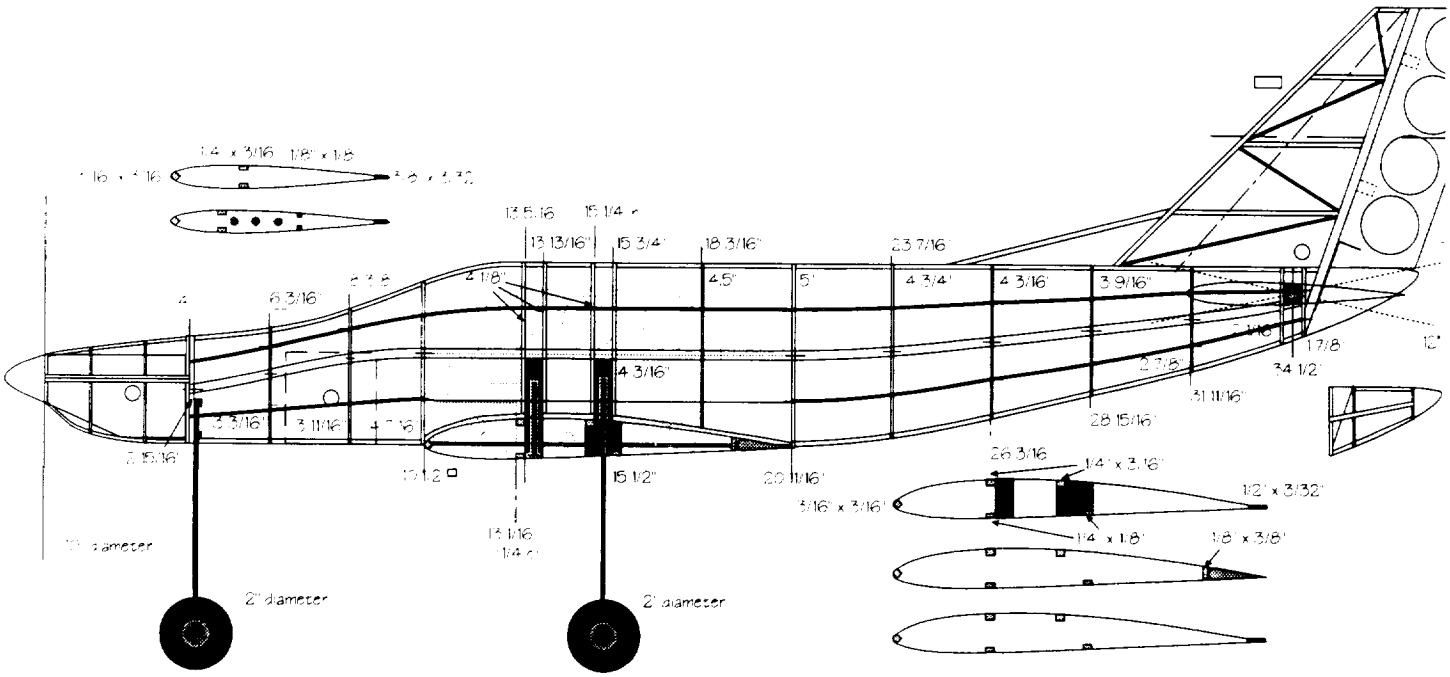

Figure 1.1.2: 2-View Internal

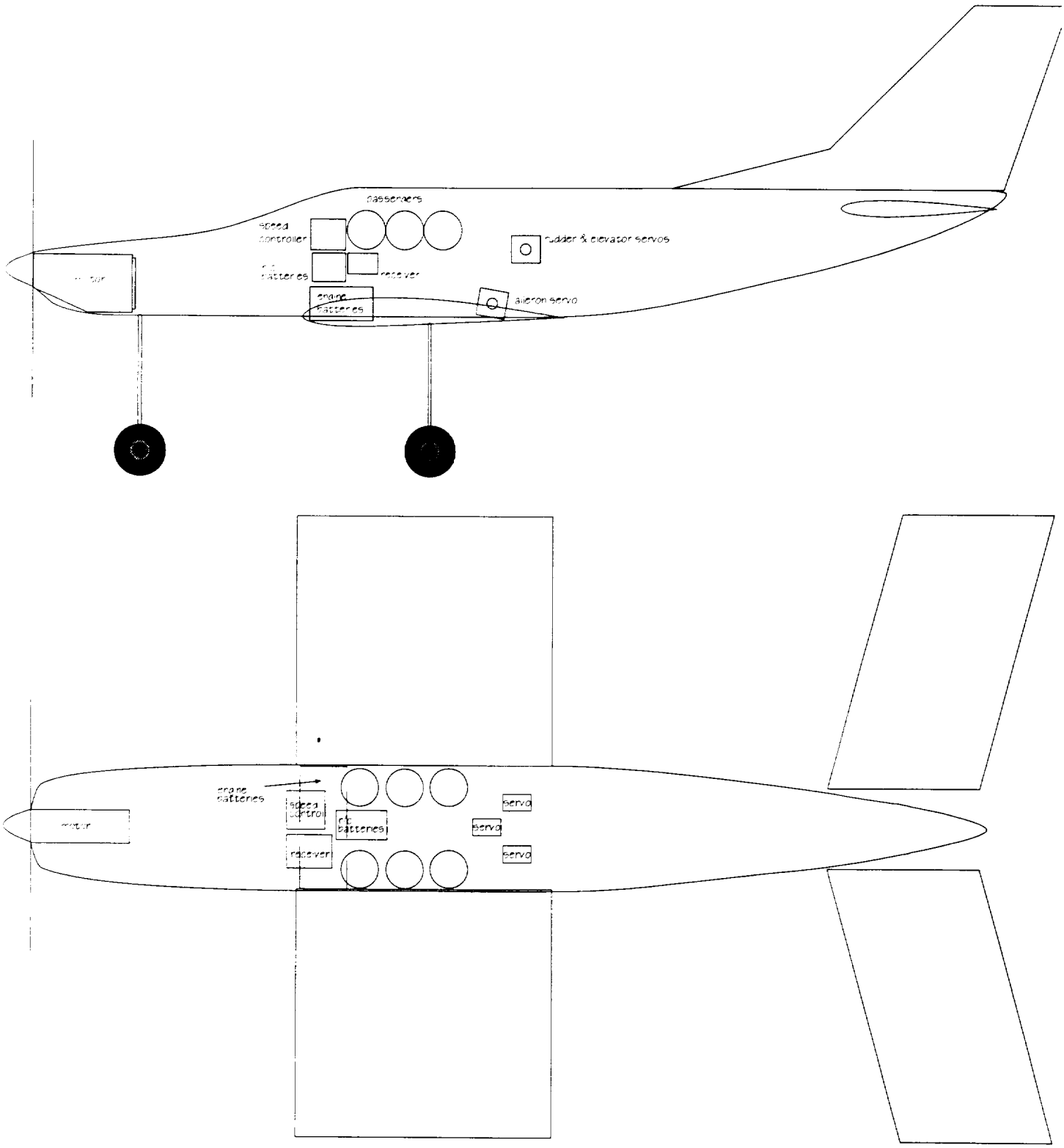

Table 1.1 Data Summary

Parameter	Final Design
[all distances are relative to aircraft nose and in common units]	
DESIGN GOALS:	
V cruise	60 ft/sec
V max	80 ft/sec
No. of passengers/crew	6
Max Range at Wmax	30500 ft
Altitude cruise	50 ft
Minimum turn radius	40 ft
Improved Field Take-Off Dist.	28 ft
BASIC CONFIG.	
Wing Area	6.5 ft^2
Maximum TO Weight - WMTO	4.88 lb
Empty Flight Weight	4.83 lb
Wing loading(WMTO)	0.75 lb/ft^2
max length	38 inches
max span	7.66 ft
max height	1.5 ft
WING	
Aspect Ratio	9
Span (including fuselage)	7.66 ft
Area (ft^2)	6.5 ft^2
Root Chord	10 3/16 in
Tip Chord	10 3/16 in
taper Ratio	1
Dihedral	5 degrees
Airfoil section	DF101
Design Reynolds number	350,000
t/c	0.11
Incidence angle (root)	1.2 degrees
FUSELAGE	
Length	38 in
Cross section shape (circular)	5 in diam.
Nominal Cross Section Area	0.0873 ft^2
Fineness ratio	7.6
Payload volume	25 in^3
Planform area	1.06 ft^2
Frontal area	0.155 ft^2

Parameter	Final Design
PROPULSION	
Type of engine	Astro15
placement	nose (tractor)
Propeller type	Zingali 10-8
Propeller diameter	10 in
Propeller pitch	8 in
Number of blades	3
battery type	P-130SCR
number	13
pack capacity	1300 mah
pack voltage	15.6
STAB AND CONTROL	
Neutral point	41% MAC
Static margin %MAC	11% MAC
Stabilator area (ft^2)	0.9 ft^2
Stabilator max deflection	12 degrees
Rudder Area	0.3 ft^2
Rudder max deflection	15 degrees
Aileron Area (ft^2)	0.75 ft^2
Aileron max deflection	15 degrees
Parameter	**Final Design**
PERFORMANCE	
Vmin at WMTO	24.8 ft/s
Vmax at WMTO	71.71 ft/s
Vstall at WMTO	24.8 ft/s
Range max at WMTO	32919.3 feet
Endurance @ Rmax	14.86 min
Endurance Max at WMTO	18.62 min
Range at @Emax	27933ft
Range max at Wmin	33790 ft @ V = 35
ROC max at WMTO	16 ft/s @ V = 36.5 ft/s
Min Glide angle	3.87°
T/O distance at WMTO	26.0 ft
Percentage of Servicable Routes @ Cruise	94.30%

Parameter	Final Design
EMPENNAGE	
Horizontal tail	
Area (ft^2)	0.9 ft^2
span	1.8 ft
aspect ratio	3.6
root chord	0.5 ft
tip chord	0.5 ft
average chord	0.5 ft
taper ratio	1
l.e. sweep	15 degrees
1/4 chord sweep	15 degrees
incidence angle	-2 degrees
Airfoil section	SD8020
Vertical Tail	
Area (ft^2)	0.3 ft^2
Aspect Ratio	1.2
root chord	0.5 ft
tip chord	0.5 ft
average chord	0.5 ft
taper ratio	1
l.e. sweep	45 degrees
1/4 chord sweep	49 degrees
Airfoil section	flat plate

Parameter	Final Design
SUMMARY AERODYNAMICS	
Cl max (airfoil)	1.14
CL max (aircraft)	1.03
lift curve slope (aircraft)	0.083 /degree
CDo (aircraft)	0.0325
Alpha stall (aircraft)	12.33 degrees
L/D max (aircraft)	14.8
WEIGHTS (pounds)	
Weight total (empty)	4.834
C.G. most forward-x&y	13.36
C.G. most aft- x&y	13.471
SYSTEMS	
Landing gear type	tricycle
Main gear position	15.5 in
Main gear length	5 in
Main gear tire size	2 in diameter
nose/tail gear position	4.375 in behind prop
n/t gear length	5 in
n/t gear tire size	2 in diameter
Control surfaces	rudder, stabilator, and ailerons
ECONOMICS:	
raw materials cost	$160.00
propulsion system cost	$172.58
avionics system cost	$280.00
production manhours	180 hours
personnel costs	$1,800.00
tooling costs	$150.00
total cost per aircraft	$4,394.45
CPF at Vcruise and Rmax	$9.37
CPFM	$1.43
CP1000	$0.40

2 DESIGN REQUIREMENTS AND OBJECTIVES

2.1 Mission Statement

The Elite was designed to satisfy the mission outlined in the Request for Proposals (Ref. 2.1). The Request for Proposals (RFP) expressed the desire to create a low-cost general aviation aircraft that displayed a significant improvement in cruise speed over existing commercial aircraft in service in Aeroworld. The RFP asked for an aircraft capable of carrying six passengers that could service any two airports in Aeroworld. The requirement to service all airports in Aeroworld included a need to service "rough" unprepared runway surfaces and shortened landing strips.

Rueter's Raiders Aeronautics decided to target their design at an upper-middle class market that would pay a slightly higher price for an aircraft that displayed superior performance and was aesthetically pleasing. This resulted in the decision to place the desire for aesthetics and performance ahead of concerns about cost.

2.2 Marketing and Economics

The market at which this aircraft was aimed was the upper-middle class private pilot, therefore, it was decided that the primary selling point of this aircraft would not be its cost. Instead, the aircraft would provide the consumer an attractive looking product with superior performance. To exhibit the performance demanded by the target market, the design included a rough and short field capability along with a range allowing the aircraft to service all of Aeroworld's airports (including a diversion to the nearest alternate airport and a loiter of one minute). The RFP required the aircraft to exhibit benign handling characteristics which would allow even a novice pilot to easily fly *The Elite* (Ref. 2.1). A summary of the marketing and economics requirements and objectives is found below.

Requirements:

1. 6 passenger capacity plus sufficient cargo space for passenger baggage (4 in^3 per passenger/pilot)
2. maximum raw material budget of $290

Objectives:

1. create an aesthetically pleasing aircraft
2. ability to service all airstrips in AEROWORLD
   - -adequate range to service any two airports with diversion to nearest alternate airport with a one minute loiter
   - -rough field capability
   - -short field capability
3. pilotable by novices
4. affordable to the upper-middle class general aviation market
5. keep the cost of the aircraft below $5000

2.3 Manufacturing

A primary driver in the overall design of *The Elite* was the desire to design an aesthetically pleasing aircraft. This desire led to the cylindrical fuselage employed in *The Elite* which required the delicate balancing of the complexity of the design with the manufacturing man-hours needed to fabricate the aircraft. In addition to this, other manufacturing related restrictions placed on the design by upper management included the ability to remove and install the complete propulsion system within 20 minutes, the use of a maximum of 4 servos, and most importantly, the batteries must be placed in the wing-box structure (Ref. 2.1). This last requirement limited the structural and weight group a great deal in the design of *The Elite*. Attention to center of gravity position and internal configuration became essential in the development of the design due to this last requirement.

Requirements:

1. radio control system and complete propulsion system must be removable with the capability of being installed within 20 minutes
2. a maximum of 4 servos may be used to control the aircraft
3. passengers and avionics must be able to withstand a crash
4. battery placement must be in the wing box

Objectives:

1. balance design complexity with manufacturing man-hours

2.4 Performance

One of the most important drivers for the design of *The Elite* was to produce an aircraft that performed well while maintaining attractive looks. To satisfy this driver of the design, *The Elite* was engineered to allow service to all airports in AEROWORLD. This objective imposed a minimum range of 30,500 feet. In addition, the RFP also required a rough and short field capability on the design of *The Elite.*

Based upon previous Aeroworld designs, a maximum velocity objective of 80 ft/s was chosen to satisfy the high-speed requirement of the design and ensure that the cruise speed of 60 ft/s was attainable. This drove the selection of the propulsion system for this aircraft.

Several requirements were imposed upon the design by upper management. These requirements involved a limit on maximum slow-speed turn radius, take-off distance and the ability for the airplane to fly to the nearest alternate airport and loiter for one minute (Ref. 2.4). These requirements drove the design of the aerodynamics, the stability and control, and the propulsion systems of the RPV.

Requirements:

1. capable of a sustained level, 60 ft radius turn at speeds of less than 30ft/s
2. rough field characteristics
   -sufficient taxi and runway handling characteristics
   -able to climb to a height of 50 ft within 200 ft of brake release

-maximum take-off distance of 60 ft

3. able to fly to nearest alternate airport and loiter 1 minute

Objectives:

1. minimum cruise speed of 60 ft/s
2. maximum velocity of at least 80 ft/s
3. sufficient range to service all AEROWORLD airports (30,500 feet including one minute loiter time at the nearest alternate airport)
4. endurance consistent with target range and cruise and loiter speeds
5. maximum take-off distance required to service all airports
   -rough field, 42 ft
   -improved runway, 28 ft
6. handling qualities consistent with private/sport recreational aircraft

2.5 Exceptions to Original DR&O

All requirements and objectives set forth in the DR&O were satisfied except the objectives of a maximum speed of 80 ft/s and a range at cruise of 30500 feet. The maximum speed objective was relatively arbitrarily chosen and was simply chosen to ensure that a cruise speed of 60 ft/s was attainable. The members of Rueter's Raiders Aeronautics decided that a maximum speed of 71 ft/s instead of 80 ft/s would not affect the marketability of their product because all of the primary speed objectives had been met.

The inability to attain the range objective was a much more difficult hurdle to overcome. A study of the number of routes not serviceable at the cruise range of 27270 feet was undertaken. This study included the need to divert to the nearest alternate airport and loiter for one minute at 30 ft/s. The study concluded that 94.3% of all routes in Aeroworld were serviceable at a range of 27000 feet. Only six routes in Aeroworld had to be serviced at speeds less than 60 ft/s. These six routes could all be serviced at speeds no slower than 50 ft/s. This was also considered acceptable by the members of Rueter's Raiders Aeronautics.

2.6 References

2.1 Batill, Dr. Stephen. " High Speed, Low-Cost General Aviation Aircraft for 'Aeroworld.'" Department of Aerospace and Mechanical Engineering, The University of Notre Dame, 1994.

3 CONCEPT SELECTION

Six different concepts were considered, each with varying configurations and levels of technology. Advantages and disadvantages of each concept were weighed against the requirements and objectives imposed on the design. Concepts were considered on the basis of their ability to satisfy the Design Requirements and Objectives, specifically the feasibility of manufacturing, high speed performance, rough field capabilities, and aesthetic appeal of the aircraft. The best aspects of each design were incorporated into the final design of *The Elite*. In particular, the final design reflected the team's desire to produce an aesthetically pleasing aircraft.

3.1 High Wing Conventional - Aileron Control

The requirements for rough-field servicing and high-speed cruise were very influential in the choice of configuration for this design shown in Figure 3.1.1. This aircraft employed tricycle style landing gear to facilitate control on unprepared runways. A three-bladed propeller was envisioned to reduce the propeller diameter needed without reducing the amount of thrust, therefore increasing propeller clearance on rough airfields. Large diameter tires would be used to improve rough field handling, however this could result in a significant increase in the weight and drag of the aircraft.

A circular fuselage was designed to decrease drag at the higher cruise speeds specified by the DR&O. The circular design would also be more aesthetically appealing. This circular design would present difficulties in construction as well as with attaching the empennages to the fuselage structure.

This design incorporated a high-wing design. The main wing was swept and tapered to decrease the induced drag at the higher cruise speeds and to decrease the weight of the structure. Roll control involved the use of ailerons. Directional control would be provided by a rudder. Pitch control would be achieved using a conventional elevator-horizontal tail configuration. Both the horizontal and vertical tails employed symmetric airfoils.

Figure 3.1.1: High Wing Conventional - Aileron Control Concept

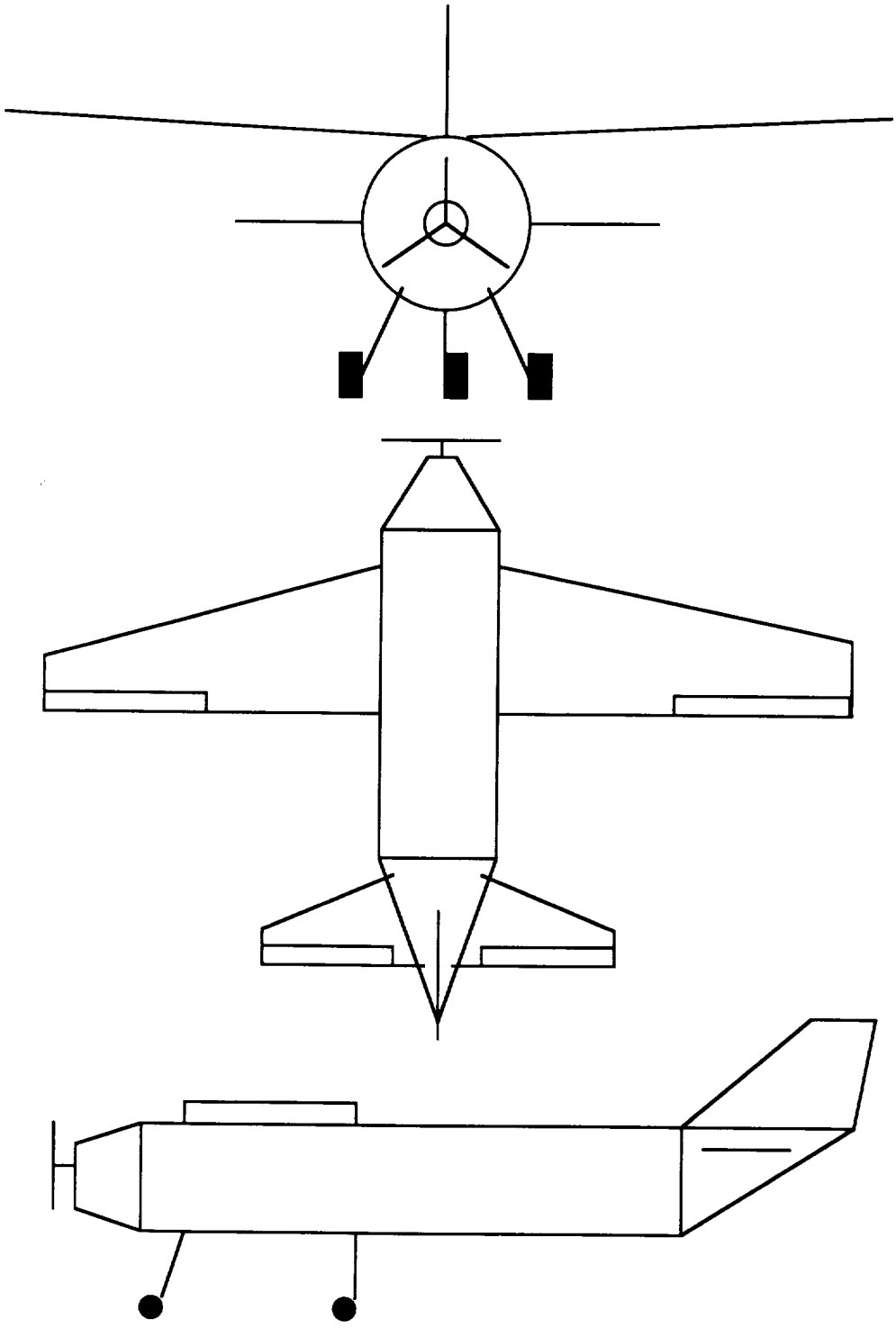

3.2 Rectangular Fuselage - Polyhedral Wing

This design concept (found in Figure 3.2.1)was driven by the desire to produce an aircraft that would be easy to manufacture. Thus, the fuselage had a uniform square cross-section, tapered to a smaller cross-section at the nose. The back end of the fuselage was tapered.

To help attain the high cruise speed objective stated by the Design Requirements and Objectives, a less cambered airfoil would be used. The use of an airfoil with less camber, it was believed, would reduce the profile drag created by the wing. The design would incorporate a high-wing configuration to allow for easier attachment to the fuselage and easy access to the avionics. Also, there was a large database for designs using a high wing. This design also used a polyhedral wing to have dihedral on the outboards of the wing where it was most needed and to allow for easier attachment of the wing to the fuselage. A possible problem with the polyhedral wing configuration was tip stall during turns.

3.3 The "Backward" Airplane

The two primary drivers of this design (found in Figure 3.3.1) were to achieve a high cruise speed and to be aesthetically pleasing. These drivers were the result of the Design Requirements and Objectives of producing a high performance, aesthetically pleasing aircraft. It employed a rounded fuselage with a swept back, tapered wing. This design was essentially a conventional aircraft flying backwards. It was a canard and fore-rudder design. A major weakness of this design was that the fore-rudder was destabilizing in yaw.

This aircraft used spoilers to provide roll control, eliminating the adverse yaw created by ailerons. The problem found with using spoiler control was the complexity of the control linkages to the servo adding to the weight of the aircraft. This design also utilized a pusher propeller, with the motor and avionics located above the main landing gear. Having the majority of the weight over the rear set of landing gear it was believed would localize most of the landing impact stress to the rear section of the aircraft. A problem with this weight distribution was that it required very sturdy, and possibly bulky, landing gear which would increase the drag considerably.

3.4 Low Wing - "T" Tail

The design in Figure 3.4.1 utilized a high horizontal tail to reduce the interference effects caused by the propeller slipstream. This configuration would increase the effectiveness of the elevator, but would require complicated control linkages. Also, the

Figure 3.2.1: Rectangular Fuselage - Polyhedral Wing

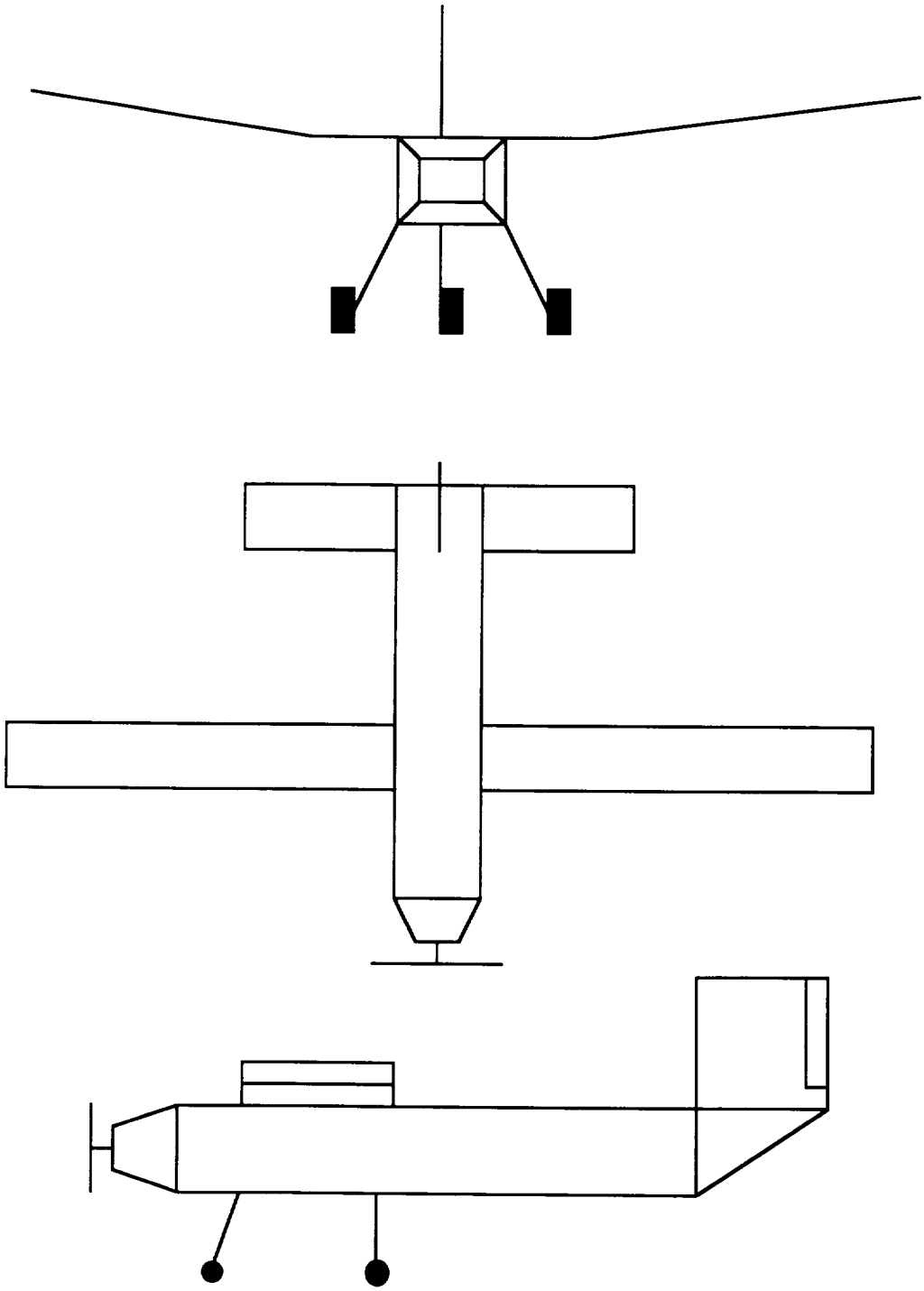

Figure 3.3.1: The "Backward" Airplane

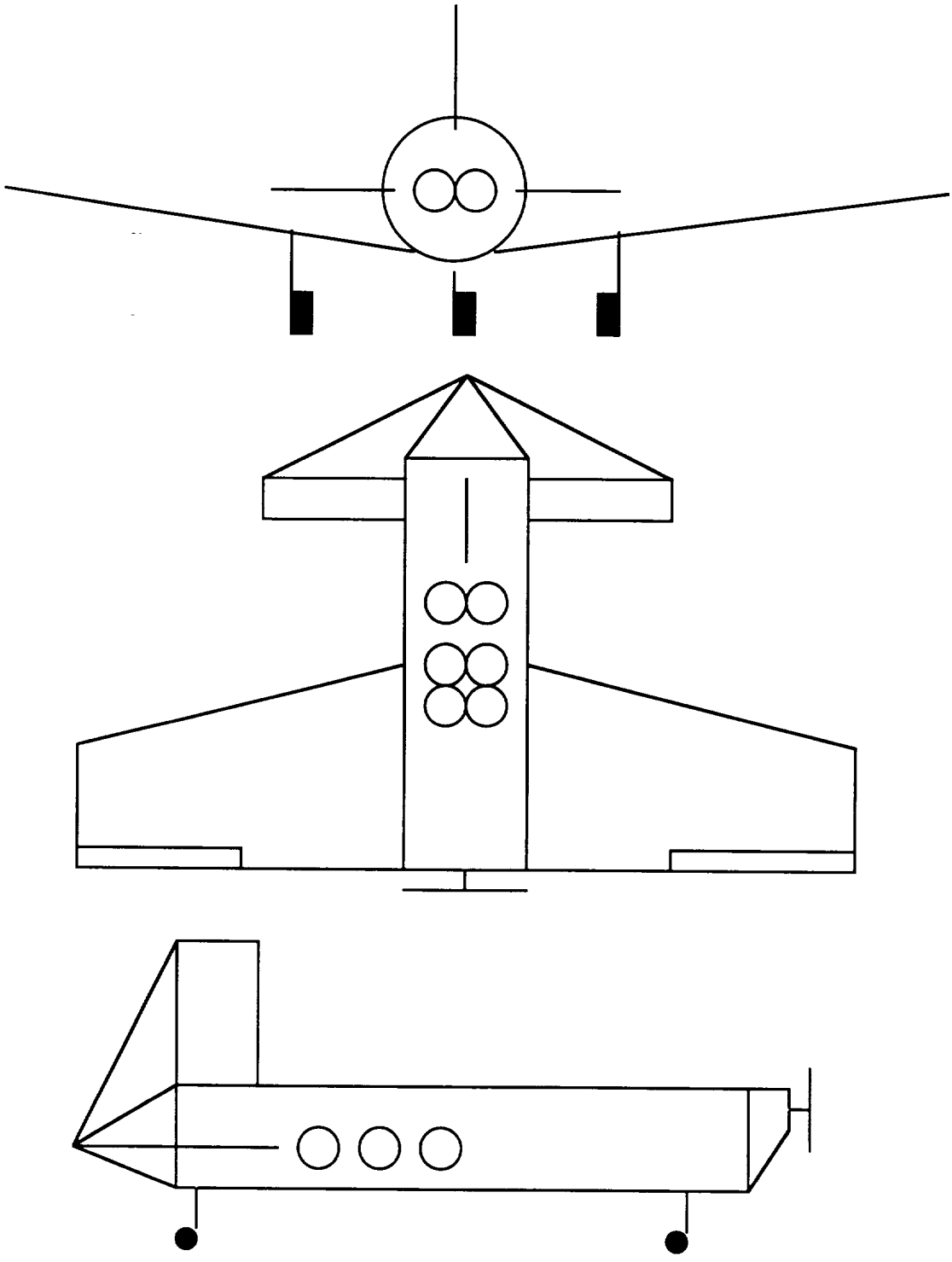

vertical tail would have to be reinforced in order to carry the loads from the horizontal tail, increasing the overall aircraft weight.

The rest of this design was fairly conventional. It incorporated a rectangular fuselage, a tapered low-wing, and a rudder, elevator, and ailerons. This design also utilized tricycle landing gear to satisfy the rough field handling requirement specified in the DR&O.

3.5 Low Wing - Winglets

The design illustrated in Figure 3.5.1 incorporated a cylindrical fuselage to minimize the wetted area and the drag. The wing was tapered to simulate a parabolic lift distribution and utilized flaps to help reduce take-off distances. Winglets were used to slightly decrease tip vortex effects and induced drag. The winglets also added to the appeal of the aircraft. Winglets would create complex loadings and reduce the structural integrity of the wing. The reinforcement of the wing to accommodate winglets would incur a weight penalty upon the design.

The landing gear of this design was of the tail dragger variety allowing the tail wheel to be linked to the rudder to steer the aircraft.

A major weaknesses of this concept was the complex structure, this would increase man-hours and thus increase the overall cost of the aircraft.

3.6 Low Wing - Stabilator Control

Figure 3.6.1 shows the low wing monoplane concept utilizing an all moving horizontal tail for pitch control. The use of a stabilator reduced the horizontal-tail area needed to control the aircraft and provide static pitch stability. It was anticipated that the stabilator would be difficult to design and manufacture because all loads were carried from the tail to the fuselage through a control rod linking the tail to the fuselage.

A tractor propeller was used to propel the design. The concept used a rounded fuselage to decrease drag and increase appeal. Control was achieved through the use of a rudder, a stabilator and ailerons.

The low wing configuration necessitated access to the avionics package through the underside of the fuselage. Lack of high lift devices necessitated a large wing area to meet take-off requirements.

3.7 *The Elite*

The final concept for *The Elite* resulted from an examination of the submitted concepts for their feasibility, performance and looks. The low wing, polyhedral design was eliminated from consideration because of its boxy appearance. The Backward Airplane was statically unstable and was eliminated from consideration. The possibility

of utilizing a "T" tail was dropped because of structural and weight considerations. The tail-dragger concept was eliminated because of the desire to avoid ground loops upon landing.

A high wing conventional design utilizing aileron control and a low wing design incorporating a stabilator were given further consideration. A decision was made between the high wing, convenient access design and the more appealing low wing concept. Despite the less accessible avionics, the low wing design utilizing the stabilator was chosen in accordance with the primary objective of creating an appealing aircraft as specified in the DR&O.

Table 3.7.1 illustrates the advantages and disadvantages of each of the concepts considered.

Figure 3.4.1: Low Wing - "T" Tail Concept

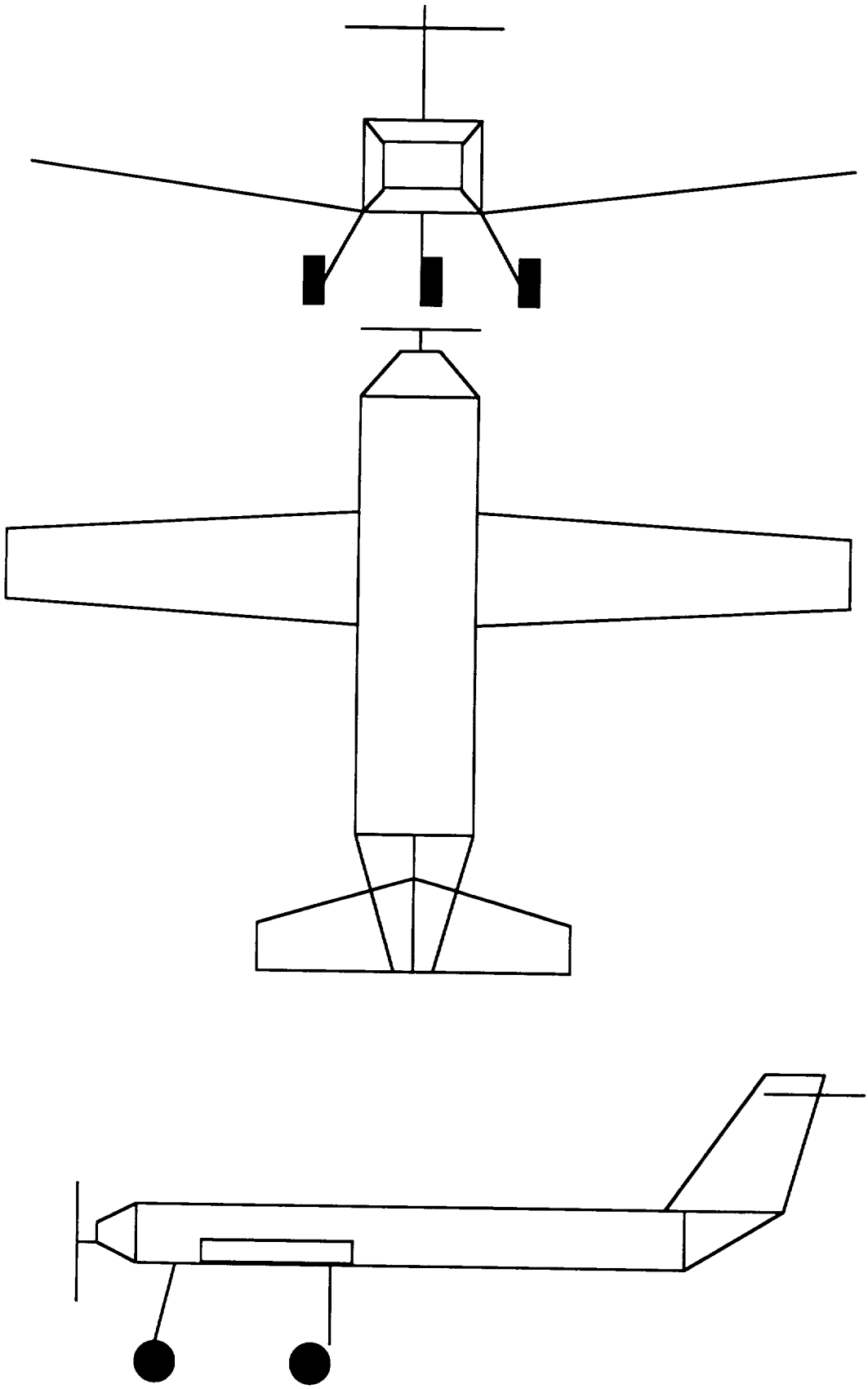

Figure 3.5.1: Low Wing - Winglets Concept

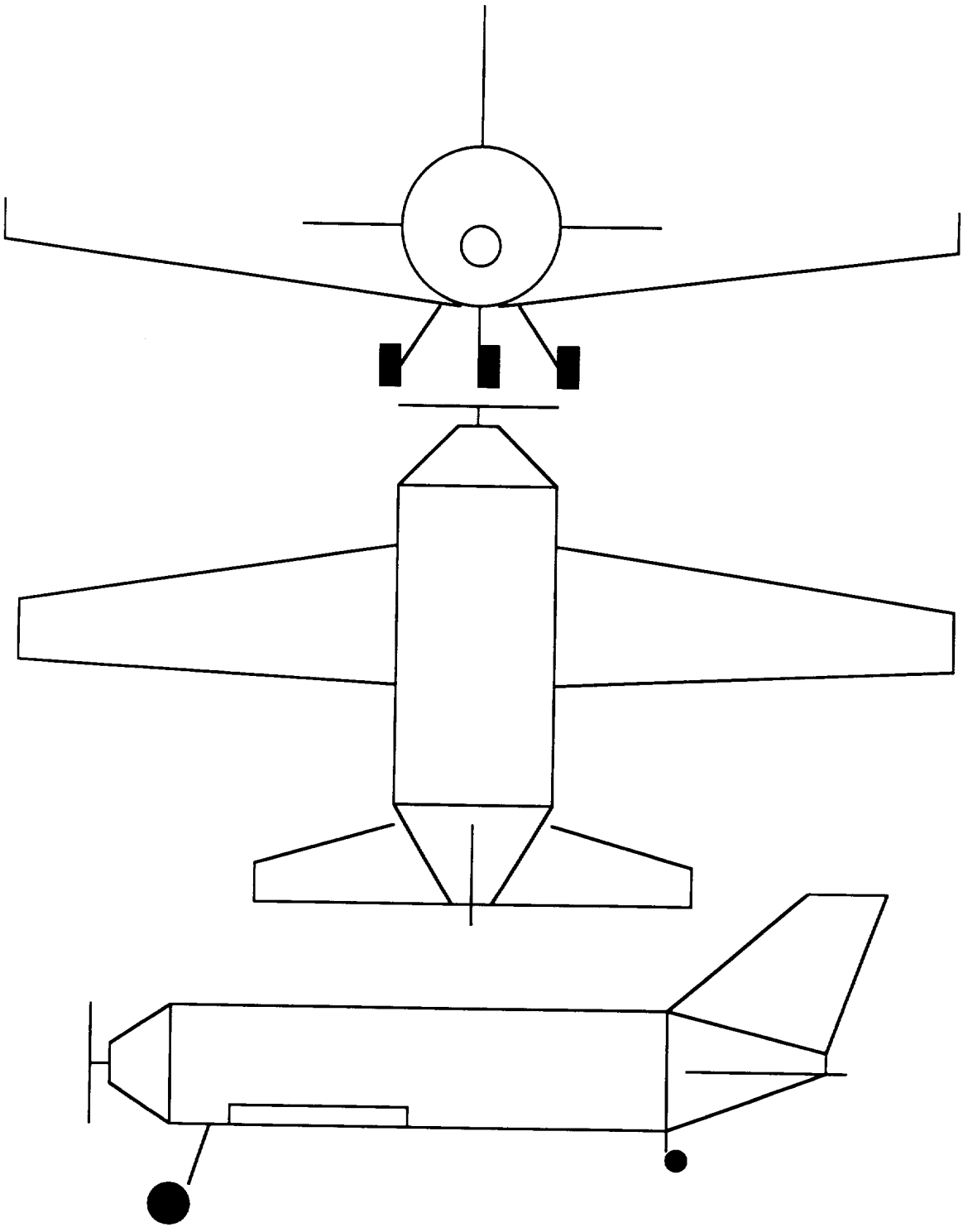

Figure 3.6.1: Low Wing - Stabilator Control

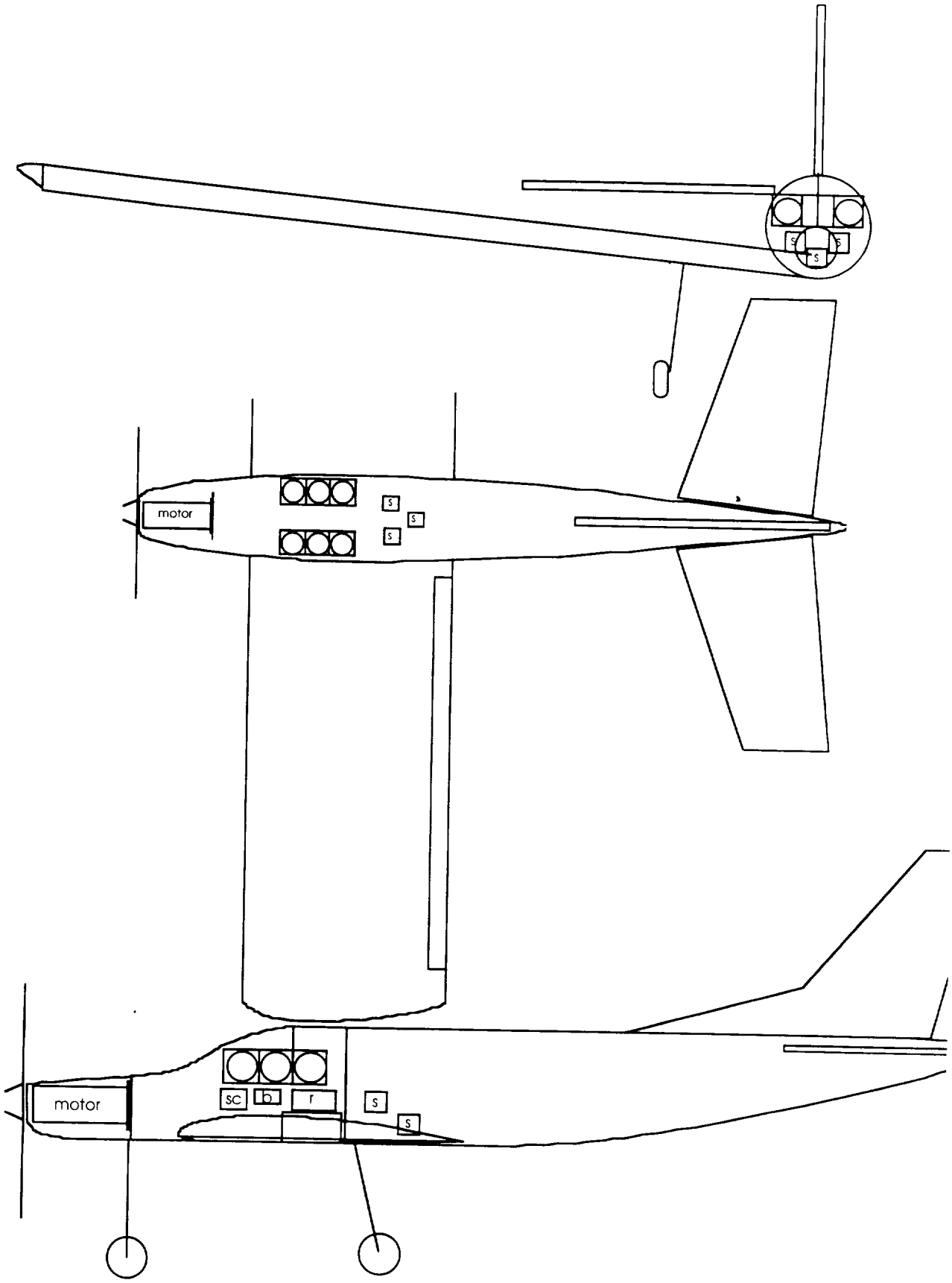

Table 3.7.1: Summary of Concept Selection

Concept	Advantages	Disadvantages
High Wing Conventional - Aileron Control	- Tricycle gear facilitates control on unprepared runways - Large tires help rough field handling - Circular fuselage increases aesthetic appeal - Extensive Database and easy avionics access with high wing configuration	- Large tires could result in significant weight and drag increases - Construction and attachment problems associated with circular fuselage
Rectangular Fuselage - Polyhedral Wing	- Easier to Manufacture - Extensive Database and easy avionics access with high wing configuration	- Not highly innovative - Flaps have been somewhat ineffective in previous designs - Large pitch down moment due to flaps
The Backward Plane	- Circular fuselage increases aesthetic appeal - Spoilers eliminate adverse yaw created by ailerons - Landing impact stress is localized to rear section	- Fore-rudder was destabilizing in yaw - Difficult to connect spoiler control linkages to servo - Requires bulky landing gear
Low Wing - "T" Tail	- High Horizontal Tail reduces interference effects - Increased elevator effectiveness	- Requires complicated control linkages - Reinforcement needed on vertical tail
Low Wing - Winglets	- Circular fuselage increases aesthetic appeal - Nose cone reduces bluff body drag effects - Winglets reduce tip vortex effects and drag	- Winglets could create complex loadings and diminish the structural integrity of wing - Reinforcement of wing could incur weight penalty
Low Wing - Stabilator Control	- Stabilator reduces size of horizontal tail - Circular fuselage increases aesthetic appeal	- Load carrying problem from stabilator control rod - Low-wing necessitates access to avionics through underside of fuselage
The Elite	- Circular fuselage increases aesthetic appeal - Stabilator reduces size of horizontal tail - Tapered vertical tail and low wing increase appeal - Placement of horizontal tail reduces the downwash on the tail	- Difficult to manufacture circular fuselage - Load carrying problem from stabilator control rod - Low-wing necessitates access to avionics through underside of fuselage - Limited database for ailerons

4 AERODYNAMIC DESIGN DETAIL

4.1 Main Wing Basic Concept

The first step in the wing design was to decide on a basic concept. The wing concept was driven by the DR&O Goals of an aesthetically pleasing aircraft that has a high cruise speed. One of the main problems with the wing was how to attain a high cruise speed and still meet the takeoff requirements. In essence, the Elite needed to have two separate wings, one for low speed and one for cruise. The standard approach at attaining this dual nature in the wing is the use of flaps. Unfortunately, previous years' reports indicated that the drag and weight associated with the flaps overshadowed any benefit the flaps provided. At takeoff, several groups noted that the decreased acceleration due to flap drag caused the takeoff length to actually increase. Also, past groups ran into difficulties balancing the increased moments caused by flap deployment. Due to the uncertain benefits and possible detrimental effects of flaps, they were not employed in *The Elite's* design. Therefore other means of attaining the desired performance had to be examined. Without flaps, the wing must be just large enough to meet the low speed requirements but as small as possible to improve the cruise qualities. This can be achieved by choosing an airfoil with a high $C_{\ell max}$. The other variable that will help improve the wing's performance is aspect ratio. The larger aspect ratio wings provide excellent lift characteristics with a decrease in induced drag. Due to manufacturing considerations, a rectangular planform shape was picked. The rectangular shape allows the use of the available wing jig and should increase the tolerances to which the wing can be built. Thus the DR&O goals and manufacturing concerns drove the wing concept to a rectangular planform with a high aspect ratio, a high C_{Lmax} and as small an area as possible.

4.2 Main Wing Airfoil Selection

The airfoil finally selected for the main wing was the DF101. This airfoil had to compete against the following list of airfoils:

Table 4.2.1: Listing of Considered Airfoils

Airfoil	% Camber	CL max	% Thickness
1) E374A	2.24	1	10.91
2) SD2030	2.25	1.05	8.56
3) DF101	2.3	1.14	11
4) NACA 2.5411	2.5	1	11
5) S3021A	2.96	1.1	9.47
6) E205B	3.01	1.1	10.48
7) S4233	3.26	1.2	13.64
8) Clark Y	3.55	1.2	11.72
9) SD6080	3.74	1.2	9.18
10) S4061	3.9	1.25	9.6
11) E214	4.03	1.3	11.1
12) FX63-137B	5.94	1.6	13.59

These twelve airfoils where selected from the many airfoils listed in references 1 and 2. They were selected on the basis of a qualitative overview of their lift curves, the drag polars, and the availability of data in the low Reynold's number regime in which our aircraft flies. To decide among the these airfoils, a trade study was performed that compared the weight of the aircraft and the drag of the wings when each of the above airfoils was used. These two criteria were chosen to select the airfoil due to their direct influence on the cruise speed and takeoff performance of the airplane.

A linear relationship was assumed to exists between the size of the wing and the weight of the wing. A lifting-line code was used (ref. 3) to iteratively adjust the wing's size until the lift just balanced the weight at a speed of 25 ft/sec (remember that weight of the aircraft was linearly dependent on the wing area). At the same time, the code adjusted the angle of attack of the wing until the $C_{\ell max}$ the tested airfoil was reached at the root of the wing. Thus the code attempted to find the wing just large enough to balance the weight of the aircraft at 25 ft/sec with a conservative stall criterion. Once the wing was sized in the above manner, the drag characteristic for the wings were found by adding the airfoil profile drag to the induced drag of the wing. The induced drag coefficient was computed by the same lifting line code only this time the area of the wing was fixed and the program searched for the angle of attack to just balance the weight of the aircraft at a cruise speed of 65 ft/sec. Once the cruise angle of attack was known, the airfoil C_D was found from the airfoil data in ref. 1. One must remember that to obtain the total drag, the drag coefficient is multiplied by $1/2\rho V^2 S$, so the total drag is also linearly dependent on

the size of the wing. The final results of the airfoil trade study are shown below. The airfoil numbers correspond to the tabular listing in table 4.2.1 above.

Figure 4.2.1: Airfoil Comparison of Resulting Wing Weights and Drag

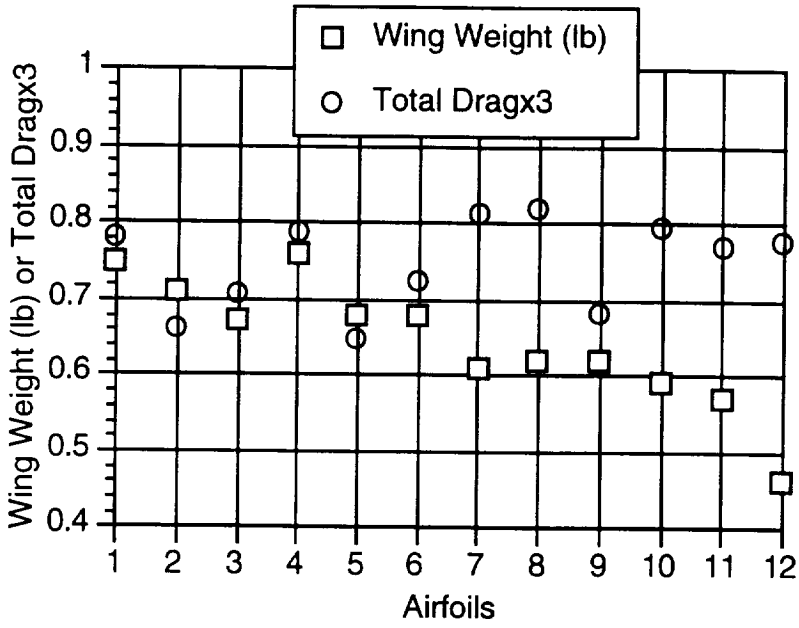

From this chart, the best airfoil choices would be numbers 2, 3, 5, 6, and 9 since they offer the best combination of weight and drag. In discussions with the structures group, it was decided that structurally a 10% airfoil thickness was the minimum allowable. This eliminated airfoils numbers 2, 5, and 9 from the running. Now, a direct comparison between airfoils 3 and 6 reveals that 3 edges out number 6 in wing weight, total drag, and thickness. Thus #3, the DF101, was chosen as the airfoil. One may wonder why the #12 airfoil was not chosen. The main reason for this was that the data for this airfoil was not available in the Low-Reynolds number regime where this aircraft flies. The large weight savings is due to the high maximum lift coefficient, 1.6, of the airfoil. However, the design group was not confident that this number would hold at the Elite's flight Reynold's numbers.

4.3 Airfoil Characteristics

From ref. 1, the DF101 has the following aerodynamic properties

Figure 4.3.1: Aerodynamic Data for the DF101 (reprint from ref. 1)

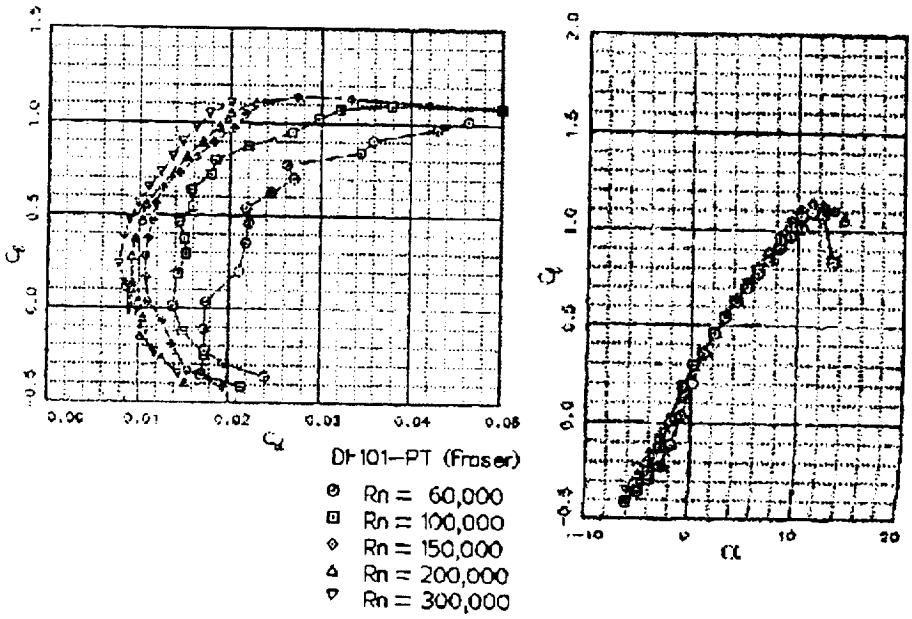

For the Elite the design Reynold's number in cruise is 348,000 and at landing is 133,000. The DF101 also has a C_{mac} of -0.0582. This C_{mac} of -0.0582 was then assumed to be the C_{mac} for the entire wing.

4.4 Wing Sizing and Aspect Ratio

With the airfoil selected and a rectangular planform picked for manufacturing reasons, only two major variables remained: the planform area and the aspect ratio. The main driver behind sizing the wing was the landing/takeoff design objectives and requirements. The DR&O specified a maximum improved runway takeoff distance of 28 ft. Preliminary studies by the propulsion group found that the we could conservatively expect to reach 25 ft/sec in the maximum takeoff distance. The planform area was sized in conjunction with the airfoil selection process. From the previous section, one can see that the planform area fell out of the airfoil trade study. Using the lifting line code that was developed and validated for AE360 (ref 3), the necessary wing area to meet the takeoff requirements with the DF101 airfoil was 6.4 ft^2. However, this had the plane taking off with the wing root in a stalled condition. In the final design, we added 0.1 ft^2 to keep the root of the wing slightly below stall at takeoff. To get a more accurate idea of the wing's stall characteristics, the lifting line code was modified to contain a more realistic stall model. One of the outputs of the lifting line code is the section lift

coefficient at fifty stations along the wing. The stall model incorporated compared these section C_ℓ's to the $C_{\ell max}$ of the airfoil. The airfoil was assumed to have a linear slope until its $C_{\ell max}$ was reached and then to linearly drop off at the same rate if its $C_{\ell max}$ was exceeded. In essence, this put the following C_ℓ vs. alpha curve for the airfoil into the lifting code.

Figure 4.4.1: Airfoil Model Incorporated into the Lifting Line Code

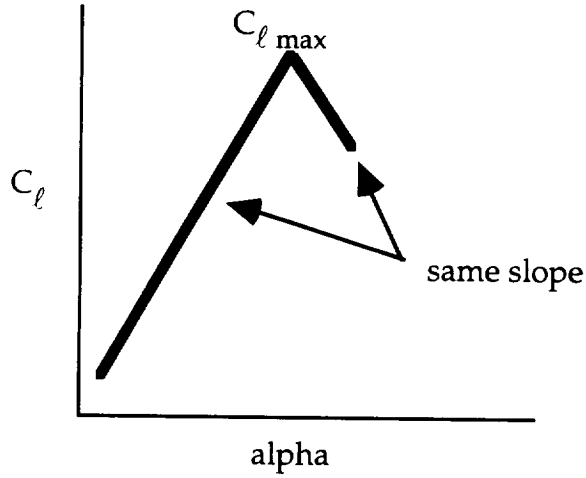

With this airfoil model, the code searched for the condition where the total integrated wing C_L was the greatest. This should give a more accurate approximation of when the wing will stall. The integration of the wing C_L distribution was found to be a maximum at 12.3 degrees. The wing C_L distribution at this condition is shown below.

Figure 4.4.2: Wing C_L Distribution at Stall

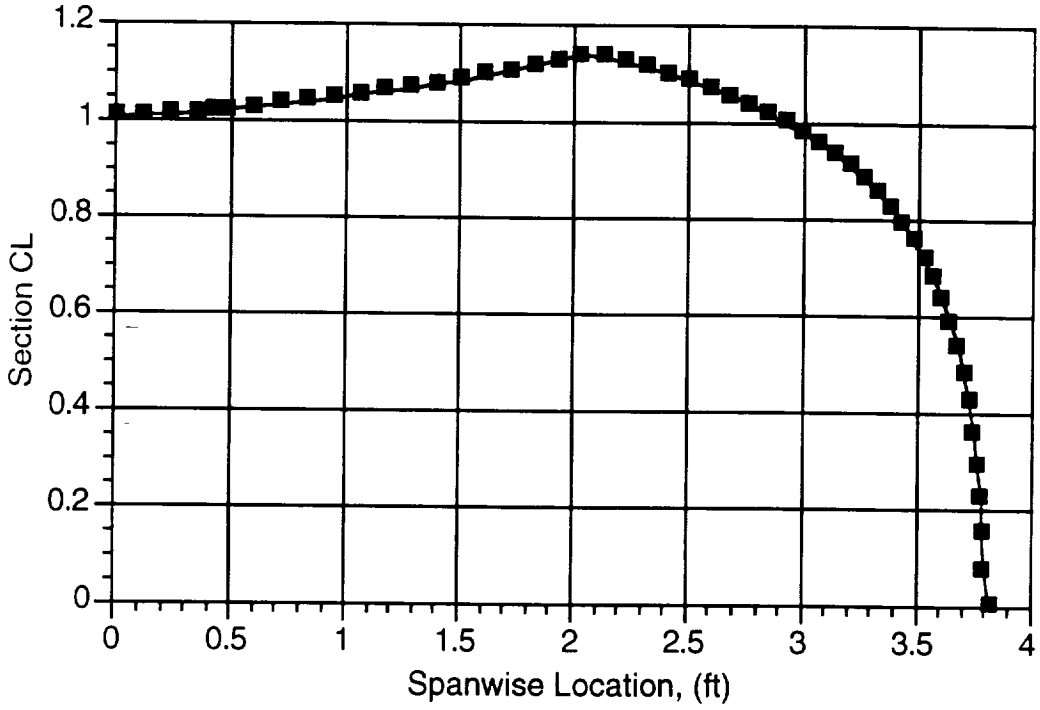

Aerodynamically, the larger the aspect ratio the better. $C_{L\alpha w}$ increases and the induced drag decreases as the aspect ratio increases. Unfortunately, this makes the wing long and narrow which is inherently structurally less sturdy. After discussions with the structures group, it was decided that the largest feasible aspect ratio was 9. Thus the wing aspect ratio was set at 9[1].

Below is a summary of the of the main wing aerodynamic characteristics. These characteristics resulted from the decisions made above based on the desire to increase the cruise speed while still maintaining adequate low speed performance.

[1] For the airfoil selection process the aspect ratio was assumed to be 8. However, the airfoils should perform the same relative to one another regardless of the aspect ratio.

Table 4.4.1: Summary of Wing Characteristics

$C_{L\alpha w}$	4.76/rad
C_{Lo}	0.0995
C_{Lmax}	1.088
e	0.978
αstall	12.33°
Re_{cruise}	347,000
$Re_{takeoff}$	133,000
Aspect Ratio	9
Planform Area	6.5 ft^2
Planform Shape	Rectangle
Span	7' 7 3/4"
Cord	10 3/16"
Airfoil	DF101

4.5 Empennage Planform and Airfoil Selection

For the tail section, we examined the follow four airfoils: NACA 0009, NACA 0012, SD8020, and a flat plate. The SD8020 was chosen for the horizontal tail and a flat plate for the vertical tail. The SD8020 had the best response in the zero angle of attack regime and had the best drag characteristics. However, one of our main design goals was the aesthetics of the airplane so it was decided to sweep the tail surfaces. It appeared to be a very difficult task to build the vertical tail in the desired trapezoidal shape with an airfoil cross-section so the design group settled upon a flat plate geometry. This difficulty was avoided in the horizontal tail by making the planform shape a parallelogram. Thus an airfoil cross-section could be used in the horizontal tail. The actual sizes of the tail surfaces were determined by the stability and control analysis.

4.6 Drag Breakdown

Since a high cruise speed is an essential part of the DR&O, drag is an extremely important issue. Unfortunately, the geometry of this aircraft was fairly fixed by other concerns (payload size, placement of servos, landing criteria etc.) so not much could be done to affect the drag. The Elite does incorporate some cosmetic changes to help with the drag but their actual impact in a low Reynold's number regime is difficult to quantify. The main cosmetic change over past designs is to have a very smooth, sleek fuselage. This helps to reduce drag while at the same time enhancing the aesthetic nature of the aircraft.

For the drag breakdown, two different sources were used to obtain a value for C_{Do}. The first was Dr. R. C. Nelson's (ref. 4) breakdown method presented in AE441. This breakdown method uses empirically determined C_{Do} values for each component. The second column of C_{Do}'s came from a variety of data sources. In the second column, the wing profile drag is assumed to be the same as the DF101 airfoil. The fuselage drag came from a fuselage drag chart on page 180 in ref 5 with a fineness ratio of 7.6. The vertical tail drag is assumed to be that of a flat plate. The horizontal tail has the C_{Do} of the SD8020 airfoil. Finally, the landing gear is assumed to have the C_{Do} of a right circular cylinder. Once the individual C_{Do}'s are obtained for each part of the aircraft, the basic equation for the total drag coefficient is:

$$C_{Do_{Total}} = \frac{\Sigma\left(C_{Do_i} S_{ref_i}\right)}{S_{ref_{Total}}}$$

Below is a tabular listing of the C_{Do} values used in determining the drag breakdown. The planform area of the wing was used as the $S_{reftotal} = 6.5\ ft^2$

Table 4.6.1: Drag Breakdown Components for Two Different Sets of Data

Component	S_{ref}	S_{ref} (ft^2)	C_{Do}-Nelson	C_{Do}-Data
Wing	Planform	6.5	0.007	0.008
Fuselage	Cross Section	0.136	0.11	0.075
Nacelles	Cross Section	0.049	0.06	0.06
Vertical Tail	Tail Area	0.55	0.008	0.013
Horizontal Tail	Tail Area	1.8	0.008	0.008
Landing Gear	Frontal Area	0.0958	0.95	1.1
Interference			+10%	+10%
		C_{Do} Result	**0.0292**	**0.0325**

From this table, one can see that the landing gear is the major contributor in terms of the drag. In fact, the landing gear accounts for 50% of the total C_{Do}. One solution to this problem would have been the use of retractable landing gear. Unfortunately, the impact of this option was not fully realized in the initial concept selection process. In the future, the use of retractable gear should definitely be considered. The drag polar is given by:

$$C_D = C_{D_o} + C_{D_i} C_L^2 \text{ where, } C_{D_i} = \frac{1}{\pi A\, Re}$$

which for the Elite equals:

$$C_D = 0.0325 + 0.03974C_L^2$$

This relation is plotted below.

Figure 4.6.1: Aircraft Drag Polar

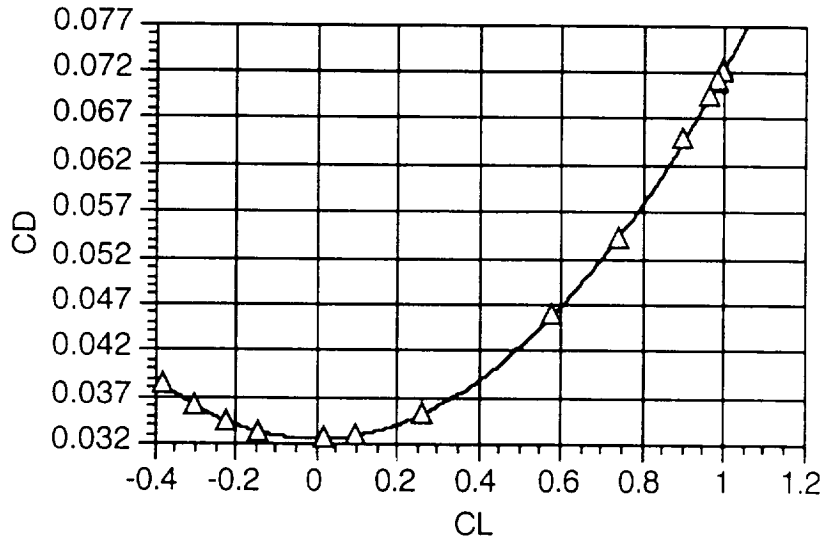

One thing to notice is the profile drag is very large compared to the induced drag. Any uncertainty in the profile drag estimates can cause dramatic changes in the performance projections for the aircraft. For *The Elite*, the pessimistic drag estimates were used to compute the performance to help insure that the objectives were met. Once a relationship between C_L and C_D has been established, the Lift/Drag curves for the airplane are easily obtained. The L/D is plotted against the angle of attack and level flight velocity below.

Figure 4.6.2: L/D Curves -- a) vs. Angle of Attack b) vs. Level Flight Velocity

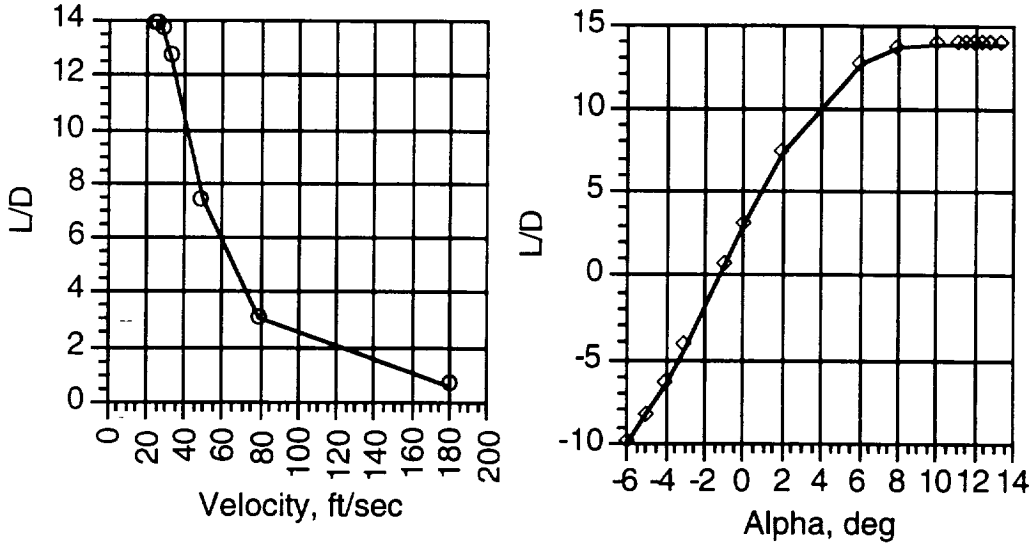

a) b)

One thing to notice about the L/D plots is that L/D_{max} occurs near stall rather than at cruise. It is desirable to have the L/D_{max} occur at cruise since that is the condition were one would fly for the maximum endurance. In the case of *The Elite*, the maximum range speed is 25 ft/sec a far cry from its cruise speed of 60 ft/sec. The main reason for L/D_{max} occurring near stall is the shallow nature of the drag polar. The large value for C_{Do} with a relatively normal value for C_{Di} never allows the drag to increase at a faster rate than the lift. Thus the L/D maximum occurs near the maximum lift condition.

4.7 Aircraft Aerodynamic Summary

Below is a summary of the aircraft aerodynamic characteristics. These values completely describe the aerodynamic quality of the Elite aircraft.

Figure 4.7.1: C_L vs α of Aircraft

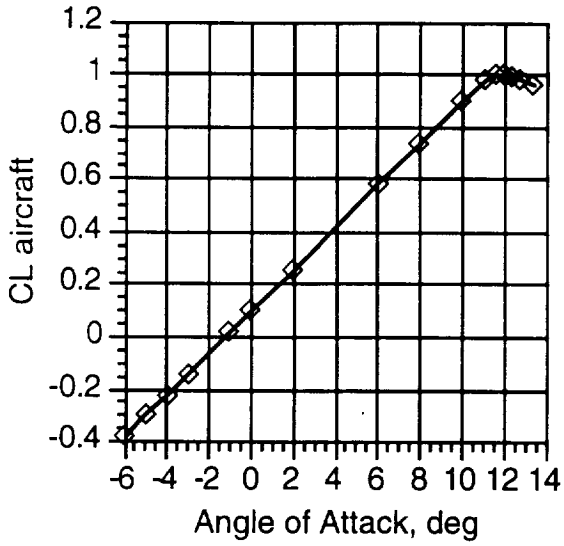

Table 4.7.1: Summary of Aircraft Aerodynamics

$C_{L\alpha}$	4.76/rad
C_{Do}	0.0325
C_{Di}	0.03974
e	0.86
L/Dmax	14
L/Dcruise	5
Planform Area	6.5 ft^2
Aspect Ratio	9

4.8 References

4.1 Selig, Michael S., Donovan, John F., and Fraser, David B. Airfoils at Low Speeds. Virginia Beach: H.A. Stokely, 1989.

4.2 Miley, S. T., A Catalog of Low Reynolds Number Airfoil Data for Wind Turbine Applications, Texas A&M, 1982

4.3 Fay, Jonathan P., Lifting Line Code written and validated for AE360 under the direction of Dr. E. J. Jumper, Department of Aerospace and Mechanical Engineering, University of Notre Dame, Spring 1993

4.4 Nelson, R. C., "Subsonic Drag Estimation: Component Build-up Method." Department of Aerospace and Mechanical Engineering, University of Notre Dame, 1993

4.5 McCormick, Barnes W. Aerodynamics, Aeronautics, and Flight Mechanics. New York: John Wiley and Sons, 1979.

4.6 Lissaman, P.B.S. "Low Reynolds-Number Airfoils", Annual Review of Fluid Mechanics, Vol 15, 1983, pg 223-239

5 PROPULSION SYSTEM DESIGN DETAIL

5.1 Requirements and Objectives

Design Requirements:

1. Environmentally safe.
2. High speed performance.
3. Maximum take-off distance of 28 feet on smooth runways and 42 feet on rough runways.
4. Propulsion system installation under 20 minutes.
5. Ability to fly to nearest alternative airport and loiter for one minute.
6. Fuel stored in the wing carry-through structure.

Design Objectives:

1. Minimum Cruise Speed of 60 feet/sec.
2. Maximum velocity of at least 80 ft/sec.
3. Short and Rough Field Take-Off Capability
4. Range of 30,500 feet to allow service of all Aeroworld airports
5. Aesthetics

5.2 System Selection

The design of the propulsion system involved the selection of the motor, propeller and fuel system. In order to be environmentally safe to Aeroworld, the RFP required that the propulsion system of the aircraft employ a state-of-the-art electric propulsion system (Ref. 5.1). The driving factors that determined the components of the propulsion system were the maximum and cruise velocities, the aircraft range, take-off distance, cost and aircraft maximum take-off weight. The final system consisted of the Astro Cobalt 15 engine, the Zingali 10-8 three-blade propeller, and thirteen Panasonic P-130SCR battery cells. The following is a table of the aircraft's values used in the calculations.

Table 5.2.1: Aircraft Data

Aircraft	
Weight	4.88 lbs
Wing Area	6.5 ft^2
Aspect Ratio	9
C_{Do}	0.0325
C_{Lmax}	1.03
Oswald Efficiency	0.89

5.3 Motor Selection

Two motors were considered for *The Elite*, the Astro 15 and the Astro 25. A third

motor, the Astro 05, was available but not considered due to its insufficient power output leading to an inability to satisfy the take-off distance objective. The motor weight and cost, maximum velocity attainable, and the take-off distance drove the motor selection. Table 5.3.1 illustrates the advantages, particularly in maximum velocity and weight, the Astro 15 motor has over the Astro 25 motor.

Table 5.3.1: Comparison of Astro 15 motor with Astro 25 motor

	Astro 15 Motor	Astro 25 Motor
Motor Weight	28 oz	38 oz
Motor Cost	$107	$174
Maximum Velocity	71.7 ft/sec	56.5 ft/sec
Take-Off Distance (28 ft max)	23.6 ft	40+ ft
Recommended Motor RPM	16,500 RPM	10,000 RPM

The maximum velocity and the take-off distance comparison were all calculated using our selected propeller, the Zingali 10-8 three-blade propeller, and the battery specifications of a pack voltage of 15.6 volts and a battery capacity of 1300 mah. These predictions were obtained using the FORTRAN programs TAKEOFF (Ref. 5.2), PROP123 (Ref. 5.3), and PAVAIL (Ref. 5.4).

Intuitively, the larger more powerful Astro 25 should have out performed the Astro 15. This would have been the case if the propeller was large enough to take advantage of Astro 25's extra torque capabilities. With a smaller ten inch diameter propeller, however, high RPM's are more important than high torque capabilities. The Astro 15 motor was ultimately selected because of its lower weight and superior velocity performance attributable to the motor's much higher maximum RPM. In addition, the Astro 15 cost significantly less than the Astro 25. Table 5.3.2 contains further information about the Astro 15 motor characteristics.

Table 5.3.2: Other Astro 15 Characteristics

Name	Astro Cobalt 15
Maximum Power	185 watts
Internal Resistance	0.12 W
Gear Ratio	31:14
Gear Efficiently	95%
k_t	1.0978 in-oz/amp
Tloss	1.3729 in-oz
k_V	7.8568 10^{-4} V/rpm

The gear efficiency was assumed to be 95% based on recommendation from AE454 Propulsion class (Ref. 5.5).The motor torque and battery constants are taken from the curve fit of the Astro 15 motor performance based upon motor data supplied by the manufacturer (Ref. 5.6). The plots used to determine the motor torque and battery constants are shown in Figure 5.3.1.

Figure 5.3.1: Motor Torque and Battery Constants

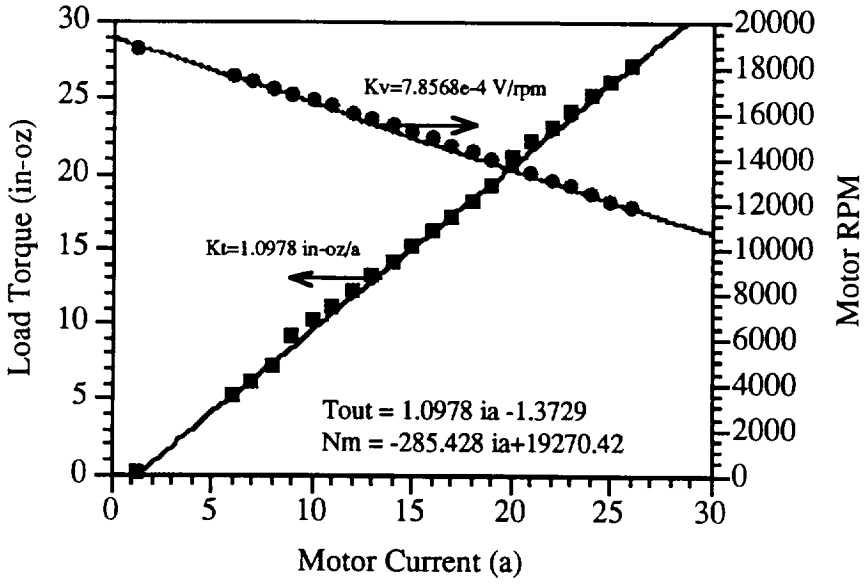

It should be noted that the PAVAIL program did not take into account a gear efficiency and torque losses (T_{loss}). This was compensated by writing our own program to

determine all the performance characteristics of the propulsion system. The program was validated by setting the gear efficiency and torque loss to 100% and zero, respectively, and compared to PAVAIL

5.4 Propeller Design

Propeller selection proved critical in the aircraft's ability to fulfill the requirements for maximum velocity and take-off distance outlined in the DR&O. Several parameters were examined during the propeller selection including diameter, pitch, manufacturer, and the number of blades. The geometric chord and thickness versus the blade radius where recorded and inputted into PROP123 to attain the results. The program accounted for induced velocity and tip losses, and Reynolds and Mach number corrections. A trade study was performed to determine the effects of the propeller diameter, pitch, manufacturer and number of blades on propeller efficiency, thrust coefficient and power coefficient. For aesthetic purposes, propeller diameter was limited to 10 inches and 11 inches so that the propeller would be somewhat proportional to the aircraft. In addition, a smaller diameter would require shorter landing gear, and thus help reduce weight and drag penalties. The propellers that were considered were the two-bladed Top Flight 10x6, Zinger 10x7, and Zinger 11x7; and the three-bladed Zingali 10x8 and Graupner 11x7. Figure 5.4.1 illustrates the improvement in thrust coefficient three-blade propellers have over two-blade propellers.

Figure 5.4.1: Thrust Coefficient as a Function of Propeller

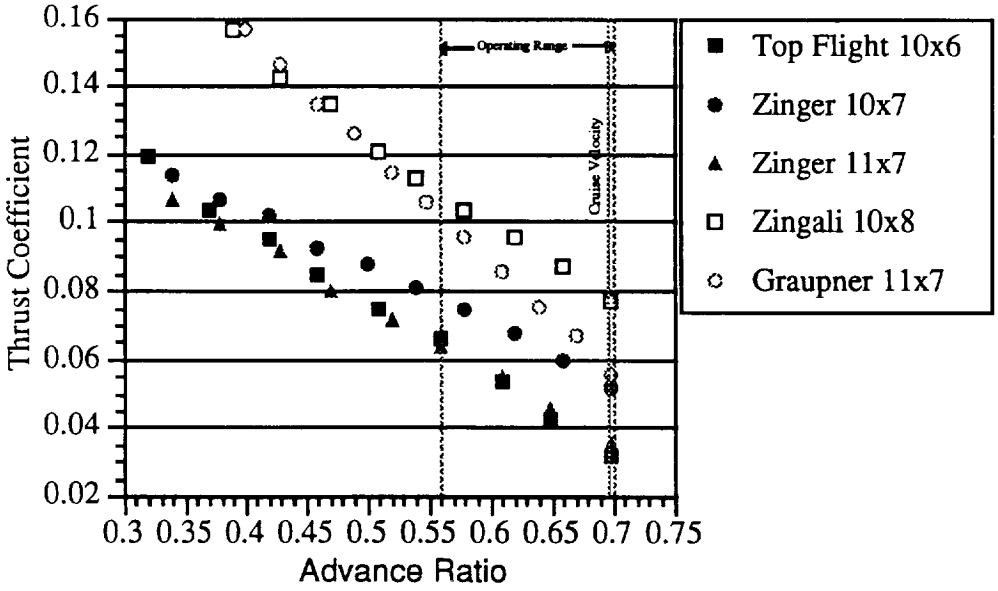

Figure 5.4.2 illustrates that although a three-blade propeller has improved thrust coefficient, it also has a higher power coefficient than two-blade propellers.

Figure 5.4.2: Power Coefficient as a Function of Propeller

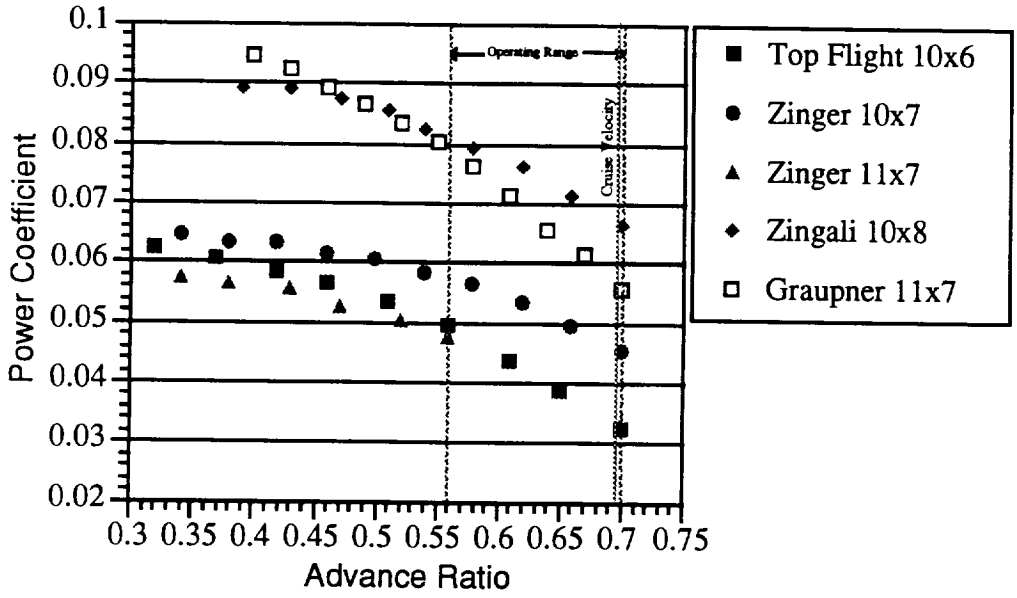

Figure 5.4.3 compares the efficiencies of three-bladed propellers and two-bladed propellers. As one can see, only the Zingali 10x8 had comparably high efficiencies with the best two-bladed propellers.

Figure 5.4.3: Propeller Efficiency as a Function of Propeller

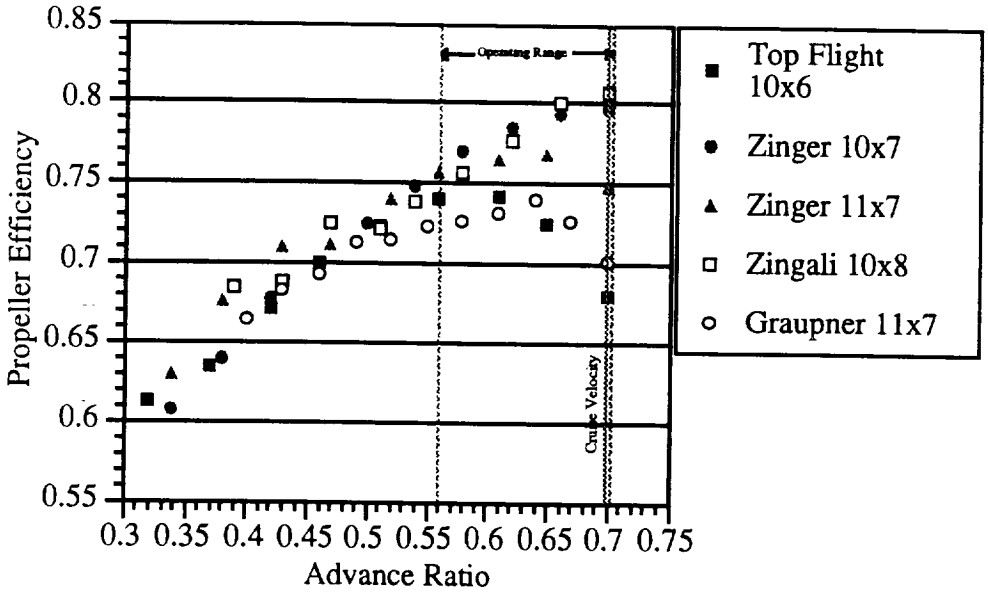

Three-bladed propellers where chosen for their higher thrust and power capability, and comparably high efficiencies. Another reason for the choice of a three-blade propeller was the more aesthetic aerodynamic appearance over two-bladed propellers. Aesthetics, again, was one of the major drivers of the design.

The selection of three-bladed propellers was very limited due the fact that few companies manufactured propellers in the desired pitch and diameter. Two three-bladed propellers were acquired and analyzed. These propellers were the Zingali 10-8 and the Graupner 11-7. Figure 5.4.4 shows the advantage the Zingali propeller had over the Graupner propeller in maximum velocity and power available at higher velocities.

Figure 5.4.4: Propeller Maximum Power Available verses Velocity

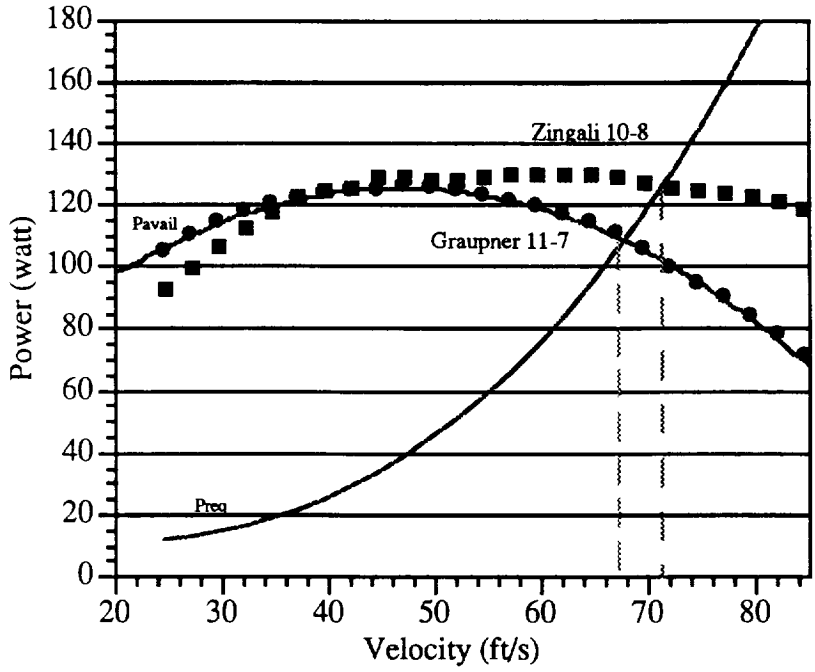

Table 5.4.1 is a break down of the propeller performances. The values are taken from a program written to determine power available, power required, range, endurance and current draw at different velocities (Ref. 5.7). Again, the Zingali's performance is superior to that of the Graupner in every category except at maximum rate of climb.

Table 5.4.1: Propeller Performance Comparison

	Zingali 10-8	Graupner 11-7
Maximum Velocity	71.7 ft/s	68.0 ft/s
Cruise Propeller Efficiency	80%	71%
Current Draw at Cruise	10.2 amps	10.8 amps
Maximum Rate of Climb	15.2 ft/s	15.36 ft/s
Range at Cruise	27401 ft	25997 ft
Endurance at Cruise	7.6 minutes	7.2 minutes

The Zingali 10-8 was ultimately selected for two reasons. Lower diameter requires a smaller landing gear which thus decreases the weight and decreases the drag while satisfying the requirement of a rough field capability. A drag breakdown performed by

the Aerodynamics Group indicated that the landing gear accounted for nearly 50% of the total parasite drag, C_{Do}. In addition, the Zingali 10-8 had a higher maximum velocity which was one of the primary drivers of the design.

Figure 5.4.5 contains the Zingali's average propeller efficiency as a function of advance ratio. This figure indicated that at cruise, the Zingali propeller was operating very closely to the propeller's maximum efficiency.

Figure 5.4.5: Zingali Propeller Efficiency as a Function of Advance Ratio

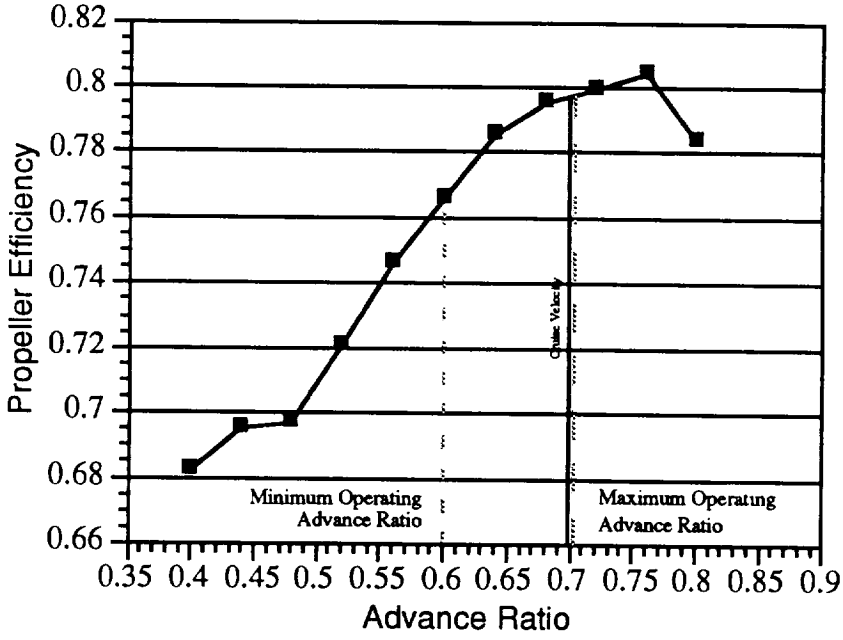

Due to some uncertainty that arose in the PROP123 program, there was considerable concern in the accuracy of its predictions, particularly at low and high advance ratios. However, as one can see, the propulsion system operates in a relatively narrow band in the linear region of the curves. Thus, within the operating advance ratios, performance predications were expected to be relatively accurate. Nonetheless, past wind tunnel data indicated that the propeller efficiencies found for the Zingali were too high. It was expected that the propeller efficiency of the fiberglass Zingali propeller would be higher than that of wooden propellers because of the capability of machine precision manufacturing, but the improvement was so dramatic as to cause suspicion of the results. The original PROP123 was used because it provided the best reasonable values of efficiencies to wind tunnel data.

5.5 Engine Control & Battery Selection

Speed and rate of climb was controlled by varying the throttle. During take off, the throttle should be opened fully to a voltage of 15.6 volts and then reduced until the required velocity is attained. The same would be done for climb maneuvers with the throttle varying between the cruise throttle and the maximum throttle. Figure 5.5.1 illustrates the power required and the power available for *The Elite* at several throttle settings during various flight regimes.

Figure 5.5.1: Effect of Throttle Setting on Power Available

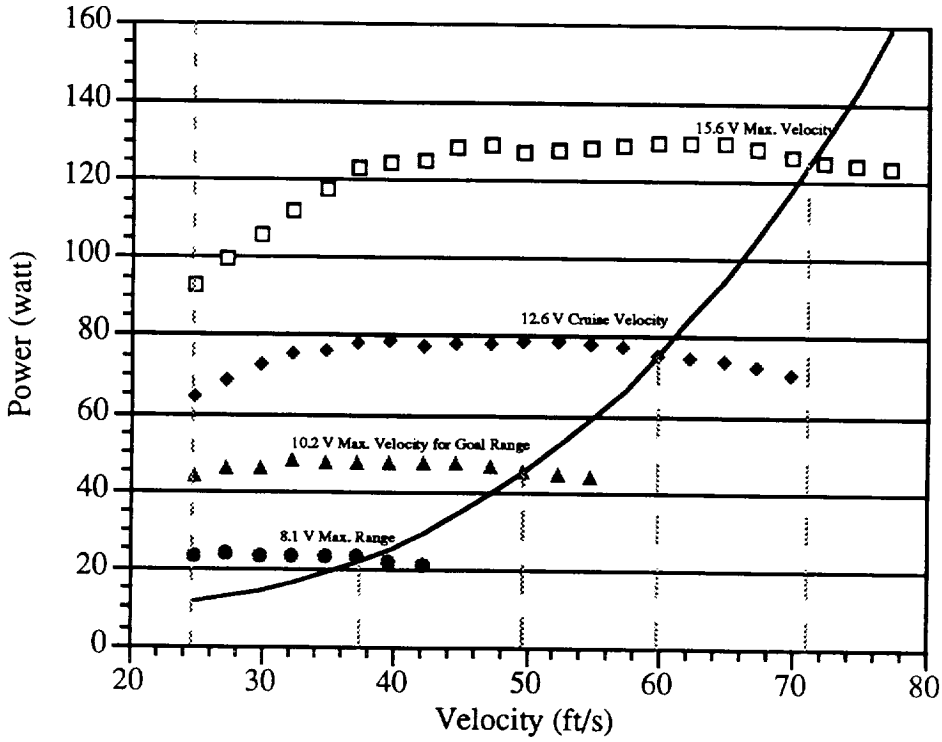

Table 5.5.1 summarizes estimates of the throttle settings that will attain the desired flight conditions for *The Elite*.

Table 5.5.1: Throttle Setting for Desired Flight Condition

Flight Condition	Velocity	Throttle
Take-off Velocity/Stall	24.8 ft/s	42%
Maximum Range at WMTO	36.9 ft/s	52%
Maximum Velocity for Range Goal of 30,500 ft	49.6 ft/s	65%
Cruise Velocity	60.0 ft/s	81%
Maximum Velocity	71.7 ft./s	100%

The Elite was designed to be powered by 1.2 volt rechargeable battery cells. The batteries chosen for *The Elite* were the P-130SCR 1.2 Volt batteries having a rated capacity of 1300 mah. This batteries were selected for the technical demonstrator based on results from PAVAIL which again proved to be erroneous when gear efficiency and torque losses were not taken into account. Figure 5.5.2 illustrates the range and endurance for *The Elite* when gear efficiency and torque losses are taken into account.

Figure 5.5.2: Range and Endurance Versus Velocity at WMTO

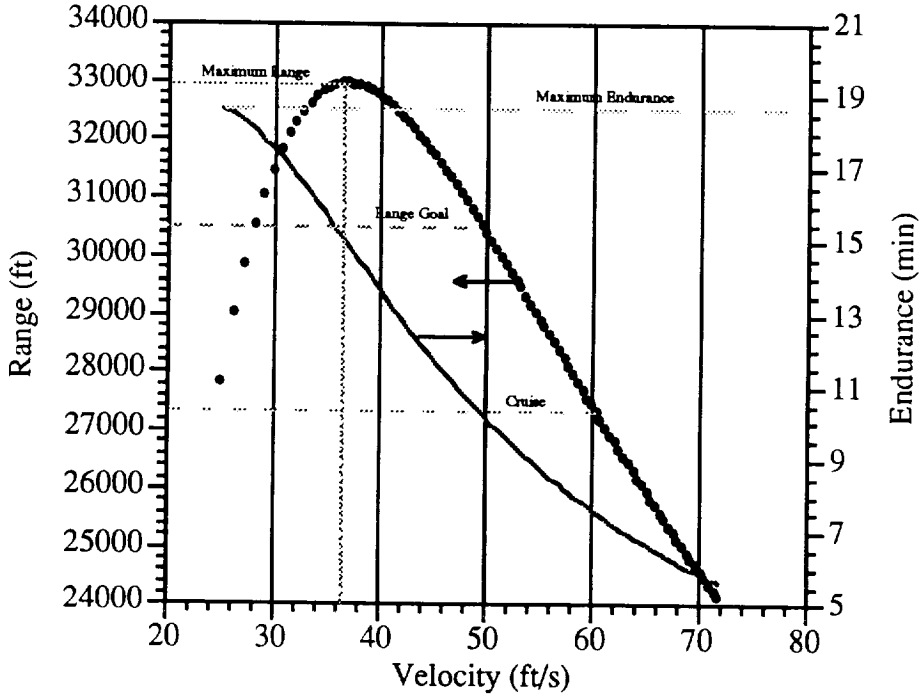

As one can see, the range requirement at cruise was not attainable with this battery. In order to have a range of 30,500 feet at a cruise speed of 60 ft/s, 1500 mah would be

required. However, such batteries were not available. The closes mah-rated battery are the 1400 mah batteries. Though all the calculations in this report are based on the 1300 mah batteries, it is suggested that the 1400 mah batteries should be used for the actual production of The *Elite*. For performance, only range and endurance would be effected. With the 1400 mah battery, the maximum range was 35,500 feet at 37 ft/s, maximum velocity for goal range was 57 ft /s, and the range at cruise was 29400 feet. This is very close to our object performance goals.

Nonetheless, with 1300 mah batteries, *The Elite* can handle 95% of the possible flight routes (see Performance Section). Thirteen cells were chosen based upon the manufacturer's suggested battery pack voltage for the Astro 15 motor. Table 5.5.2 contains the specifications on the 1300 mah batteries.

Table 5.5.2: Battery Specifications

Panasonic P-130SCR	Cell Battery	13 Cell Pack
Voltage	1.2 V	15.6 V
Capacity	1300 mah	1300 mah
Internal impedance	6 mW	78 mW
Weight	1.7 oz.	22.1 oz
Cost	$4.00	$52.00

5.6 Installation

One of the requirements of the propulsion system was that it could be installed and removed from *The Elite* in under 20 minutes. To achieve this, the batteries would be sealed together and placed in the wing carry-through structure. The wing will be able to be screwed off the bottom of the fuselage allowing easy access to the batteries and radio control equipment. The batteries will be fixed within the wing box spars with velcro.

The motor will slide into the nose mount attached to the firewall with four mounting screws. A nose cone and spindle will be mounted for aerodynamics and aesthetics. Further detail on engine and battery mount structure can be found in the Structures section of this document.

5.7 Propulsion System and Performance Summary

Propulsion System	
Motor	Astro Cobalt 15
Propeller	Zingali 10-8
Battery	13 Panasonic P-130SCR
Speed Controller	Tekin Model
Radio Control System	Futaba 4NBL/Attack
Weight	2.04 lbs
Cost	$ 172.58
Performance	
Maximum Velocity	71.7 ft/s
Cruise Velocity	60.0 ft/s
Maximum-Range Velocity	49.57 ft/s
Maximum-Velocity Range	24,099 ft
Cruise Range	27,401 ft
Maximum Range	32,919 ft
Maximum Velocity Endurance	5.6 minutes
Cruise Endurance	7.62 minutes
Maximum Range Endurance	14.9 minutes

5.8 References

5.1 Batill, Dr. Stephen. "High Speed, Low-Cost General Aviation Aircraft for 'Aeroworld.'" Department of Aerospace and Mechanical Engineering, The University of Notre Dame, 1994.

5.2 Batill, Dr. Stephen. TAKEOFF FORTRAN program. Department of Aerospace and Mechanical Engineering, The University of Notre Dame, 1994.

5.3 Batill, Dr. Stephen. PROP123 FORTRAN program. Department of Aerospace and Mechanical Engineering, The University of Notre Dame, 1994.

5.4 Batill, Dr. Stephen. PAVAIL FORTRAN program. Department of Aerospace and Mechanical Engineering, The University of Notre Dame, 1994.

5.5 Dunn, Dr. P.F. "AE454 - Propulsion Class Notes - Electric Motor - Propeller Propulsion (with application to Remotely Piloted Vehicles)." Department of Aerospace and Mechanical Engineering, The University of Notre Dame, 1993.

5.6 Batill, Dr. Stephen. Group A Design Databook. Department of Aerospace and Mechanical Engineering, The University of Notre Dame, 1994.

5.7 Le, Tuan. A FORTRAN program to compute range and endurance, 1994.

6 WEIGHT ESTIMATE DETAIL

6.1 Level Zero Weight Estimate

A preliminary component weight breakdown is presented in Table 6.1.1. These estimates were based on the data base of prior airplane designs in Aeroworld. The initial weight estimate was a low value of 4.2 lbs. Several of the components were taken directly from RPV catalogues. These include the motor, servos, receiver, speed controller, propeller, and batteries. The wing, fuselage, and empennage weights were all estimated as 2/3 to 3/4 of the values observed in past airplane designs. An uncertainty of ± 10 % was added to find the high and low end weight estimations.

Table 6.1.1: Zero Level Weight Component Breakdown

Component	Weight (lb)	Weight %
Structure		
Wing	0.75	17.9
Empennage	0.16	3.8
Fuselage	0.5	11.9
Landing Gear	0.35	8.3
Subtotal	1.76	41.9
Control Systems		
Servos	0.113	2.7
Receiver	0.059	1.4
Speed control	0.11	2.6
System batteries	0.125	3.0
Subtotal	0.407	9.7
Propulsion		
Motor (Astro 15 w/ gear box)	0.64	15.2
Propeller	0.044	1.0
Batteries	0.94	22.3
Subtotal	1.624	38.7
Payload	0.05	1.1
Total	3.8 ± .38	
High-end weight	4.2	

A preliminary center of gravity estimation was made by placing the aircraft components at desirable positions. The position was located at 13.25 inches behind the nose of the airplane.

6.2 Improved Weight and C.G. Estimate

A more detailed weight estimation was then calculated after a better understanding of the aircraft layout was obtained. The weight component breakdown is presented in Table 6.1.2. The table is an inclusive summary of all the of the structural weight needed to design the airplane. Each spar that is needed for manufacturing is included. Also in Table 6.1.2 is the x location of the center of gravity of each component measured from the nose of the aircraft and the moment that each creates about the leading edge of the aircraft (the nose). The center of gravity of the entire aircraft resulted in a location of 13.565 inches behind the nose. This was very close to the initial c.g. estimate of 13.25 inches.

Table 6.1.1: Improved Weight Component and C.G. Breakdown

System	Part Name	Weight (lb)	X-Location (in)	Moment about nose
Propulsion				
	Propeller	0.097	0.000	0.000
	Astro 15 motor w/mount	0.640	2.500	1.600
	Motor Batteries	1.380	12.000	16.560
	Speed Controller	0.117	11.500	1.346
	Wires			
	batteries--> Speed Controller	0.032	11.750	0.376
	motor --> Speed Controller	0.032	7.000	0.224
	Propulsion Total Weight	**2.298**		
Avionics				
	Servos			
	Aileron	0.038	18.000	0.675
	Rudder	0.038	19.250	0.732
	Elevator	0.038	19.250	0.732
	Receiver	0.059	12.250	0.723
	Servo Batteries	0.125	11.500	1.438
	Receiver Wires	0.020	15.000	0.300
	Antenna	0.010	25.000	0.250
	Control Rods/Links/Horns			
	Rudder			
	Balsa Rod	0.007	26.625	0.197
	Control Horn	0.004	34.000	0.150
	Wire Rod with Link (@ servo)	0.008	21.250	0.178
	Wire Rod with Link (@ horn)	0.008	32.000	0.268
	Elevator			
	Balsa Rod	0.007	26.625	0.197
	Control Horn	0.004	34.000	0.150

	Wire Rod with Link (@ servo)	0.008	21.250	0.178
	Wire Rod with Link (@ horn)	0.008	32.000	0.268
	Aileron			
	Wires	0.037	19.000	0.703
	Links	0.004	18.500	0.065
	Nose Gear			
	Sheathed Plastic Rod	0.016	11.625	0.187
	Link (@ gear)	0.002	5.000	0.009
	Link (@ servo)	0.002	18.250	0.032
	Total Avionics Weight	**0.445**		
Landing Gear				
	Nose Gear with Horn and Screws	0.150	4.125	0.619
	Main Gear	0.256	16.100	4.122
	Main Gear Straps and Screws	0.053	16.100	0.850
	Total Landing Gear Weight	**0.459**		
Payload		**0.046**	14.500	0.671
Main Wing	Leading Edge Location		10.500	
	Spars			
	Main Top (Balsa)	0.041	13.050	0.535
	Main Bottom (Balsa)	0.027	13.050	0.352
	Leading Edge (Balsa)	0.031	10.560	0.327
	Trailing Edge (Balsa)	0.027	19.130	0.517
	Secondary Top (Spruce)	0.017	16.100	0.274
	Secondary Bottom (Spruce)	0.017	16.100	0.274
	Monokote	0.167	15.590	2.604
	Ribs	0.093	15.340	1.427
	Aileron	0.032	20.020	0.641
	Tips (Soft Balsa Blocks)	0.050	13.750	0.688
	Gear Blocks (Spruce)	0.062	15.750	0.983
	Fuselage Mating Blocks (Spruce)	0.040	14.575	0.583
	Webbing (Balsa)	0.015	12.930	0.194
	Hinges	0.053	19.190	1.013
	Glue	0.063	18.660	1.166
	Fiberglass Spar Mating	0.188	18.660	3.508
	Total Wing Weight	**0.923**		
Fuselage				
	Longerons			
	Top (Balsa)	0.018	19.000	0.334
	Bottom (Balsa)	0.019	19.000	0.361
	Port Side	0.009	19.000	0.171
	Starboard Side	0.009	19.000	0.171
	Shaping (All 4 Combined)	0.018	19.000	0.342
	Bulkhead (#'s start @ Firewall)			
	1 (Spruce)	0.008	4.000	0.031

	2 (Balsa)	0.004	6.000	0.027
	3 (Balsa)	0.006	10.500	0.066
	4 (Spruce)	0.014	12.925	0.178
	5 (Spruce)	0.014	13.175	0.183
	6 (Spruce)	0.014	15.975	0.224
	7 (Spruce)	0.014	16.225	0.227
	8 (Balsa)	0.008	20.500	0.167
	9 (Balsa)	0.008	24.000	0.192
	10 (Balsa)	0.006	28.000	0.168
	11 (Balsa)	0.005	32.000	0.160
	12 (Spruce)	0.008	34.000	0.272
	Monokote	0.050	19.000	0.950
	Servo Tray	0.039	15.500	0.605
	Tail Cone	0.025	36.000	0.900
	Engine Mounting Blocks (Spruce)	0.030	4.000	0.120
	Fuselage Mating Blocks (Spruce)	0.040	14.575	0.583
	Glue	0.063	19.000	1.197
	Empennage Mating Blocks (Spruce)	0.025	34.000	0.850
	Total Fuselage Weight	**0.454**		
Vertical Tail				
	Spars			
	Leading Edge (Balsa)	0.008	34.000	0.286
	Hinge Line (Balsa)	0.008	36.000	0.288
	Truss Pieces	0.015	35.000	0.536
	Rudder	0.018	37.000	0.681
	Tip Spar	0.001	36.000	0.035
	Root Spar	0.003	34.500	0.099
	Fuselage Blending Block	0.003	29.000	0.087
	Hinges	0.004	36.000	0.144
	Monokote	0.022	34.000	0.748
Horizontal Tail				
	Spars			
	Main Top (Balsa)	0.009	34.000	0.289
	Main Bottom (Balsa)	0.009	34.000	0.306
	Leading Edge (Balsa)	0.009	32.500	0.293
	Trailing Edge (Balsa)	0.004	39.000	0.156
	Graphite Rod	0.034	34.000	1.156
	Ribs	0.024	35.000	0.851
	Tip Blocks (Soft Balsa)	0.020	34.000	0.680
	Hardwood Connecting Blocks	0.025	34.000	0.850
	Monokote	0.010	35.000	0.350
	Glue (Vertical and Horizontal)	0.030	34.000	1.020
	Total Empennage Weight	**0.257**		

	SUMS--------->	**4.881**		**66.211**
	Xcg	**13.565**		
	With 5% Fudge Factor	**5.125**		
	% Cmac of Xcg	**0.303**		

Figure 6.2.1: Weight & Balance Diagram

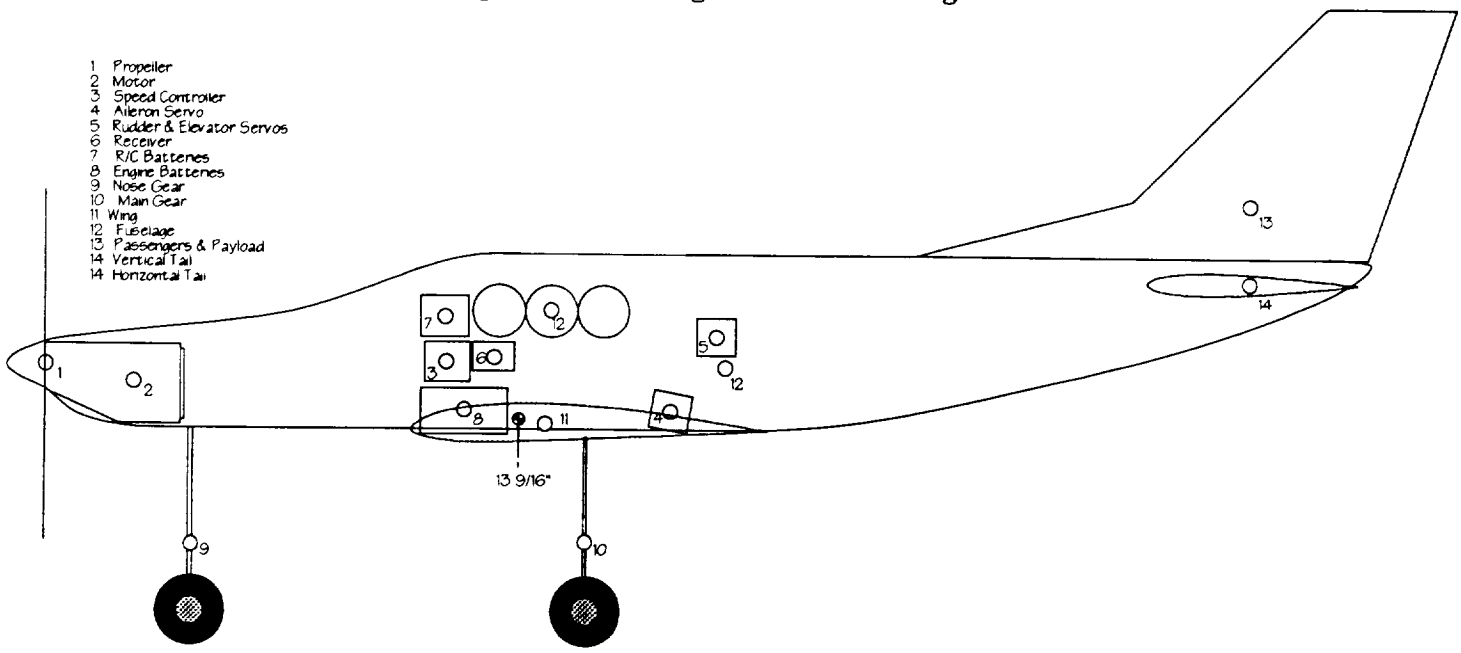

7 STABILITY AND CONTROL

7.1 Requirements and Objectives

Requirements:

1. The stabilator must be able to rotate the airplane at take-off, trim the airplane at cruise and at landing (stall angle), and maintain static stability while in the air.
2. Must execute a steady, level 60-ft-radius turn at 25 ft/sec in order to maneuver in Aeroworld.
3. Must achieve a coordinated turn with the rudder and aileron deflections. The rudder must be able to overcome the adverse yaw created by the ailerons while at a bank angle.

Objectives:

1. Longitudinal static stability must be achieved with static margin > 10%. This is to enable a novice pilot to fly the airplane.
2. Aircraft is to fly at cruise at zero angle of attack with a zero stabilator deflection in order to minimize the drag of the fuselage.
3. The horizontal and vertical tails and their corresponding control control surfaces should be selected as small as possible, as long as they satisfy stability parameters. This is to keep with the design objective of a lightweight aircraft.

Note: All of the equations an methods used for the stability analysis in this airplane design are taken from (Ref. 7.1).

7.2 Longitudinal Stability

The Elite utilized an all-movable tail in order to achieve longitudinal stability and control. This was chosen since it can have a smaller area and still provide the same control power as a conventional tail with an elevator. It also adheres to the design objective of an aesthetically pleasing airplane since its size is proportional to the short fuselage. Past Aeroworld designs had relatively large empennages which looked somewhat awkward on their aircrafts.

The sizing and positioning of the stabilator were initially driven by the need to rotate the airplane at take-off. The stabilator surface area and location were both varied in order to find when they provide a zero moment about the wheel at a certain tail deflection angle. The computer code for this trade study can be found in Appendix C. The location of the wheel was placed as far forward as possible in order to give a large moment arm for the tail. There was a certain restriction on this position since it had to be a minimum distance away from the main fuselage spar so that loads can be distributed when mounting the wing. The resulting graph is presented below in Figure 7.2.1

Figure 7.2.1: L_t vs. Tail Area for Rotation at Take-off

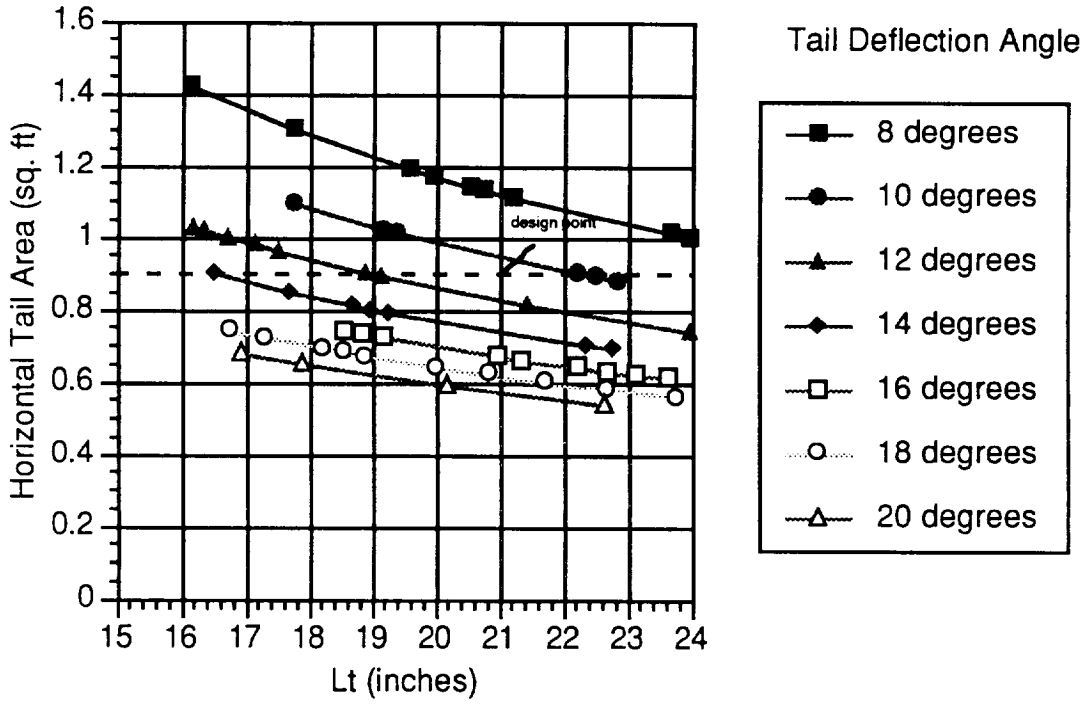

Given a certain horizontal tail location (l_t), Figure 7.2.1 shows the tail area and tail deflection angle that was required in order for the airplane to rotate at take-off. It was decided to set the maximum tail deflection angle to ± 12 degrees, because this was just below the airfoil's stall angle. Also, greater deflections would interfere with the movement of the rudder as well as create possible problems with the avionics necessary to control the tail. Figure 7.2.1 shows that there was a wide range of acceptable combinations. Therefore, additional measures of merit were needed in order to help determine the tail parameters.

The pitching moment curve slope (C_{ma}) measures the longitudinal static stability of the airplane. When an airplane experiences an increase in its angle of attack due to a positive (nose-up) moment, it must be able to create a negative (nose-down) pitching moment which tends to rotate the airplane back to its equilibrium position. In order for this to occur, the C_{ma} slope must be negative:

$$\frac{dC_m}{d\alpha} < 0$$

The wing, fuselage, and horizontal tail all contribute to the pitching moment of the aircraft. The contribution of the fuselage to the pitching moment in previous

Aeroworld airplanes was relatively small. An example of a typical general aviation airplane in (Ref 7.1) also had a negligible fuselage pitching moment. Therefore, since the method for calculating the C_{maf} of the fuselage is tedious and time-consuming, its effect was neglected. This is one aspect of the design that can be improved upon. An accurate estimate of the fuselage pitching moment would help insure the stability of the airplane since the fuselage contributes a destabilizing effect. The wing also produces a destabilizing effect on the aircraft. Therefore, the horizontal tail of *The Elite* must provide a large enough pitching moment to overcome the destabilizing effect of the wing and fuselage.

Static margin is the other measure of merit which was explored. The static margin helps to measure the responsiveness of the airplane. It is defined as the distance between the neutral point (X_{NP}) and the airplane's center of gravity position (X_{cg}), both referenced from the wing's leading edge:

$$\text{Static Margin} = \frac{X_{NP}}{c} - \frac{X_{cg}}{c}$$

The neutral point is the furthest aft location that the center of gravity can be located. A center of gravity beyond the neutral point results in an statistically unstable aircraft.

The static margin is normally between 5 and 10 percent for conventional aircraft. However, for this class of airplanes a slightly larger static margin is desired. This is due to the fact that the pilot is stationed on the ground with limited visual cues resulting in a slower response time than if he were sitting within the aircraft. A larger static margin would make the airplane respond more slowly to control inputs. Thus, a static margin greater than 10% would be desirable for this type of airplane. An experienced RPV pilot may be able to handle an aircraft with a lower static margin, however this airplane was designed for the novice pilot to fly.

The stabilator should then be able to provide a suitable C_{ma} value and a static margin of at least 10 percent while also being able to rotate at take-off. A computer code was written to observe the effects of the tail size and location on the pitching moment and static margin values. The resulting graph can be seen in Figure 7.2.2.

A typical general aviation aircraft (Ref 7.1) has a C_{ma} of -0.68 rad^{-1}. From Figure 7.2.2, the smallest tail area and shortest location possible were chosen which would still give a static margin of at least 10 % and a sufficient C_{ma} value. A smaller tail will provide less weight in raw materials and help with reducing the drag. It also satisfies the design objective of an aesthetically pleasing airplane. A significantly large tail will make the airplane look awkward and dissuade potential buyers. As long as the airplane maintains sufficient handling qualities, a smaller tail should not present a problem.

Because of these reasons, a tail area of 0.9 ft^2 and a location of 21 inches behind the center of gravity was chosen. This provides the airplane with a C_{ma} value of -0.485 rad^{-1} and a static margin of 10.5 %. The C_{ma} value was comparable with (Ref 7.1) and other past Aeroworld aircraft. The all-moveable tail was given a sweep angle so that it could maintain its aesthetically pleasing appearance. The angle was arbitrarily chosen to be 15 degrees.

Figure 7.2.2: Variation of Static Margin and C_{ma}

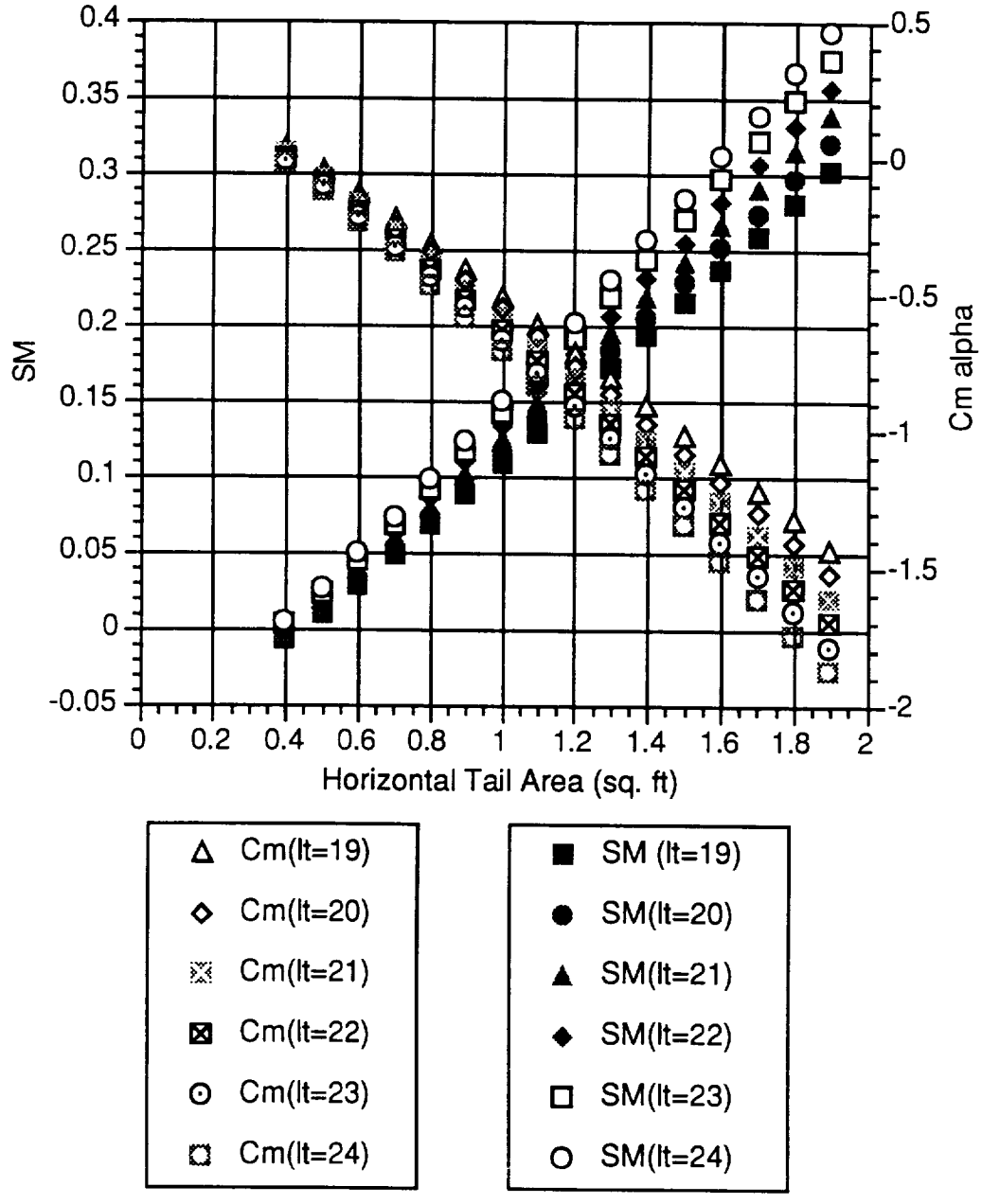

The following is a table summarizing the design values for longitudinal stability:

Table 7.2.1: Longitudinal Stability Parameters

Horizontal Tail Area (S_H)	0.9 ft^2
S_H / S	0.14
V_H	0.30
mean chord, c	6 inches
span, b	21.6 inches
AR tail	3.6
Moment arm (lt)	21 inches
Tail incidence (i_t)	-2.0 degrees
Static Margin	10.5 %
X_{NP}	40.5 %
C_{ma}	-0.485 rad^{-1}

The tail and wing incidence angles were selected in order to enable the airplane to be trimmed at cruise with a zero wing angle of attack and a zero tail deflection. This would make the drag of the airplane at cruise as small as possible since it eliminates any unnecessary drag due to the fuselage at angles of attack. The incident angles necessary to accomplish this were, $i_w = 0.85$ degrees and $i_t = -2.0$ degrees. The pitching moment of the airplane as a function of the angle of attack is presented in Figure 7.2.3 below.

It was evident from Figure 7.2.3 that the wing pitching moment curve had a positive slope, and was therefore unstable. The C_{mo} of the airplane must be a positive value in order for the airplane to trim at positive angles of attack. The C_{mo} of the wing had a negative value. Therefore, the tail must have a large enough C_{mo} to counteract the wing's effect. The results can be seen in Figure 7.2.3.

Figure 7.2.3: Pitching Moment Coefficient vs. alpha

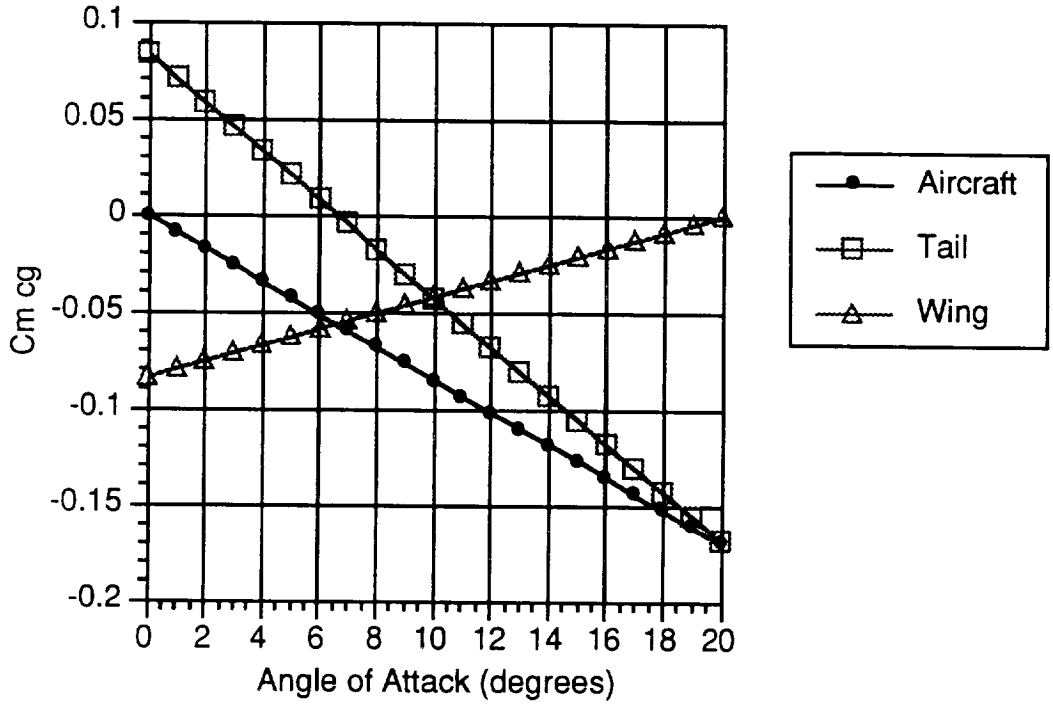

The Elite, was designed to fly at cruise with a zero angle of attack of the fuselage. The drag on the fuselage is least when the fuselage was at 0° angle of attack. Mounting the wing at the incidence angle equal to the angle of attack needed for cruise thereby minimizes the aircraft's drag. Placing the wing at a particular incidence is a difficult task because of all the imprecision involved. However, for *The Elite*, the incidence angle was small (less than 1°), so mounting the wing should not pose a problem. For this configuration, the pitching moment should be zero (the aircraft is trimmed) at an a of zero degrees. Figure 7.2.3 shows that this is indeed the case. The equation of the pitching moment curve is :

$$C_m = 0.001 - .009*a$$

where a is in degrees.

The movement of the center of gravity is very small when the passengers and payload are removed. They only make up 1.0 % of the weight and thus do no affect the c.g. location to any extreme. The resulting shift in the center of gravity position is presented in Figure 7.2.4. The two curves are very similar. Even at the forward c.g. position, the airplane will be able to trim at cruise at essentially a zero angle of attack. As long as the c.g stays in front of the neutral point the airplane will remain statistically stable and will be able to trim at positive angles of attack. This requirement did not seem

to pose any problems.

Figure 7.2.4: Pitching Moment Coefficient for Aft and Forward C.G.

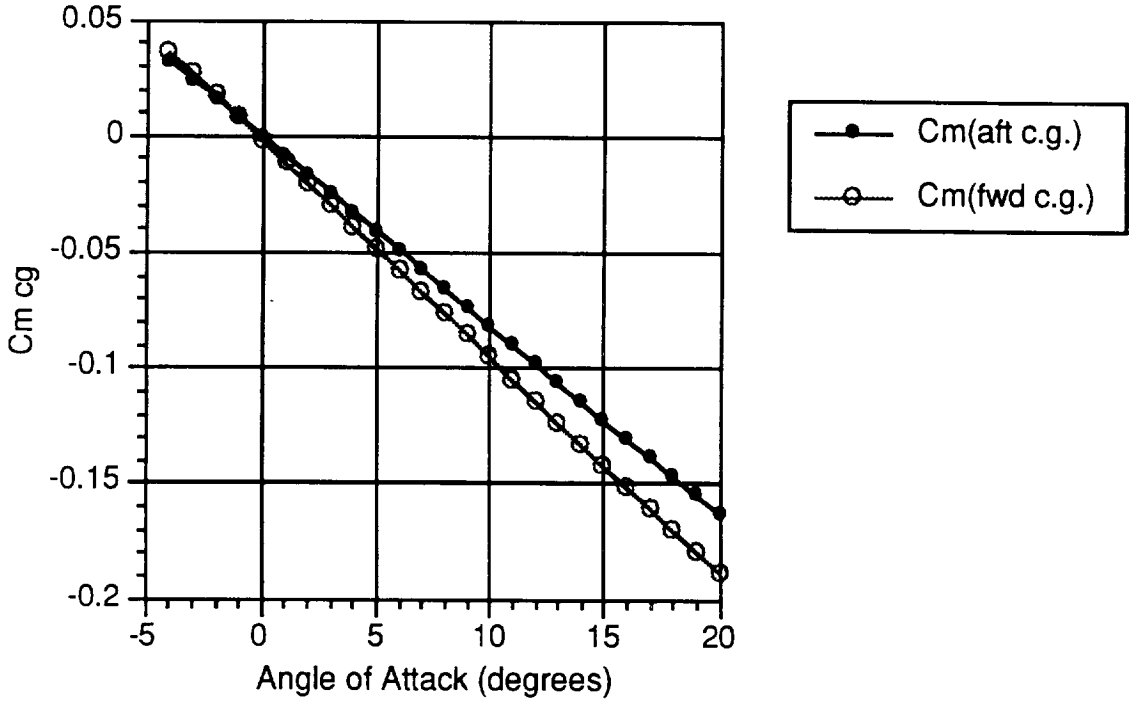

7.3 Longitudinal Control:

The control mechanism of The *Elite* was the same as the horizontal tail since it utilized an all-moveable tail. It has already been observed that the tail provides enough control in order to rotate the airplane at take-off. It remains to be seen whether the stabilator will be able to trim the airplane at various flight conditions while in the air and at landing. Figure 7.3.1 shows the different trim condition of the aircraft at angles of attack from 0 to 20 degrees. The airplane will stall at an angle of attack just over 12 degrees.

Figure 7.3.1: Effect of Tail Deflection on Pitching Moment

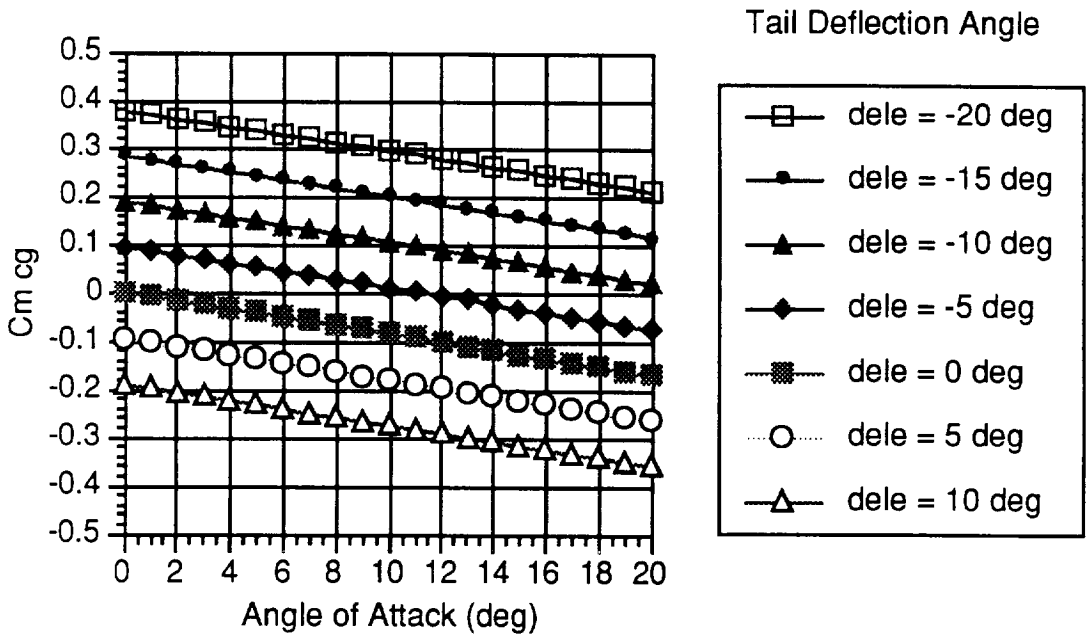

Figure 7.3.1 shows that *The Elite* could be trimmed at a wide range of angles of attack with minimal tail deflection angles. This enabled the airplane to remain at equilibrium while in flight. When the airplane is landing, it will have an extreme angle of attack close to the stall angle of 12.3 degrees. The stabilator must be able to provide a sufficient pitching moment to trim the airplane with a maximum deflection angle of 12 degrees. Deflection greater than this value were undesirable because the tail will stall at a slightly higher angle. Since it was an all moveable tail, it will have significant control power and a deflection of 12 degrees should be sufficient to trim. The procedure for determining longitudinal control (Ref. 7.1) was simplified since there was an all-moveable tail. For this case, the effective elevator area was the same as the horizontal tail area. The flap effectiveness parameter (t) therefore would simply be set equal to one. Setting, the a of the airplane at 12.3 degrees and the C_m equal to zero, the corresponding d of the tail could be determined. The tail must deflect an angle of d = -6.2 degrees in order to trim at landing. This was well within its range of ± 12 degrees and can thus trim at landing. Similar results can be obtained directly by using Figure 7.3.1.

In Figure 7.3.1, the effect of the stabilator deflection angle on the pitching moment curve was observed. As the tail was given a positive deflection angle (deflected leading-edge up), the pitching moment curve shifted downward. This was because a positive deflection would cause a pitch-down moment on the aircraft. A negative deflection caused the opposite to be true.

Table 7.3.1: Characteristics of Stabilator

d_e (landing)	-6.2 degrees
C_{mde}	-.218 rad^{-1}
Se / St	1.0
$d_{e\,max}$	± 12°

7.4 Directional and Lateral Stability:

Directional stability was necessary in order to return the airplane to an equilibrium condition when subjected to a form of yawing disturbance such as sideslip. The requirement for directional stability was for $C_{nb} > 0$. The contribution of the fuselage and the wing to the directional stability was determined by way of the equations and graph in (Ref. 7.1). The fuselage and wing create a destabilizing effect on the directional stability. The tail position (l_v) was set equal to the horizontal tail location (l_t). The tail area was then varied over a range from 0.2 to 1.0 ft^2 and the different C_{nb} values were observed. An area of 0.3 ft^2 was chosen which gives a vertical tail volume ratio of 0.011 and a C_{nb} of 0.025. This is a compatible C_{nb} value when compared to past Aeroworld airplanes. This area was chosen also based on rudder requirements which will be discussed in section 7.6. There were many uncertainties when calculating the contribution of the fuselage and the wing. They may in actuality contribute more of a destabilizing effect. Therefore, a large vertical tail was used in order to ensure directional stability. The sizing of the vertical tail was re-affirmed when determining the rudder size in the section on directional control.

The lateral or roll stability of the airplane was what enabled it to create a restoring moment when disturbed from a wings-level attitude. For roll stability, the coefficient of the roll moment due to the sideslip should be less than zero ($C_{lb} < 0$). Since *The Elite* used ailerons for the turning of the airplane, dihedral was needed only to insure the lateral stability and not turn the aircraft. Therefore, a dihedral angle of 5 degrees was chosen for this airplane design. This angle gives a C_{lb} of -0.104. A table of the aircraft stability coefficients are shown in Table 7.4.1.

Table 7.4.1: Directional and Lateral Stability Parameters

S_v	0.3 ft^2
V_v	0.012
S_v / S	0.046
mean chord	6 inches
Span	7.2 inches
AR_v	1.2
C_{nb}	0.025 rad^{-1}
Wing Dihedral G	5.0 degrees
C_{lb}	-0.104 rad^{-1}

7.5 Lateral Control

Lateral Control would be achieved by the deflection of ailerons. The size and location of the ailerons were determined using the steady state roll equations (Ref. 7.1, Eq. 5.2):

$$\dot{p} = L_p p + L_{\delta_a} \delta_a$$

$$\left(\frac{pb}{2v}\right) = -\frac{C_{l_{\delta_a}} \delta_a}{C_{l_p}}$$

The aileron control power is a function of the span, chord, and location of the ailerons (Ref. 7.1, Eq. 2.97):

$$C_{l_{\delta_a}} = \frac{2C_{L_{\alpha w}} \tau}{Sb} \int_{y_1}^{y_2} cydy$$

Note that these equations were included in this report to make clear the method used in determining the roll control of the airplane. The velocity was taken as 28 feet/second to meet the requirement of making the turn in under 30 feet/second and to ensure some margin above the stall speed of 25 feet/second. The maximum aileron deflection angle was set at 15 degrees. The flap effectiveness parameter, t, was found for aileron chord lengths of 1, 1.25, 1.5, 1.75 and 2 inches. At each of these chord lengths, the roll rate was computed for various aileron spans and wing locations.

It was found that a 0.25 inch increase in the chord length would give approximately a 10% increase in the roll rate produced for a given span and location. Also, a 0.5 feet increase in the span of the aileron for a given chord length increases the roll rate by 25%-30%. (Ref.7.2) suggested that the best way to increase aileron control is

to increase the aileron span rather than increase the aileron chord because increasing the chord increases the effectiveness only slightly but greatly increases the loads placed on the servo. These additional loads may cause the control rods to bend or the aircraft's structure to be slightly distorted. Also the chord should not be so small that the aileron effectiveness is lost. Thus the aileron chord length was set at 1.5 inches.

A plot of the roll rate versus different aileron spans and locations with a chord length of 1.5 inches is found in Figure 7.5.1. Note that the roll rate was a maximum with the inboard edge of the aileron closest to the fuselage and with the outboard edge closest to the wing tips. However, a roll rate of 40 or 50 degrees/second is not desirable because this would be too fast a roll for this type of aircraft. Based on the aircraft's load factor while turning, and a 50 feet turning radius at a velocity of 28 ft/sec, the expected bank angle was between 25 and 29 degrees. To achieve this bank angle in 1.5 seconds, the required roll rate was 16-20 degrees/second. Thus it was desired that the ailerons produce a roll rate of at least 20 degrees/second.

Figure 7.5.1: Inboard and Outboard Location vs. Roll Rate

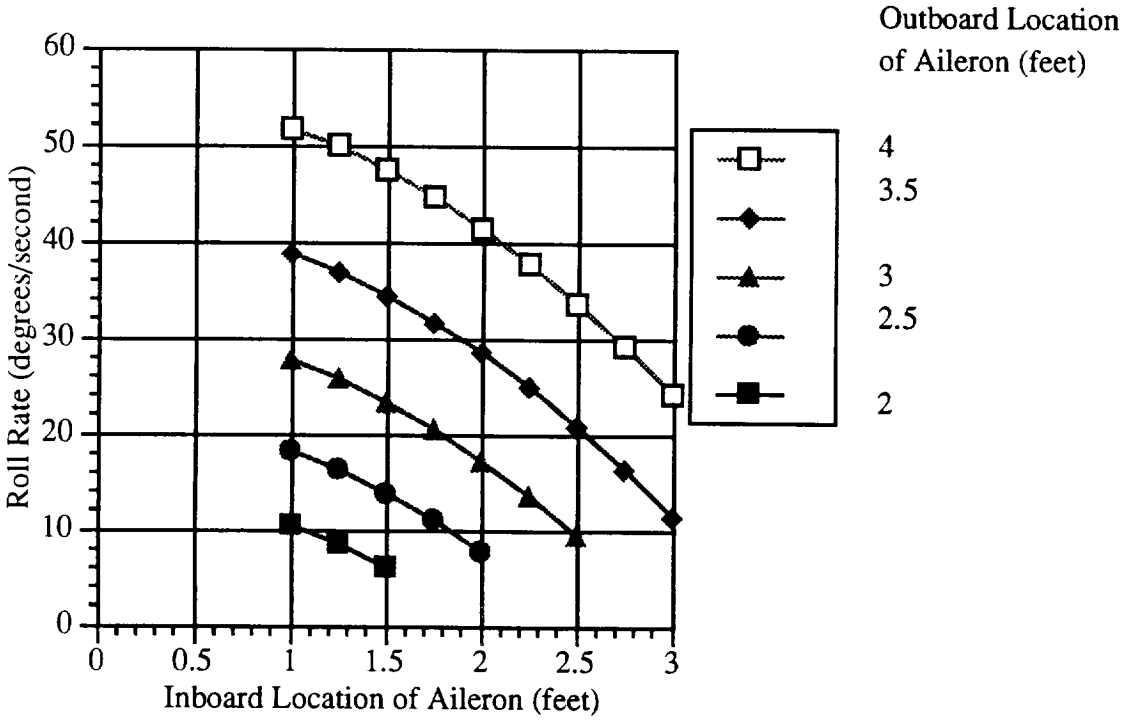

The manufacturing team suggested that the ailerons run as close inboard as possible so that the control wire would not have to be run very far out along the wing. Also, (Ref. 7.3) suggested that the ailerons be placed two-thirds to three-fourths of the

way out along the wing for maximum effectiveness. This placement considered the possibility of a tip stall condition, whereby the wing tip would stall before the root. By placing the ailerons approximately two-thirds of the way out along the wing, neither tip stall nor root stall was favored. Thus, if either the root or the tip does stall, there will still be a substantial portion of the aileron in the freestream to sustain its effectiveness. Thus, the inboard location of the aileron was chosen as 1.75 feet and the outboard location was chosen as 3 feet to give a roll rate of 20.5 degrees/second.

One weakness of the ailerons was that at low speeds and on airplanes with large spans, induced drag was dominant. The ailerons tend to produce "adverse yaw", or yaw due to the down-going aileron producing more drag than the up-going aileron. This tendency of the ailerons to pull the aircraft away from the turn can be countered with simultaneous application of a rudder.

Table 7.5.1: Lateral Control Parameters

y1 (inboard distance)	1.25 ft
y2 (outboard distance)	1.75 ft
Roll rate (p)	20.5 deg/sec
span	1.25 ft
chord	1.5 inches
C_{lda}	0.155

7.6 Directional Control:

The directional control of the aircraft was created by deflecting the rudder on the vertical tail. The size of the rudder was driven by its need to provide a sufficient yawing moment to overcome the adverse yaw created by the ailerons. The control power for the rudder was investigated in Figure 7.6.1 for different rudder sizes and vertical tail sizes.

Figure 7.6.1: Control Surface Area Ratio vs. Control Power

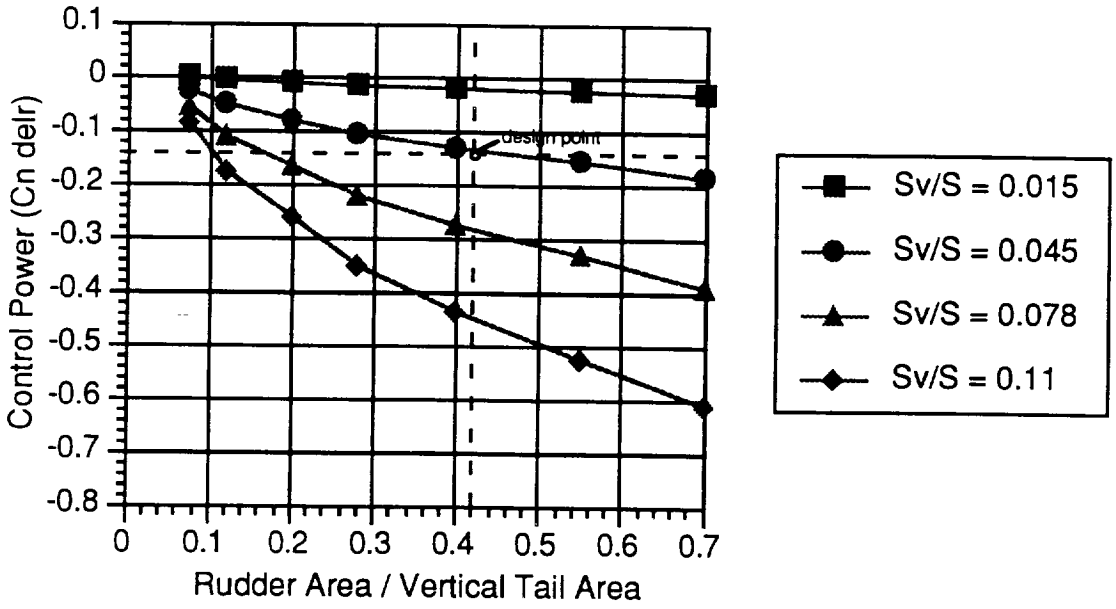

The yawing moment needed to counteract the adverse yaw due to the ailerons was calculated. The necessary counteracting yaw moment of the rudder requires a rudder control power of at least -0.08 rad^{-1} at a maximum deflection angle of ± 15 degrees. The top horizontal dashed line in Figure 7.6.1 shows that no parameters above the line can be considered. This control power results in a minimum ratio of rudder area to vertical tail area of 0.42. This fact can be seen by the vertical dashed line in Figure 7.6.1. Ratios to the left of this line are not valid since the rudder sizes will not provide sufficient yaw moment. When the minimum ratio was chosen, a rudder area of 0.12 ft^2 resulted. The previously chosen vertical tail area of 0.3 ft^2 ($S_v/S = 0.46$) resulted in a sufficient control power for overcoming the adverse yaw, providing a C_{ndr} value of -0.14 rad^{-1}. This value was significantly lower than previous Aeroworld airplanes, however this may be due to the fact that many of them did not have ailerons. The rudder for those airplanes had to have more control power in order to turn the airplane, coupled with the wing dihedral. The control power obtained for this particular aircraft should be quite sufficient.

The minimal vertical tail area was not chosen because of the uncertainties involved. This results in a large vertical tail that does not look like it belongs to this particular airplane design, making the aircraft appear "awkward". This decision goes against the design goal of an aesthetically pleasing airplane, one of the objectives which helped determine the stabilator size. However, the greater uncertainties involved in directional stability and control requires a conservative tail size in order to ensure

stability. This decision seems justified. Clearly, even a good-looking airplane was not worth much if it cannot be controlled.

Table 7.6.1: Directional Control Characteristics

Sr / Sv	0.046
Sr	0.30 ft^2
C_{ndr}	-0.103
d_r max	± 15 degrees

7.7 Control Mechanisms:

The Elite utilizes three different control surfaces: a rudder, an all-moveable tail, and ailerons. The rudder will have a maximum deflection of ± 15 degrees and the all-moveable tail will be able to deflect up to ± 12 degrees. The tail will be mounted at an incidence angle of -2 degrees for zero deflection at cruise condition.

Control will be provided by way of control rods connected to each surface and a series of servos. Plastic control rods will be used due to their simple operation and flexibility. The plastic rods maneuver freely within the nylon tubing, thus allowing smooth movement of the control surfaces. The flexible rods will enable them to be bent around other components such as the batteries.

Each control rod will be connected to the control surface by way of a control horn. The control horns have adjustable connection joints so that the surfaces deflections can be altered. One servo will link the control of both the rudder and the nose gear. The ailerons and horizontal tail will both operate on separate servos. All control rods will be internal to the aircraft in order to help decrease any unnecessary drag.

7.8 References:

7.1 Nelson, Robert C., Flight Stability and Control, New York, McGraw-Hill Book Company, 1989.

7.2 Simons, Martin, Model Airplane Aerodynamics, Great Britain, Argus Books Limited, 1978.

7.3 McCormick, Barnes W., Aerodynamics, Aeronautics, and Flight Mechanics, New York, John Wiley & Sons, 1979.

7.4 Avis, Daniel, Fortran computer code for take-off rotation, February, 1994.

8 AIRCRAFT PERFORMANCE

8.1 Requirements and Objectives

Requirements:

1. capable of a sustained, level 60 foot radius turn at a speed of less than 30 feet/second
2. rough field characteristics
    a. adequate taxi and runway handling characteristics
    b. able to climb to a height of 50 feet within 200 feet of brake release
    c. maximum take-off distance of 60 feet
3. able to fly to nearest alternate airport and loiter for one minute

Objectives:

1. minimum cruise speed of 60 feet/second
2. maximum velocity greater than 80 feet/second
3. sufficient range to service all Aeroworld airports
4. endurance consistent with target range, cruise and loiter speeds
5. maximum take-off distances
    a. rough field, 42 feet
    b. improved runway, 28 feet
6. handling qualities consistent with private/sport recreational aircraft

8.2 Summary of Performance

The upper-class market at which *The Elite* is aimed demands an aircraft that will not only be aesthetically pleasing, but will exhibit a high level of performance for its class of aircraft. The performance requirements outlined in the Design Requirements and Objectives drove the design of *The Elite*. Specifically, the required take-off distance of 28 feet, the cruise velocity of 60 feet/second and a maximum velocity of 80 feet/second were primary drivers in the choice of propulsion system. The desire to service all airports in Aeroworld was also a major concern as was the ability to execute a 60 foot radius turn at 28 feet/second. Table 8.1.1 illustrates the performance specifications of *The Elite*.

Table 8.2.1: Performance Specifications for *The Elite* Aircraft

Speed Performance:	
Cruise Velocity	60 ft/s
Minimum Velocity (Stall Velocity) at WMTO	24.8 ft/s
Maximum Velocity at WMTO	71.71 ft/s
Range and Endurance:	
Maximum Range at WMTO	32900 ft (at V=36.9 ft/s)
Endurance at Maximum Range at WMTO	14.9 minutes
Design Range at WMTO	30500 feet (at V=49.6 ft/s)
Endurance at Design Range (WMTO)	10.3 minutes
Cruise Range at WMTO	27268 ft (at V=60 ft/s)
Endurance at Cruise Range (WMTO)	7.5 minutes
Climb and Glide Performance:	
Maximum Rate of Climb at WMTO	16 ft/s (at V=36.5 ft/s)
Maximum Climb Angle	29.9 degrees (at V=30 ft/s)
Minimum Glide Angle	3.87 degrees
Take-Off Performance:	
Take-Off Distance at WMTO	25.54 ft

8.3 Take-Off Performance

In order to service all of the runways in Aeroworld, the DR&O set a maximum take-off roll on an improved runway at 28 feet. This requirement influenced the choice of the Astro 15 motor combined with a Zingali 10-8 three-blade propeller as the propulsion system. The FORTRAN program TAKEOFF (Ref. 8.1) was used to determine the distance required by *The Elite* to lift-off. The TAKEOFF program, which uses a numerical integration routine to compute take-off roll, indicated that the distance required by the aircraft to take-off was 25.5 feet. This value was determined using pessimistic values of a $C_{l\text{-max}}$ of 1.00, a weight of 4.88 pounds, and a rolling friction coefficient of 0.19. In order to achieve these values, TAKEOFF assumes the aircraft runs its propeller up to maximum rpm and then releases brakes. Since the RPV is not equipped with brakes it is anticipated that the take-off roll will be slightly longer than predicted by the program.

Figure 8.3.1 illustrates the results of an investigation of the dependence of take-off distance upon manufacturing imperfections. Because of the uncertainty in the

maximum coefficient of lift of a manufactured airfoil, the variation of take-off distance with weight and maximum coefficient of lift were investigated. Figure 8.3.1 indicates that a maximum take-off weight of approximately 5.2 pounds is the most the technology demonstrator may weigh to satisfy the take-off distance requirement. This result comes from the belief that it is possible to achieve a maximum coefficient of lift of 0.95 for the airfoil as opposed to the design value of 1.14.

Figure 8.3.1: Effect of Manufacturing Imperfections upon Take-Off Performance

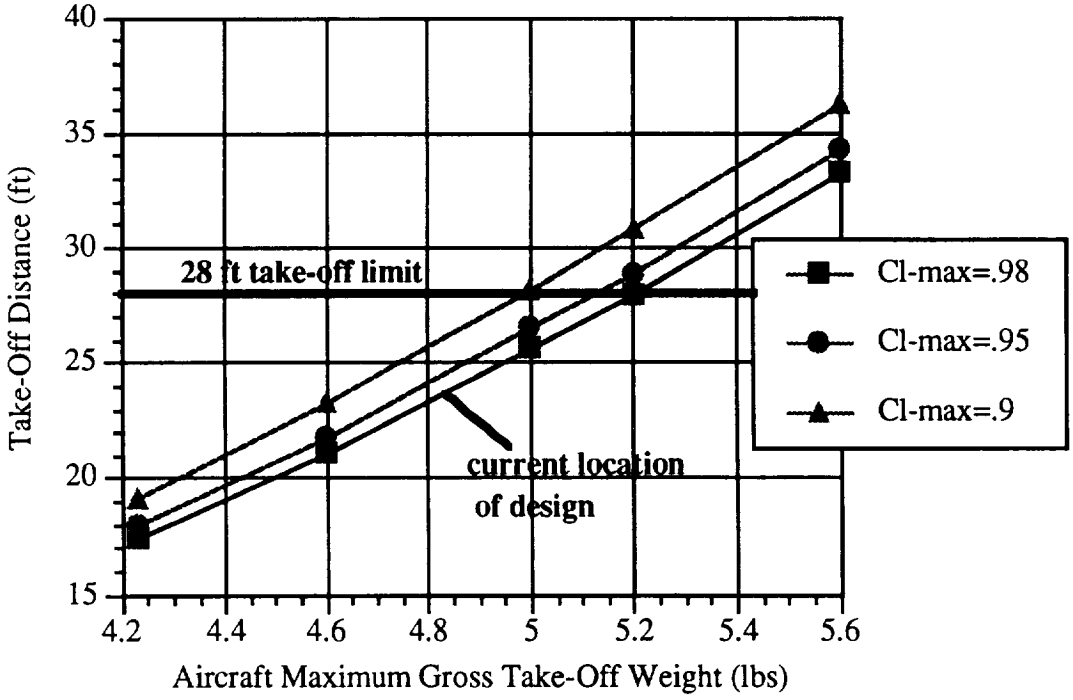

8.4 Range and Endurance

The Design Requirements and Objectives Document specified a range sufficient to service all airports in Aeroworld allowing for diversion to an alternate airfield including a one minute loiter. The range specified in the DR&O was found by determining the distance to each airport and its closest alternate and adding 1 minute of loiter time at a velocity of 30 ft/s. Using this method, a design range of 30500 feet was deemed necessary to serve all airports in Aeroworld. This study used a computer program (Ref 8.2) written to determine range and endurance as a function of velocity. Upon completion of the study it was determined that it was not possible to achieve the range specified in the DR&O at the cruise speed of 60 ft/s with the current propulsion system. A study was then undertaken to determine how much of Aeroworld was

serviceable with a range of 27268 ft at the cruise velocity of 60 ft/s. After examining every possible route (including distances to alternate airstrips and loiter time) in Aeroworld, it was determined that only six routes were not serviceable at a velocity of 60 ft/s. At the design cruise speed of 60 ft/s, *The Elite* can service 94.3% of all possible routes in Aeroworld. The six routes that cannot be serviced at a speed of 60 ft/s can be serviced at a minimum speed of 49.6 ft/s. This compromise was deemed adequate and it was decided not to reduce cruise speed or reconsider the propulsion system.

Figure 8.4.1 illustrates the relationship between range, endurance and velocity at the maximum take-off weight of this aircraft. This figure indicates that the maximum range for *The Elite* is 32900 ft at a speed of 36.9 ft/s. Also indicated on this plot is the location of the maximum endurance and the design range and the cruise range for this aircraft.

Figure 8.4.1: Variation of Range and Endurance with Velocity

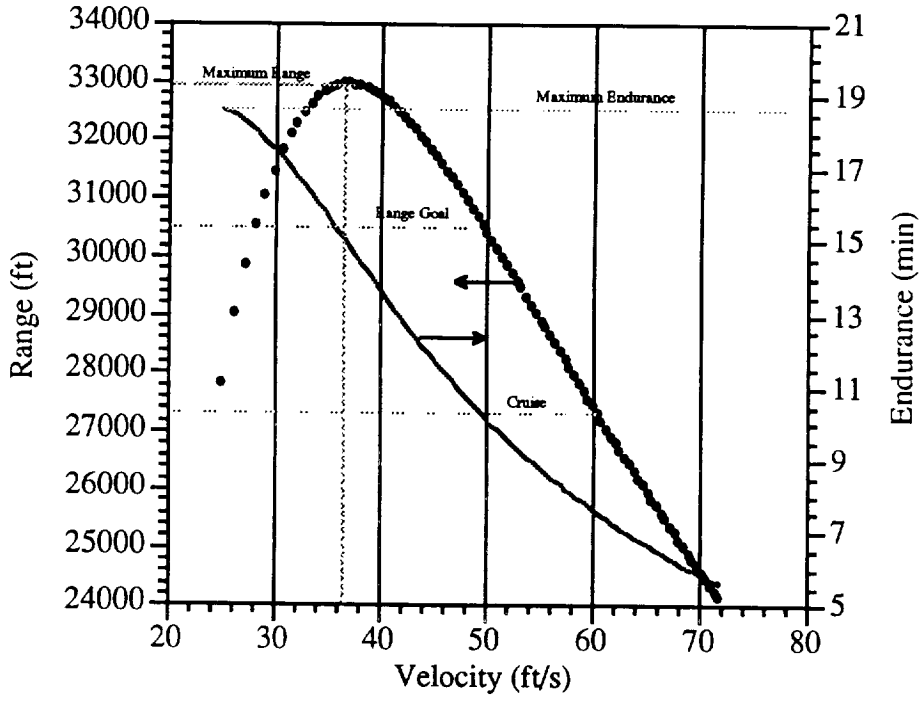

The effect of weight on range was also investigated in Figure 8.4.2. This figure shows the linear dependence of range on weight and the minimal variation of the range for this small general aviation aircraft. This minimal variation is due to the small weight of the payload carried by *The Elite*.

Figure 8.4.2: Dependence of Range and Endurance Upon Payload

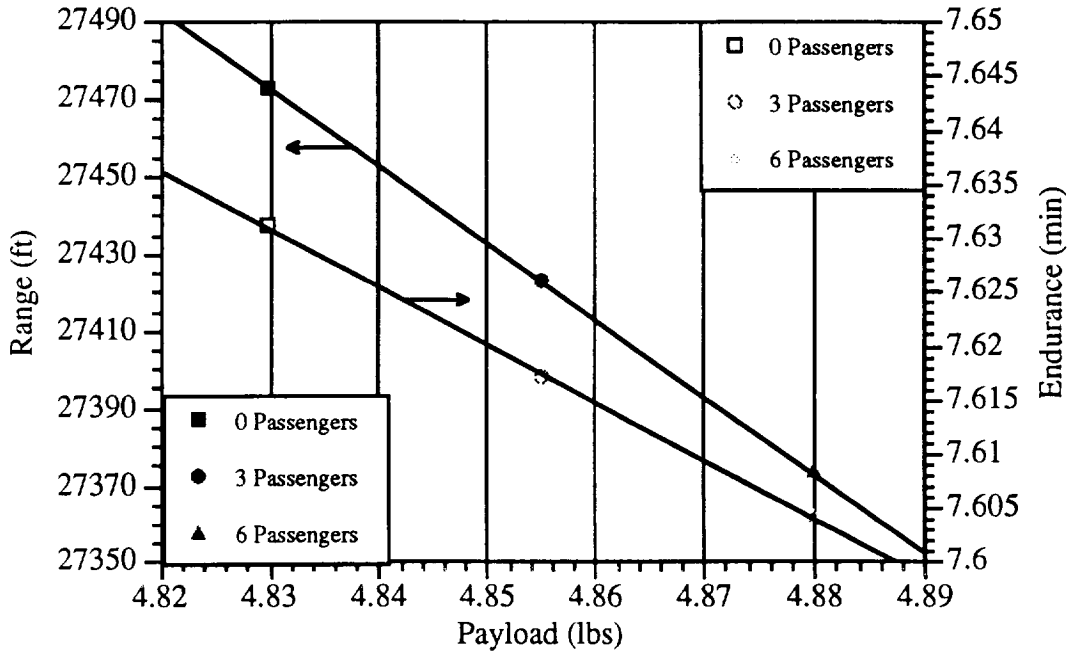

8.5 Power Required and Power Available

Figure 8.5.1 shows the power required and power available curves at varying motor voltage settings obtained using Ref. 8.3. The maximum velocity of 71.7 ft/s is evident at the far right intersection of the power required and power available curves. This velocity is the maximum velocity at which the aircraft may fly and still maintain steady, level flight. Also indicated on the plot is the voltage setting of 12.9 volts necessary to maintain steady cruise and the voltage settings for maximum range (8.0 volts) for the maximum velocity (15.6 volts) and for the velocity necessary to service all Aeroworld routes (10.5 volts). In addition to the higher maximum velocities induced by higher voltage settings, the climbing ability of the aircraft also improves because of the dependence of rate of climb on the difference between power available and power required at specific velocities.

Figure 8.5.1: Power Required and Power Available Curves

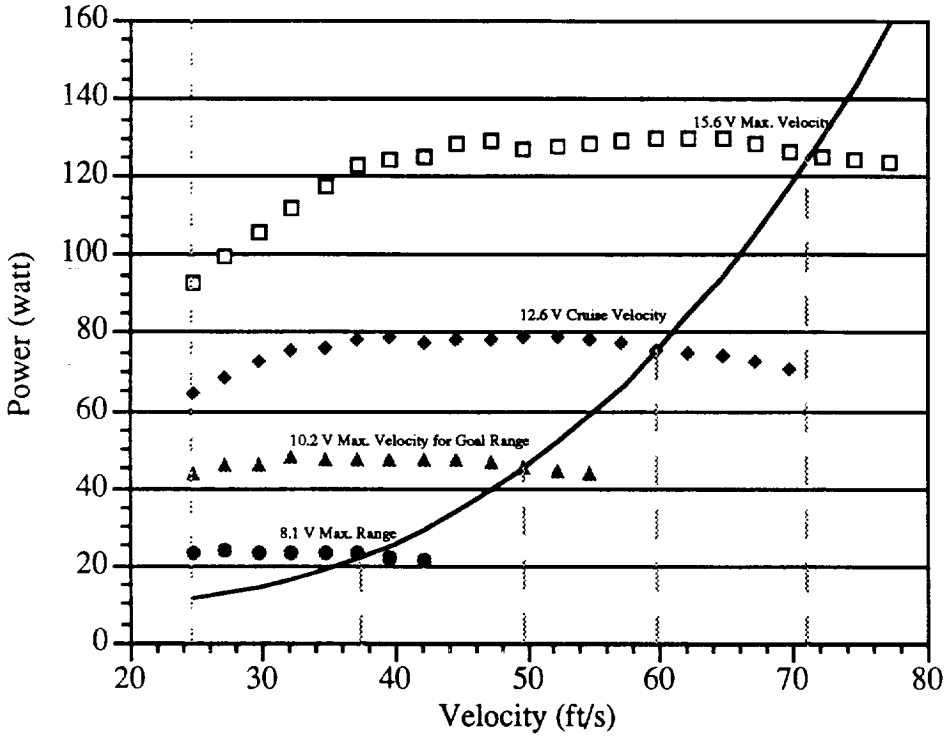

8.6 Climb and Gliding Performance

Using the power available and power required curves acquired in the previous section the rate of climb for the aircraft was determined by simply taking the difference between the power curves and then dividing by the weight of the aircraft (Ref 8.4). Using this method, the maximum rate of climb for *The Elite* was determined to be 16 ft/s at a velocity of 36.5 ft/s. This velocity is slightly greater than the take-off velocity meaning that the aircraft will be flying at or close to the maximum rate of climb in the portion of the flight regime where good climbing ability is necessary. Assuming a cruising altitude of 25 feet and a climb-out angle of 23.67 degrees at the maximum rate of climb *The Elite* will reach the cruising altitude of 25 feet in 1.6 seconds while covering a ground distance of 57 feet. Including the ground roll distance, this allows the aircraft to be in cruise approximately 67 feet before encountering the first turn in the Loftus Center. This rate of climb also ensured that the aircraft would be able to satisfy the design requirement of being able to climb to an altitude of 50 feet within 200 feet of brake release. Assuming a take-off roll of the design objective length of 42 feet and a maximum rate of climb, the aircraft would be able to climb to a height of 50 feet within 156 feet of brake release

satisfying this design requirement.

Examining the glide performance of *The Elite* simply involved knowledge of the maximum lift-to-drag ratio of the aircraft (Ref 8.5). By inverting the maximum lift-to-drag ratio and taking the arctangent of the result, the minimum glide angle was obtained. This method resulted in a minimum glide angle of 3.87 degrees. This value is important in an engine out scenario. If the single engine of *The Elite* were to fail, a gentle glide slope was desirable to ensure a safe landing. If, perhaps, the engine were to shut down at an altitude of 25 feet, at the minimum glide-slope the RPV will cover 370 feet at the minimum glide angle before touching down.

8.7 Turn Performance

The Elite is required to perform a 60 foot radius turn at a speed of less than 30 ft/s as specified in the DR&O. In order to satisfy that requirement, the aircraft will have to bank an angle of 23.9 degrees and make the turn at a speed of 28 ft/s. Using the formulas supplied by Ref 8.6 the radius determined for the turn was 55 ft and the g-factor was found to be 1.1g. A maximum bank angle of 70 degrees was found using a maximum load factor of 3 as provided by the structural design of *The Elite*. This maximum bank angle results in a turn radius of 41 feet at the cruise speed of 60 ft/s.

8.8 References

8.1 Batill, Dr. Stephen. TAKEOFF FORTRAN program. Department of Aerospace and Mechanical Engineering, The University of Notre Dame, 1994.

8.2 Le, Tuan. A FORTRAN program to compute range and endurance, 1994.

8.3 Batill, Dr. Stephen. PAVAIL FORTRAN program. Department of Aerospace and Mechanical Engineering, The University of Notre Dame, 1994.

8.4 McCormick, Barnes W. Aerodynamics, Aeronautics and Flight Mechanics. New York: John Wiley and Sons Inc., 1979. p. 432.

8.5 Jumper, Dr. Eric J. "AE441 - Flight Mechanics/Intro to Design Class Notes - Aircraft Performance." Department of Aerospace and Mechanical Engineering, The University of Notre Dame, 1993.

8.6 Jumper, Dr. Eric J. "AE441 - Flight Mechanics/Intro to Design Class Notes - Turn Performance." Department of Aerospace and Mechanical Engineering, The University of Notre Dame, 1993.

9 STRUCTURAL DETAIL DESIGN

9.1 Requirements and Objectives

Design Requirements:

1. Fuselage must contain 6 passengers and avionics.
2. Structure must be designed so as to ensure the survivability of passengers and radio components in a crash from any flight condition.
3. Structure must allow for easy access to avionics and propulsion system so that complete system installation can be accomplished in no more than 20 minutes.
4. All propulsion system batteries must be placed in the main wing carry-through structure.

Design Objectives:

1. A lightweight structure of less than 4.88 lbs so as achieve performance objectives.
2. An aerodynamically efficient aircraft with aesthetic appeal so as to be marketable in the higher end of the general aviation market.
3. A structure capable of withstanding flight load factors of no greater than 3.0 and no less than -2.0 and ground loadings of up to 3.0 G's with a factor of safety no less than 1.5.
4. Readily accessible avionics and propulsion system components allowing installation in less than 20 minutes.

9.2 Main Wing Spar Design

To determine the best structural design for the wing, an extensive trade study was performed on six different balsa spar configurations for the cross section of the wing. The loads used in this test subjected the wing to three times the landing load distribution and at the same time put three times the weight of the aircraft on the main gear. This should provide a worst case scenario that will not be experienced in the operation of the aircraft. The shear and bending moment graphs associated with this loading configuration are shown in Figure 9.2.1.

The cross section was idealized into four lumped normal stress carrying booms and four shear panels (see Figure 9.2.2). Table 9.2.1 presents a summary of the analyzed configurations. One thing to note is that the fifth and sixth configurations use graphite tape on the bottom main spar. The modulus of elasticity of the tape enforced spar was 11,000,000 lb/in^2 versus the un-enforced spar 800,000 lb/in^2. In effect, this stiffens the total beam against a tip up deflection.

Figure 9.2.1: Limit Loading of Wing a) shear b) moment

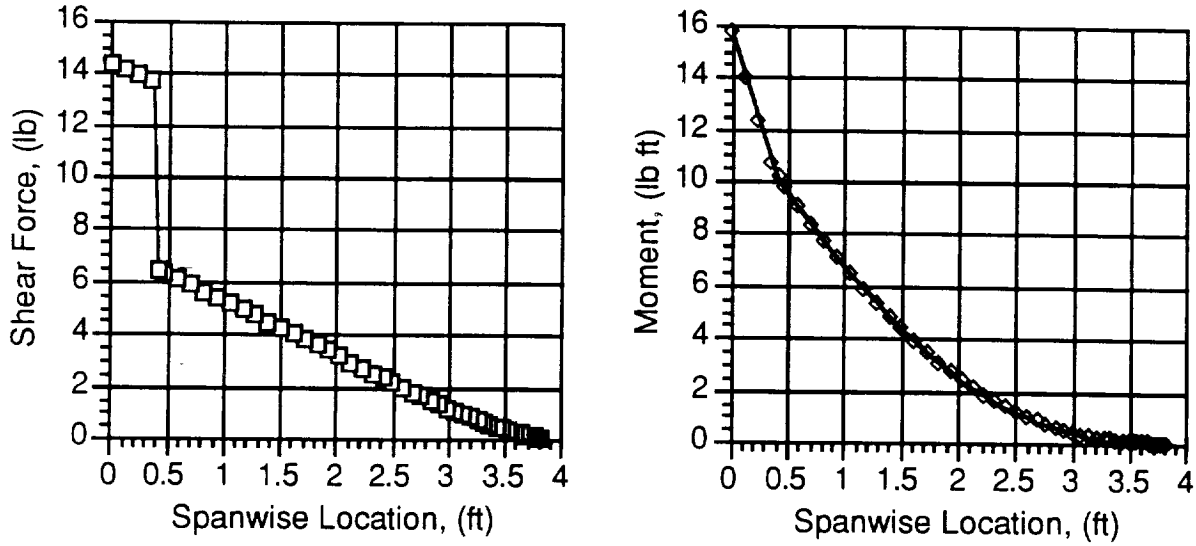

a) b)

Figures 9.2.1 a) and b) show the shear and bending moment diagrams for the wing in the limit load configuration previously described. The jump in the shear diagram is due to the landing gear loads placed 4.5 inches from the root.

Figure 9.2.2: Idealized Cross-Section

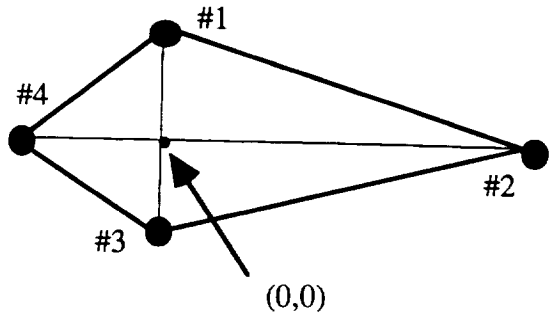

Table 9.2.1: Idealized Cross-Section Coordinates and Dimensions

lump #	z-loc (in)	y-loc (in)	Different Tested Configurations--Spar Areas (in^2) 1	2	3	4	* 5	* 6
1	0.0	0.6875	0.03125	0.0469	0.0625	0.0625	0.03125	0.0469
2	-6.578	0.0625	0.03125	0.03125	0.03125	0.03125	0.03125	0.03125
3	0.0	-0.3125	0.03125	0.0469	0.03125	0.0625	0.0391	0.0391
4	2.547	0.0	0.0352	0.0352	0.0352	0.0352	0.0352	0.0352

The trade study was performed with a code that Jonathan Fay wrote for AE346-Aircraft Structures. The code was validated in that class. The trade study attempted to find the configuration with the lowest weight, highest stiffness, and lowest stress. The weight of each design was calculated from the total volume of the main wing spars multiplied by an average density of balsa. The stiffness of the beam was evaluated on the basis of how far the tip would deflect under a constant load distribution.

$$\delta_{tip} = \frac{wL^4}{8EI} \text{ (ref. 2)}$$

Finally, the stress in each lump was outputted from the computer code under the loading conditions described above. These three factors were combined into a single figure of merit, Z, based on their relative importance to the design. The weight of the design received a weighting of 3 while the tip deflection received a weighting of 1.5 and the stress in the #1 lump received a weighting of 1. The result of this study is shown graphically in Figure 9.2.3.

Figure 9.2.3: Comparison of Tested Cross-Sections

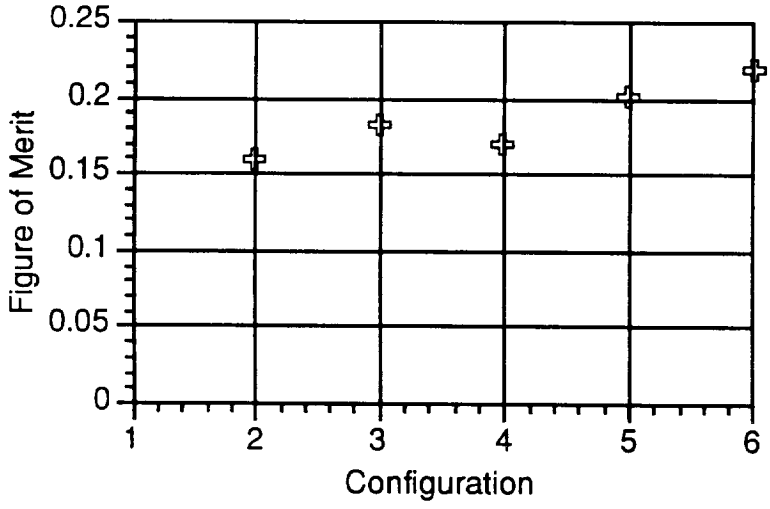

* These two analyzed cross-sections contain a strip of graphite re-enforcing tape along the length of the third lump (i.e. the bottom main spar).

where the Figure of Merit, Z,

$$Z = \frac{1}{3 \times \text{Weight} + 1.5 \times \text{Tip Deflection} + \text{Stress in \#1 lump} / (-4000)}$$

Since it is desirable to have the lowest possible weight, with the smallest tip deflection, and lowest stress, the best design is represented by the maximum value of the figure of merit. Thus the sixth configuration was chosen as the design for the wing.

9.3 Main Wing Rib Spacing

A trade study was conducted to determine the proper rib spacing for the wing. To save on structural weight, it is desirable to space the ribs as far apart as possible . Two main factors played a role in determining the final value of 4" for the rib spacing. The first major factor in determining the rib spacing was the shaping of the monokote. There is a point when the monokote sags between the ribs enough to hurt the wing performance aerodynamically. By examining past years wings, 4" was found to be the largest value at which a reasonably consistent airfoil shape can be maintained.

The second factor was the buckling of the wing spars. The ribs must be close enough together to prevent the main wing spars from buckling under the worst case scenario loads. The buckling characteristic of the spars was determined using the a pinned end approximation in conjunction with the stress analysis output by the computer code. From reference 2, the buckling length of a rod pinned at both ends is given by:

$$L_{buckle} = n\pi\sqrt{\frac{EI}{P}} \text{ (ref 2)}$$

P is the applied force to the end of the rod. To determine the value of P, the normal stress in each spar given by the computer code was multiplied by the spar's cross-sectional area. To prevent buckling under the worst case scenario loading conditions, the ribs would have to be spaced 1.5" apart at the sections near the wing root. This was an unacceptable solution because it added too much weight to the aircraft. Ideally, a spacing of 4" would be used since that is the largest value possible due to aerodynamic (wing shaping) concerns. To solve the buckling problem, some balsa webbing was added to the inboard four sections of the wing. The webbing effectively increases the mode of buckling (n in the above equation) that the spars would undergo, thus increasing the length at which buckling would occur. The final webbing configuration to prevent buckling at the limit loads with a 4" rib spacing is shown below. The inboard most section has a full sheet of 1/16" balsa running across the main spars. The next three sections of the wing use 3/16" square balsa pegs as the webbing.

Figure 9.3.1: Webbing Between Main Spars (Wing Front View)

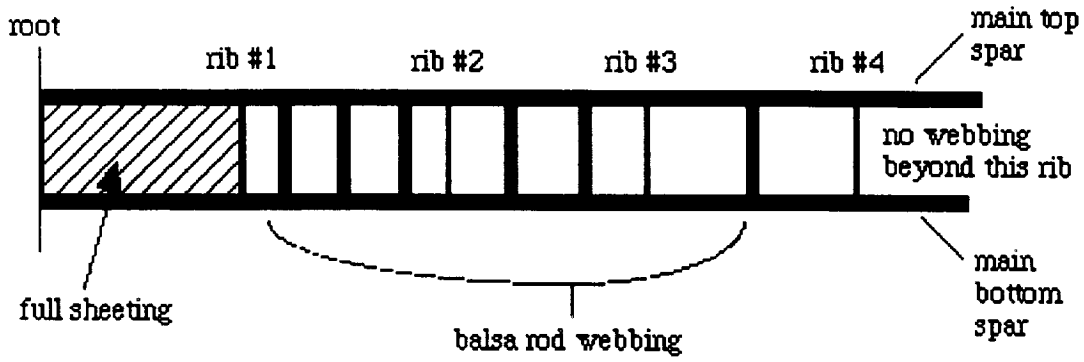

9.4 Fuselage Structural Design

The primary design objectives for the fuselage design were low weight, low drag, aesthetics, strength, and system access. After consideration of the initial concepts, a rounded fuselage composed of longerons and bulkheads was chosen because it satisfied each of the above.

Of primary concern were the sizes of the longerons and the bulkheads. Two studies were conducted, the first of which determined the dimensions of the longerons needed to provide the necessary strength while minimizing the weight. The software developed to conduct the wing structure analysis was modified to model the fuselage as a right circular cylinder with a 4" diameter (the average diameter of the tapered fuselage) formed by four longerons (see Figure 9.4.1). Though spruce and basswood were considered initially, balsa proved to be more than adequate to withstand the loads while minimizing the weight, a primary design concern. Figure 9.4.2 depicts the idealized cross section composed of four lumped booms and shear panels. Table 9.4.1 lists the three configurations examined under flight loads during cruise and ground loads during landing (see Figures 9.4.3 and 9.4.4).

Figure 9.4.1: Fuselage Model for Stress Analysis

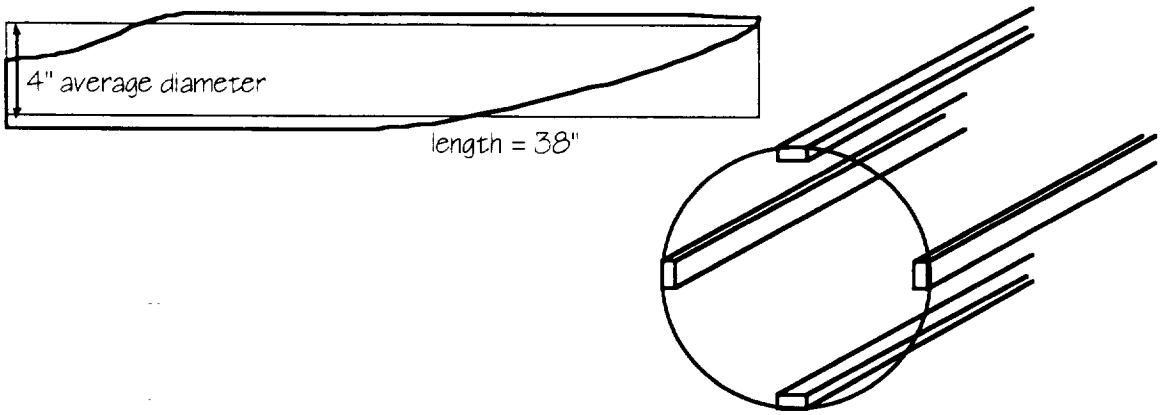

Figure 9.4.2: Idealized Cross-Section

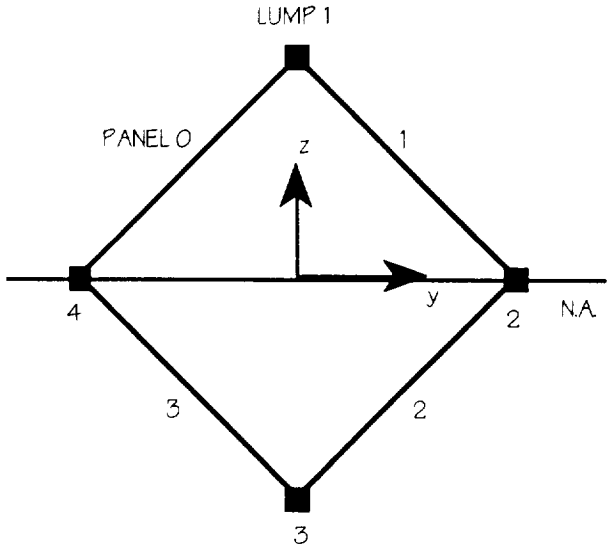

Table 9.4.1: Idealized Cross-Section Coordinates and Dimensions

lump #	z-loc (in)	y-loc (in)	Configuration--Longeron Dimensions (in) 1	2	3
1	2.0	0.0	1/4 x 1/8	1/4 x 3/16	1/4 x 1/4
2	0.0	2.0	1/4 x 1/8	1/4 x 3/16	1/4 x 1/4
3	-2.0	0.0	1/4 x 1/8	1/4 x 3/16	1/4 x 1/4
4	0.0	-2.0	1/4 x 1/8	1/4 x 3/16	1/4 x 1/4

Figure 9.4.3: Fuselage Ground Loading a) shear b) bending moment

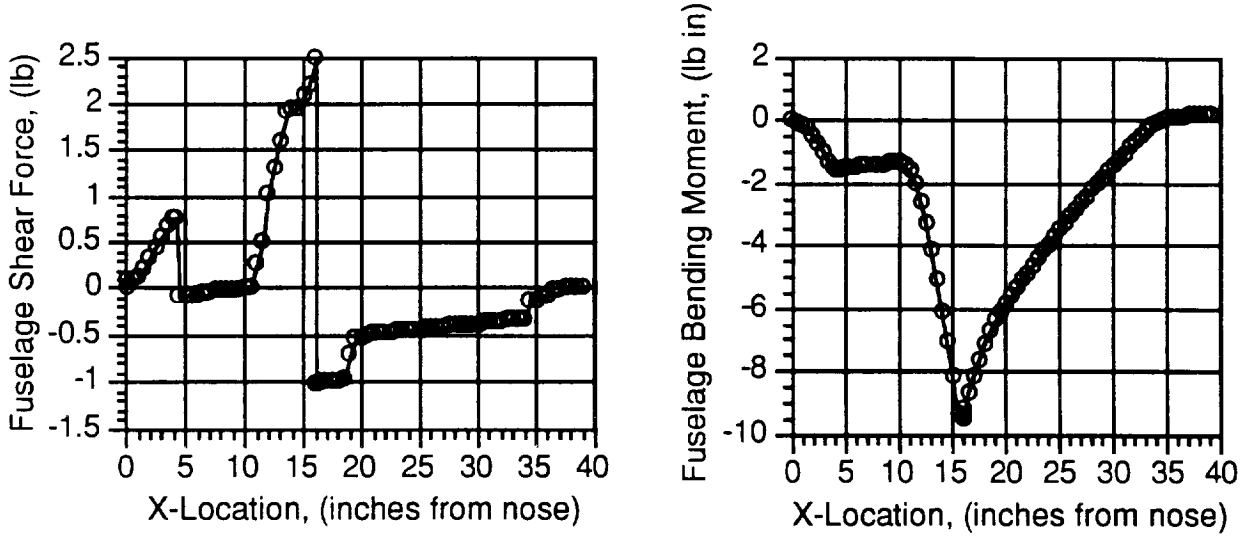

a) b)

Figure 9.4.4: Fuselage Loading at Cruise a) shear b) bending moment

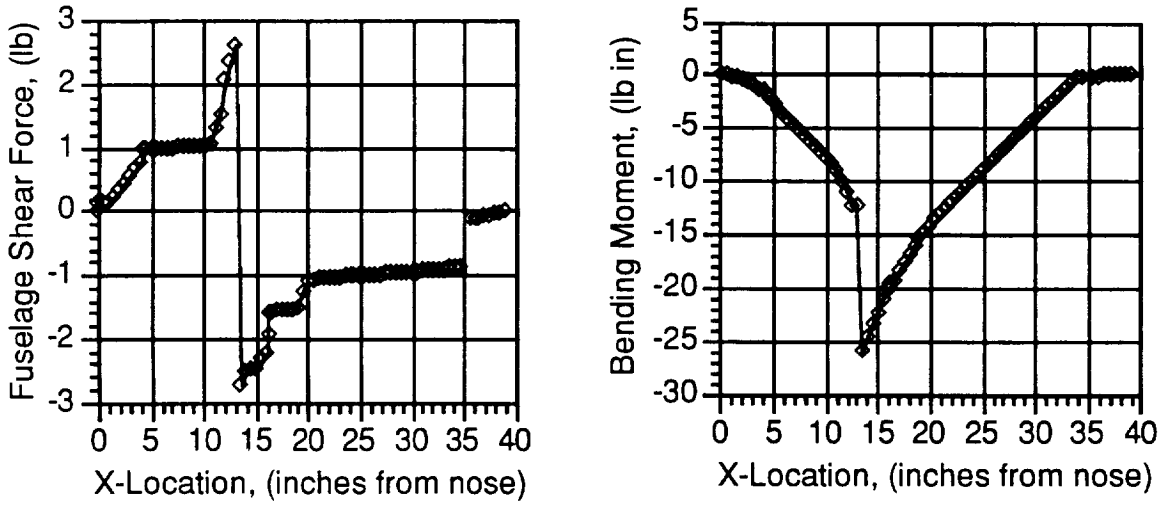

a) b)

The shear diagrams were obtained by discretely integrating the weight of the aircraft from the nose to the tail and including the point loads due to the gear and the lifting surfaces. Similarly, the moment diagrams were calculated by discretely integrating the shear along the length of the aircraft. One thing to note is that the moment charts were extremely sensitive to the placement of the major forces. Even a relatively small (0.5 in) movement in the landing gear or lift forces would prevent the moment diagrams from returning to zero at the tail. Once these loading distributions were known,

the resulting stresses in the longerons could be calculated so as to select the minimum longeron size which would sustain the loads while satisfying the design objective of a margin of safety no less than 0.5. Table 9.4.2 summarizes the results of the stress analysis (Ref. 9.1 provided σ_{fail} for balsa).

Table 9.4.2: Longeron Stress Analysis Results

Configuration	σ_{fail} (psi)	σ_{max} (psi)	margin of safety
1	5337	2914	0.8
2	5337	1942	1.7
3	5337	1457	2.7

The study indicated configuration one (1/4" x 1/8" longerons) would achieve the design objectives of minimizing the weight and attaining a margin of safety of at least 0.5. There were two additional concerns, though, which were addressed before arriving at a final longeron design. First, the fuselage tapers considerably fore and aft of the wing, a feature of the design unaccounted for in the stress analysis. As a result of the taper, the moment of inertia of the longerons along the top and bottom of the fuselage decreases as the longerons approach the neutral axis. Recalling that stress is inversely proportional to moment of inertia, and also considering that the top and bottom longerons bear the greatest stresses in the fuselage structure, it was apparent that configuration one may not be sufficient to withstand the loads with a margin of safety of at least 0.5. Second, a calculation of the buckling length of the longerons when $\sigma = \sigma_{max}$ indicated the bulkheads would have to be spaced less than 1 7/8" apart to prevent buckling. This was undesirable because the need for so many bulkheads largely negated any weight savings derived by selecting the longerons with the least cross-sectional area. Clearly, a means of strengthening the top and bottom longerons with a minimum weight penalty was needed.

Carbon fiber tape proved to be the solution. The addition of strips of carbon fiber tape epoxied along the top and bottom longerons greatly strengthened the longerons. With a modulus of elasticity of 11.0E6 lb/in^2, the combination of the longeron and 1/4" x 7/1000" tape can withstand any tensile load the fuselage will experience (the modulus of elasticity of the composite longeron was determined in Section 9.2). Thus, the final longeron design was 1/4" x 1/8" balsa stock with carbon fiber tape epoxied along the top and bottom longerons. Four additional longerons were added to help support the Monokote covering. Since the four primary longerons bear the loads, lightweight 1/16" x 1/16" balsa stock was chosen for the secondary longerons. The addition of the carbon fiber tape increased the buckling length to 5", though the bulkhead spacing aft of the

wing was set at 2 3/4" and the bulkheads fore of the wing were spaced 2 3/16" apart so as to support the secondary longerons and prevent the Monokote from sagging. Within the wing carry-through structure, the bulkheads were spaced to accommodate the wing attachment structure (see Figure 9.4.5).

Figure 9.4.5: Fuselage Structure

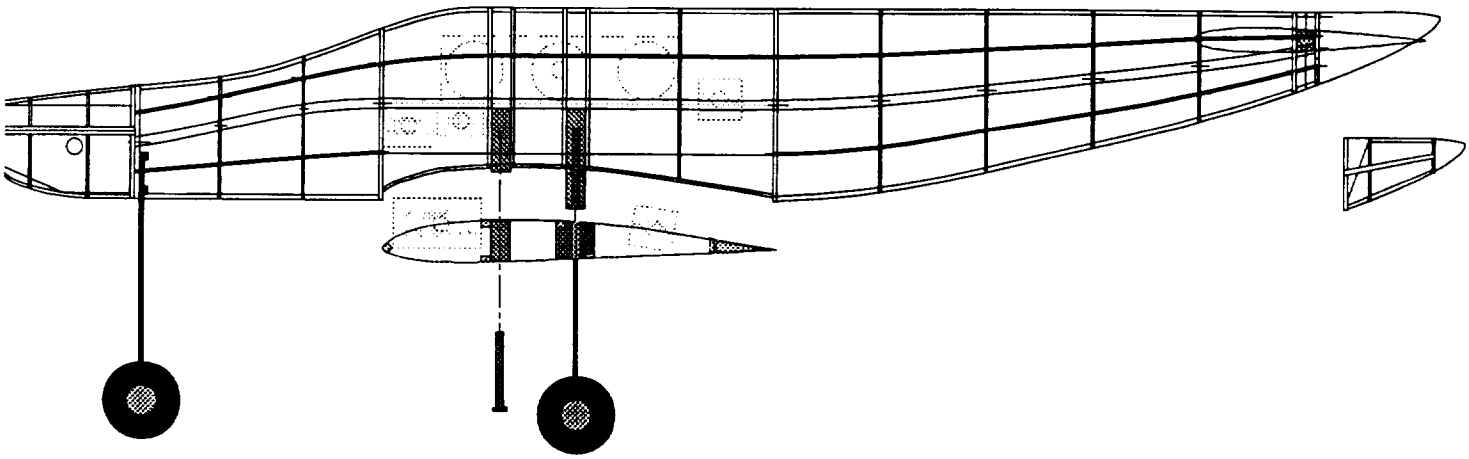

The second study involved sizing of the fuselage bulkheads. In particular, an analysis of the shear flow through the bulkheads was conducted so as to determine the minimum cross-sectional thickness necessary to withstand the loads. Minimizing the thickness will in turn minimize the weight so as to attain the design objective of a lightweight structure.

The bulkhead study employed the fuselage model and idealized cross-section used in the longeron analysis (see Figures 9.4.1 and 9.4.2). For this study, however, the shear flow in each panel was calculated given the flight and ground loads (recall Figures 9.4.3 and 9.4.4). With the bulkhead modeled as a slice of a thin-walled member, the average shear could then be estimated (see Figure 9.4.6 and Ref. 9.2).

Figure 9.4.6: Bulkhead Model for Shear Analysis

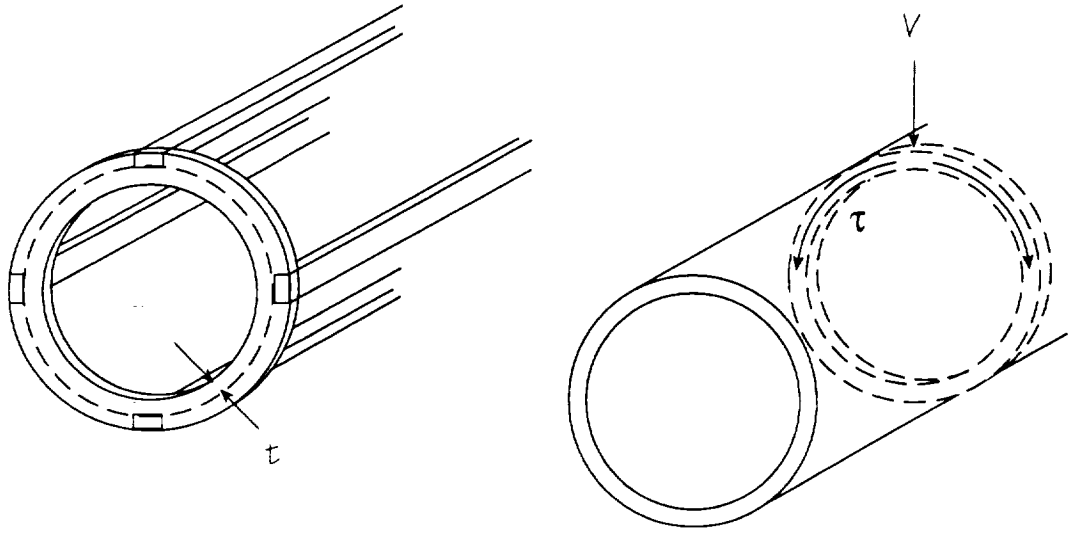

Note that the thickness is measured inside of the notches for the longerons and not from the outer circumference. Doing so increased the overall thickness so as to provide for stress concentrations at the cuts. As with the longerons, balsa was chosen due to its high strength-to-weight ratio. The three configurations examined were t = 1/8", 3/16", and 1/4". As with the longeron study, low weight and a margin of safety of at least 0.5 were the primary figures of merit. Table 9.4.3 summarizes the results (Ref. 9.3 provided t_{fail} for balsa)..

Table 9.4.3: Bulkhead Shear Analysis Results

Configuration	t_{fail} (psi)	t_{max} (psi)	margin of safety
1	300	24.32	11.3
2	300	16.21	17.5
3	300	12.16	23.7

The above results indicate that the first configuration (t = 1/8") would attain the design objectives. However, due to concerns about the stress concentrations at the notches, configuration two (t = 3/16") was selected. A further concern was the orientation of the grain of the balsa; the bulkhead would be weak at the points where the grain was oriented radially (see Figure 9.4.7). Therefore, the material was changed from sheet balsa to 3-ply balsa sheets. The grains within the plywood balsa are mutually perpendicular, thus eliminating the weaknesses due to unidirectional grains.

Figure 9.4.7: Balsa Sheet versus 3-Ply Balsa

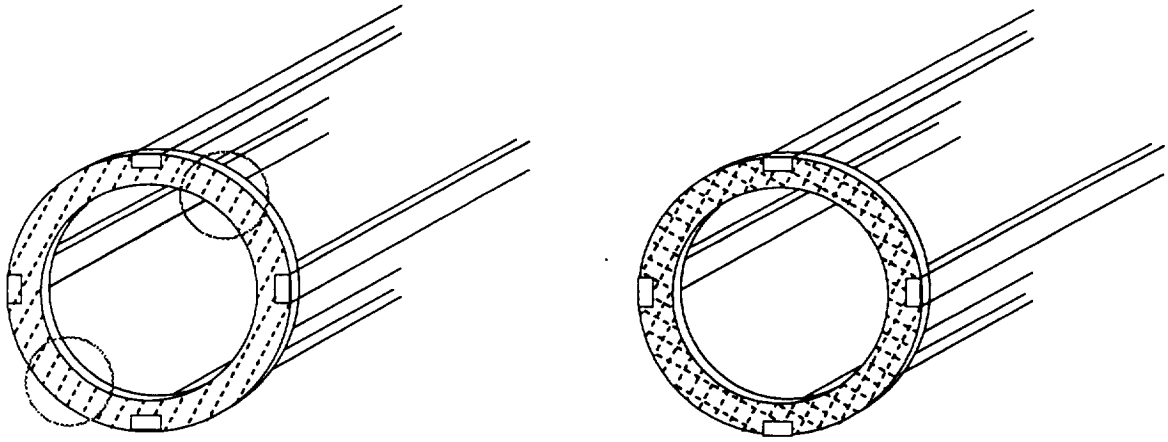

The final consideration was the thickness of the balsa stock from which to fabricate the bulkheads. In order to minimize weight without sacrificing strength, several thicknesses were used for the bulkheads depending upon the estimated load on each. For instance, 1/8" stock was chosen for the firewall due to the sizable loads placed upon it by the power plant and nose gear. Likewise, the bulkheads within the wing carry-through structure are sturdy 3/32" 3-ply balsa as are the bulkheads fore and aft of the stabilator hinge. The remaining bulkheads are 1/16" thick (see Figure 9.4.5).

9.5 Wing Carry-Through and Fuselage Mating Design

The wing carry-through design warranted particular attention due to the many design objectives it needed to satisfy. First and foremost, the structure had to be lightweight yet strong enough to withstand the flight load extremes as well as the ground loads experienced by the main gear. Furthermore, the placement of the avionics and propulsion system batteries within the carry-through structure posed its own difficulties, for in order to attain the design objective of complete system installation within 20 minutes, the wing would have to be simple to remove and mount. A bolt system was chosen due to the ease of removal and remounting that it offered (see Figure 9.5.1). Though such a design demands careful cunstruction for proper mating of the wing and fuselage, it offers distinct advantages over a rubber band system or a "plug-in" system by which the sing spars detach from the carry-through structure. Bolts offer an internal mounting system without the drag of external rubber bands and wooden dowels, while it also avoids the weight penalty incurred in strengthening the wing spar joint in a plug-in system.

The wing is connected to the fuselage by four nylon bolts. The bolts are screwed through spruce blocks epoxied to the wing's main and secondary spars and continue into

spruce blocks sandwiched between fuselage bulkheads. The wing sits in a saddle formed in the bottom of the fuselage by the bulkheads and thin balsa sheeting (see Figure 9.4.5). The bottom longeron terminates at the wing's leading edge and resumes at the trailing edge so that the wing can be placed flush with the fuselage. As a result, the load paths run form the wing, through the carry-through structure bulkheads, and then into 3/16" x 3/16" spruce beams running along the inside of the bulkheads. The two beams serve the dual purpose of providing strength while providing a platform to mount the avionics.

The wing spars are joined at the fuselage center line and wrapped with a thin strip of fiberglass cloth and epoxy. The bottom of the wing box is sheeted so as to provide a floor to which the propulsion system batteries are velcroed. The top of the wing box is partially sheeted where the wing contacts the bottom of the sides of the fuselage. Partial top sheeting in the aft section of the wing box provides a mount for the aileron servo.

Figure 9.5.1: Wing Mounting System

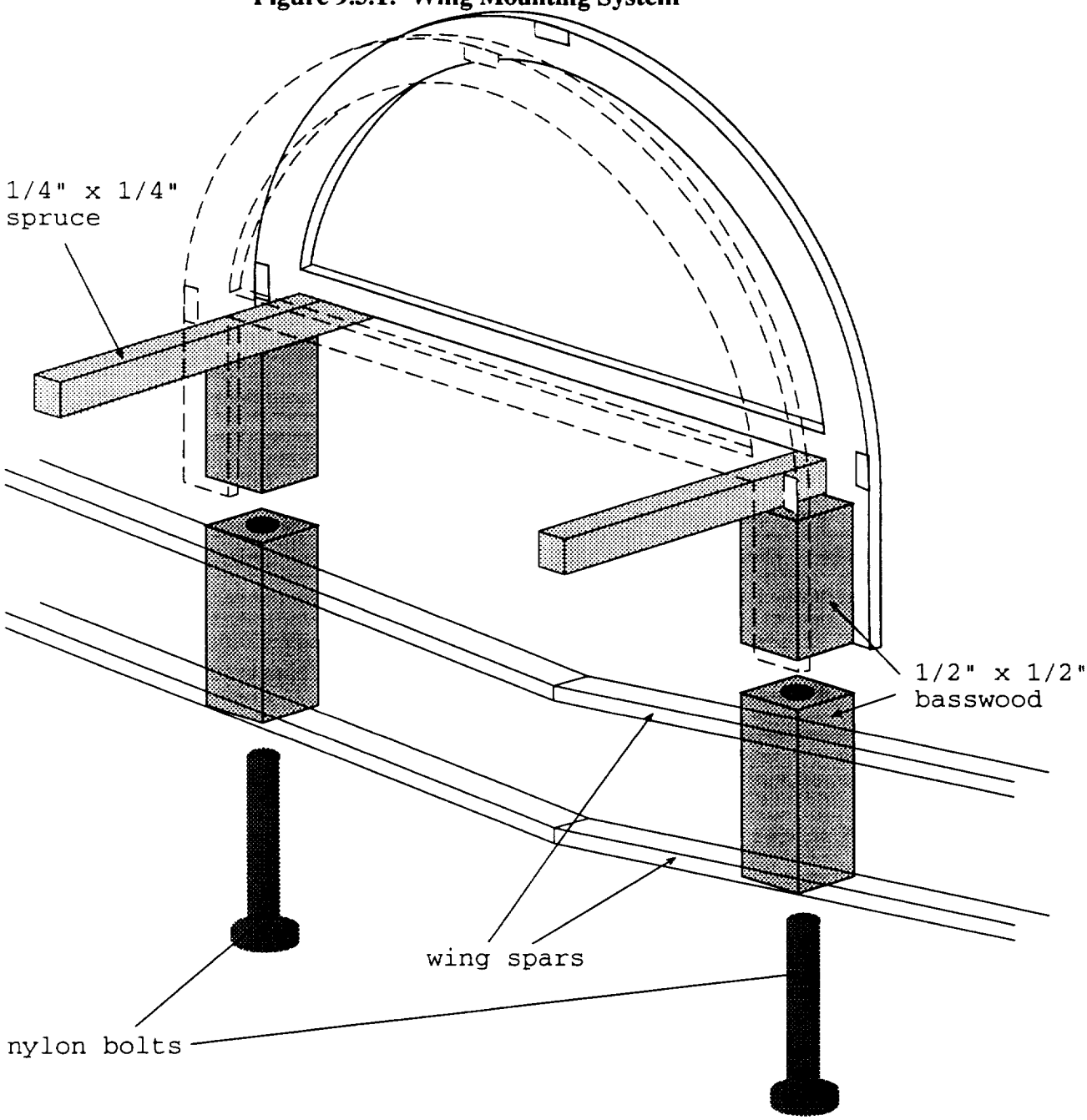

9.6 Empennage Design

The tail structure was driven by the design objectives of a lightweight structure with the strength to withstand the flight loads. Though ground loads are not of particular concern in designing the empennage, the flight loads are compounded by the additional loads induced by control surface deflections. A further concern is the sensitivity of the

center of gravity location to additional weight at the tail.

With these considerations in mind, the empennage was designed with a simple structure. The vertical tail is merely a flat plate with a truss structure whereas the rudder is 1/4" sheet balsa with holes drilled to reduce the weight (see Figure 9.6.1). Two nylon hinges and an internal wire actuator connect the rudder to the vertical tail. A 1/4" x 1/4" balsa beam extending to the bottom longeron serves as the main spar of the vertical tail, whereas 1/8" x 1/4" balsa forms the leading edge and horizontal truss members. The diagonal truss members are 1/16" x 1/4" balsa. Empirical data from previous designs provided a base for decisions concerning the dimensions of the various members.

The decision to incorporate a stabilator rather than a horizontal tail/elevator combination was driven primarily by performance considerations, though the all-moveable tail offered structural advantages as well. Though mounting the stabilator required a more complex design, weight was saved by eliminating the nylon hinges and additional trailing edge structure needed for elevators. The design objective to create an aesthetically pleasing aircraft was the basis for sweeping the stabilator 15° aft.

The primary component of the hinge design is a lightweight 1/4" diameter 12" long carbon fiber rod which can withstand the stabilator's torsional and transverse loads (see Figure 9.6.2). So as to minimize the hinge moment, the centerline of the rod was

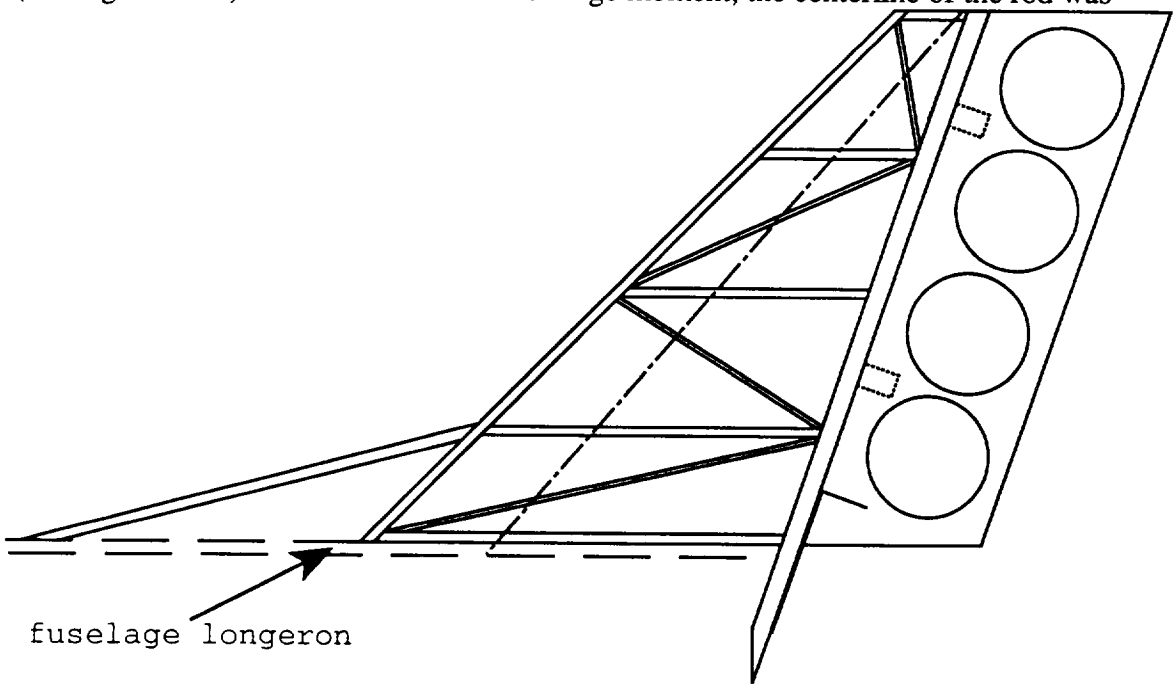

Figure 9.6.1: Vertical Tail Structure

designed to pass through the intersection of the quarter chord and the mean aerodynamic chord. Recall that for a symmetric airfoil, the coefficient of moment about the quarter

chord is zero. Hence, the hinge moment will be near zero (the addition of a small fillet between the inboard rib and the fuselage will produce a small moment). The rod serves as a partial spar for the stabilator, extending to the third rib. Holes drilled in the three inboard ribs serve as the attachment points. A rounded piece of 3/16" x 3/16" balsa serves as the leading edge, whereas 3/8" x 3/32" balsa forms the trailing edge. Two forward 1/4" x 3/16" spars and two aft 1/8" x 1/8" spars serve to strengthen the tip of the stabilator outboard of the rod and support the Monokote covering. The stabilator mounts to the fuselage via two 1/2" x 1/2" spruce blocks held in place between the two aft bulkheads (see Figure 9.6.3).

Figure 9.6.2: Stabilator Structure

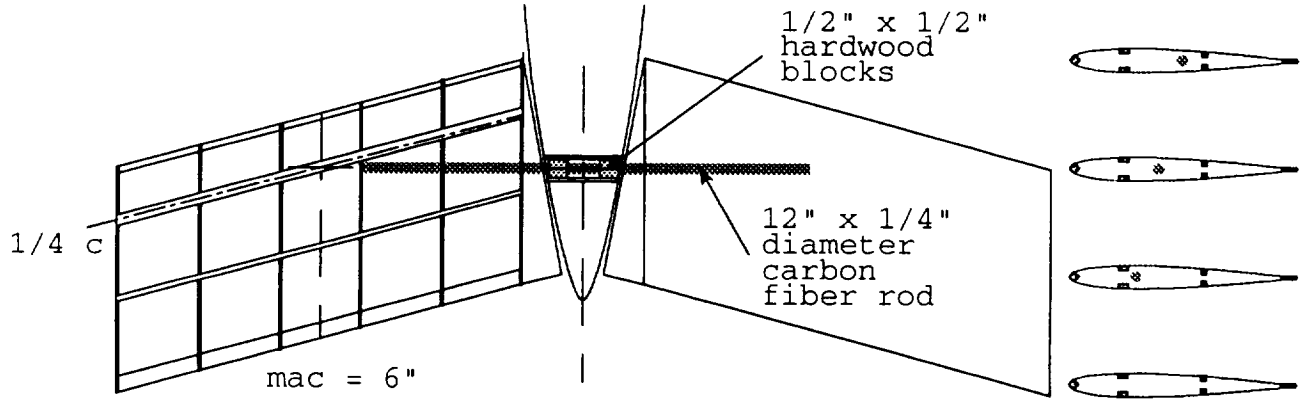

Figure 9.6.3: Stabilator Mounting System

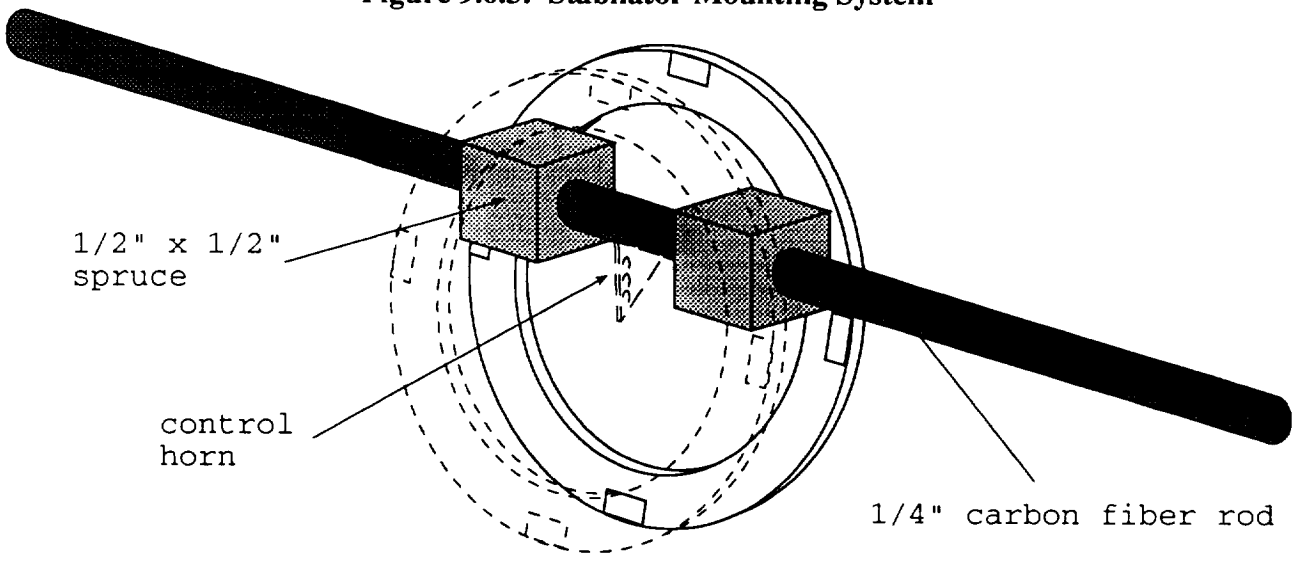

9.7 Aircraft Loading

Based on the ultimate loads placed on the fuselage and wing when they were structurally designed, a good estimate for the limit load factor for positive angles of attack is 3, while -2 should roughly approximate the allowable load factor for negative angles of attack. These values provide the pilot with a reasonable operation's envelope while still adequately safeguarding the structural integrity of the aircraft. Figures 9.7.1 and 9.7.2 show the velocity/load factor envelope and the corresponding velocity/angle of attack envelope for our aircraft respectively.

Figure 9.7.1: V-n diagram for Elite Aircraft

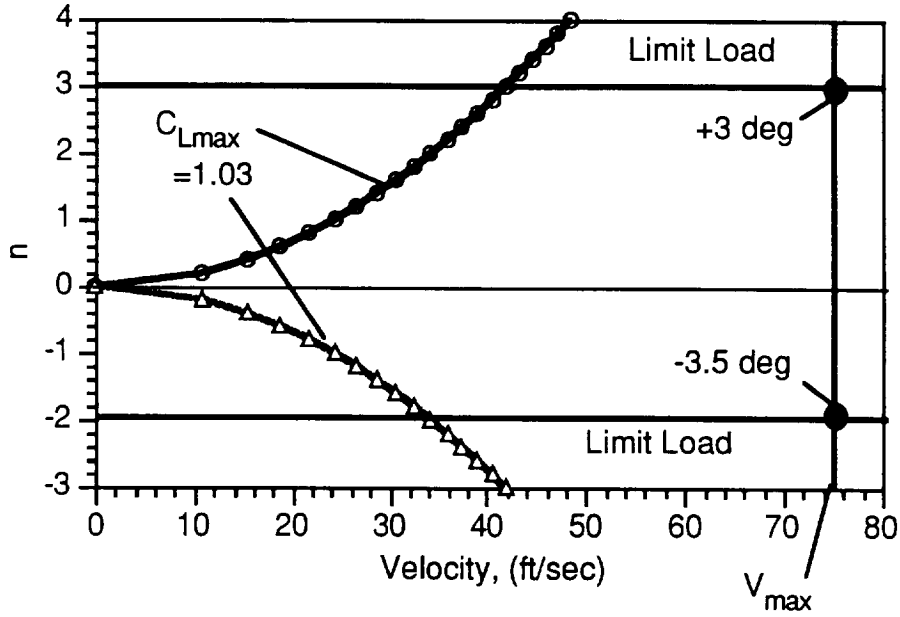

Notice in the V-n diagram that the extreme allowable angles of attack at V_{max} are a modest 3 and -3.5 degrees. This could present some difficulties in preventing the pilot from over stressing the aircraft at the higher flight speeds. Figure 9.7.2 shows the full dependence of allowable angle of attack on velocity. Once the airplane gets above 36 ft/sec the pilot is no longer allowed to stall the aircraft without the danger of damaging the aircraft. In fact, if the n=3 and n=-2 load factor curves are carried out to 150 ft/sec, as could be encountered in a dive, the allowable angle of attack range narrows to -0.18 degrees to -1.87 degrees.

Figure 9.7.2: Angle of Attack and Velocity Envelope for Elite Aircraft

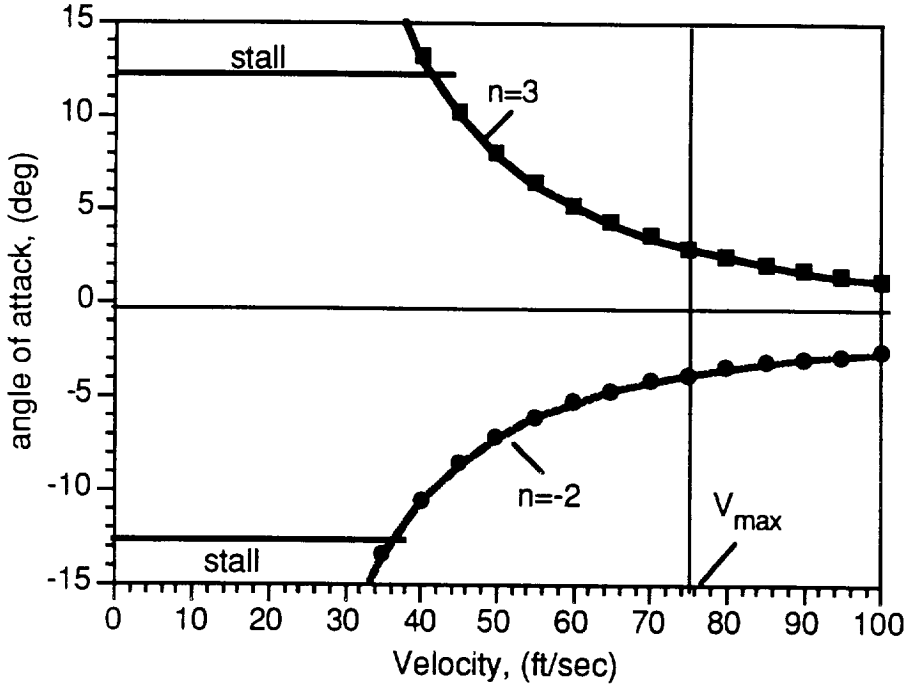

9.8 Landing Gear Design

The landing gear system employed is the standard RPV steel strut gear in a tricycle pattern. The 1/8" steel struts, main gear basswood blocks, and nose gear mounting brackets will withstand the ground loads during takeoff and landing from unimproved fields. However, there are other concerns surrounding the landing gear that should warranted some attention.

First, the gear must be long enough to provide adequate ground clearance for the propeller. Second, in a tricycle formation, the main gear must be behind the center of gravity, but not so far behind as to prevent the aircraft from rotating at takeoff. The rear gear should also have a large enough spacing between them to prevent the aircraft from tipping over during ground maneuvers. Lastly, the landing gear must attach to a very sturdy part of the aircraft to prevent structural damage if the aircraft hits the ground during a landing attempt. To meet this last requirement, secondary wing spars placed 5" behind the leading edge support 1" thick basswood blocks to which the main gears mount (see Figure 9.8.1). These secondary spars are made of 3/16" square spruce and allow a stable attachment point for the gear. The use of spruce should also prevent the gear from tearing out of the wing.

Figure 9.8.1: Main Gear Mounting System

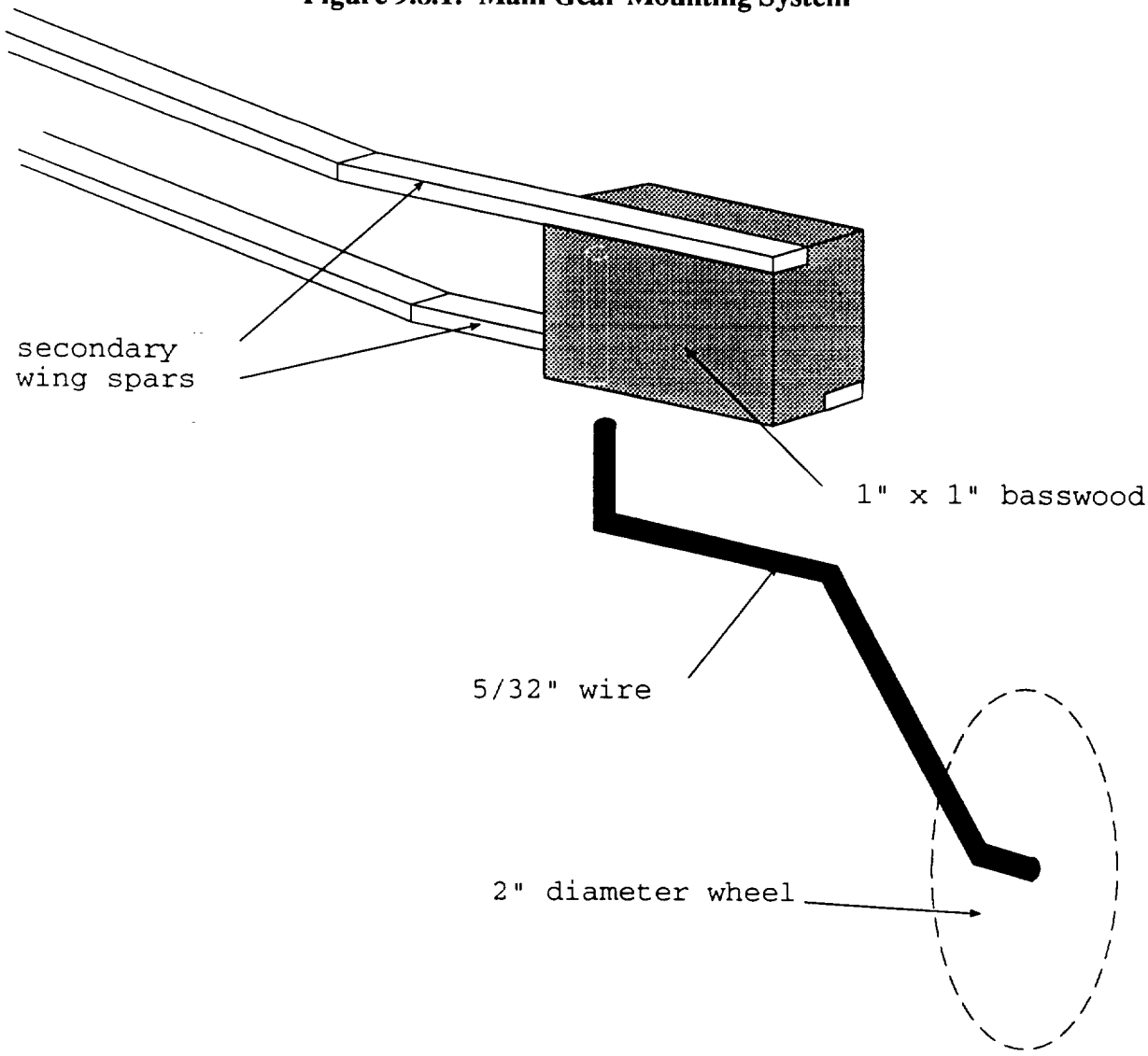

Table 9.8.1 below summarizes the landing gear properties that meet all the above stipulations for our aircraft.

Table 9.8.1: Summary of Landing Gear Properties

Material	Diameter	Nose Gear Position	Main Gear Position	Main Gear Spacing	Gear Length
steel	1/8"	4.125 in	15.5 in	21 in	6 in

In terms of the overall design, the landing gear did not receive much attention and is one area that could probably use a more detailed analysis.

9.9 References

9.1 Solbreken, Gary L. "Balsa Wood Breaking Experiment" (memo to Dr. S. M. Batill). 30 July 1992.

9.2 Beer, Ferdinand P. & Russell Johnston, Jr. Mechanics of Materials. New York: McGraw-Hill, Inc. 1992.

9.3 Wood Engineering Handbook. ed. Forest Products Laboratory. Englewood Cliffs, N.J.: Prentice Hall. 1990.

10 ECONOMIC ANALYSIS

10.1 Requirements and Objectives

Design Objective:

1. Make *The Elite* affordable to the upper-middle class general aviation market.

10.2 Cost Breakdown

The total cost per aircraft was a function of the fixed subsystem costs, the raw materials costs, and the manufacturing costs. The complete cost breakdown is found in Table 10.2.1. The total cost of the fixed subsystems was $462.58. The cost of the raw materials was estimated as $160. Manufacturing costs were estimated at $2190. Included in the manufacturing costs were the personnel costs, the tooling costs, and the waste disposal costs. The personnel costs are based on 180 hours of manufacturing time, a conservative estimate based on the complexity of our design versus that of previous designs. Waste disposal was approximated at 1.5 lbs, also a conservative estimate based on the prediction of excess material after cutting out the circular fuselage and swept empennage. The total cost of the subsystems, raw materials, and manufacturing was $2812.58. Assuming an overhead factor of 1.4 and a 12% profit, the total cost of *The Elite* was $4410.13.

A breakdown of the three main components affecting the total cost is found in Figure 10.2.1. Manufacturing costs make up the largest percentage of the total cost of the aircraft (78%). The subsystems make up 16% and the raw materials only 6%. Thus, to decrease the total cost of the aircraft, the area to target is manufacturing. Manufacturing costs can be reduced dramatically through careful planning of material acquisition and tooling time. Figure10.2.2 shows a breakdown of the factors affecting the manufacturing costs. Personnel costs dominate 82% of the manufacturing expenses, thus comprising 64% of the total aircraft cost. Waste disposal comprises 11% of the manufacturing cost or almost 9% of the total cost of the aircraft. Tooling comprises 7% of the manufacturing costs and only 5% of the total aircraft cost. Thus the top three dominating factors affecting the total cost of the aircraft were the personnel (64%), the subsystems (16%), and the waste disposal (9%). The costs of the subsystems were fixed by the design. The personnel and waste disposal costs depend on the efficiency of the manufacturing process.

Table 10.2.1: Cost Breakdown of *The Elite*

Fixed Subsystems:	
Radio Transmitter	$ 75.00
Radio Receiver	$ 35.00
Avionics Battery Pack	$ 10.00
Switch Harness	$ 5.00
Miniature Servos (3 @ $35)	$ 105.00
Electric Motor Speed Controller	$ 50.00
Astro-15 Motor	$ 107.00
Batteries (13 @ $4)	$ 52.00
Motor Power Wiring (2 feet)	$ 4.00
Landing Gear	$ 10.00
Zingali 10-8 Propeller	$ 9.58
	$ 462.58
Raw Materials:	
	$ 160.00
Manufacturing:	
Personnel Costs (180 hrs @ $10/hr)	$1800.00
Tooling	$ 150.00
Waste Disposal (1.5 lbs @ $10/oz)	$ 240.00
	$2190.00
Subsystems+Materials+Manufacturing	**$2812.58**
TOTAL COST OF AIRCRAFT	**$4410.13**

Figure 10.2.1: Breakdown of Total Aircraft Cost

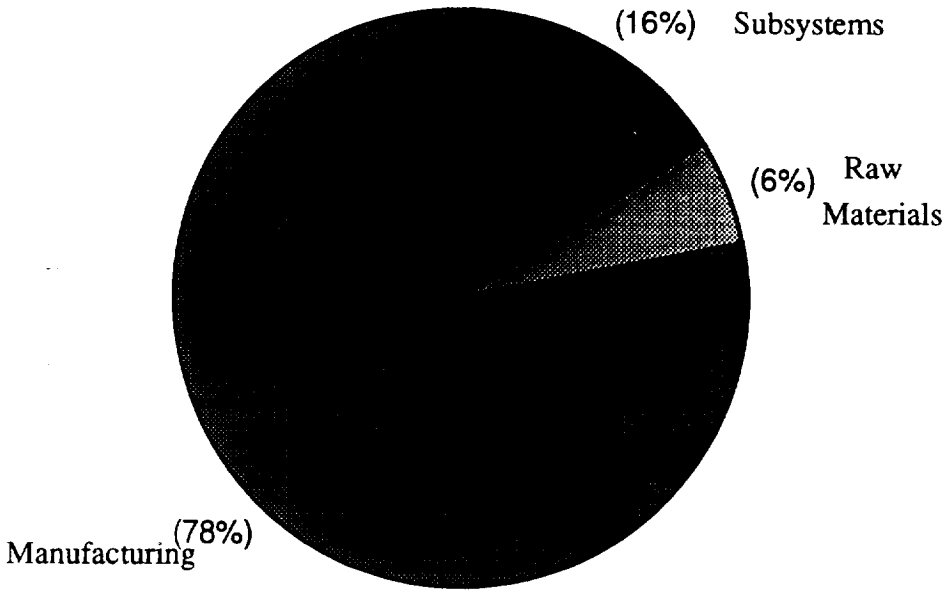

Figure 10.2.2: Breakdown of Manufacturing Costs

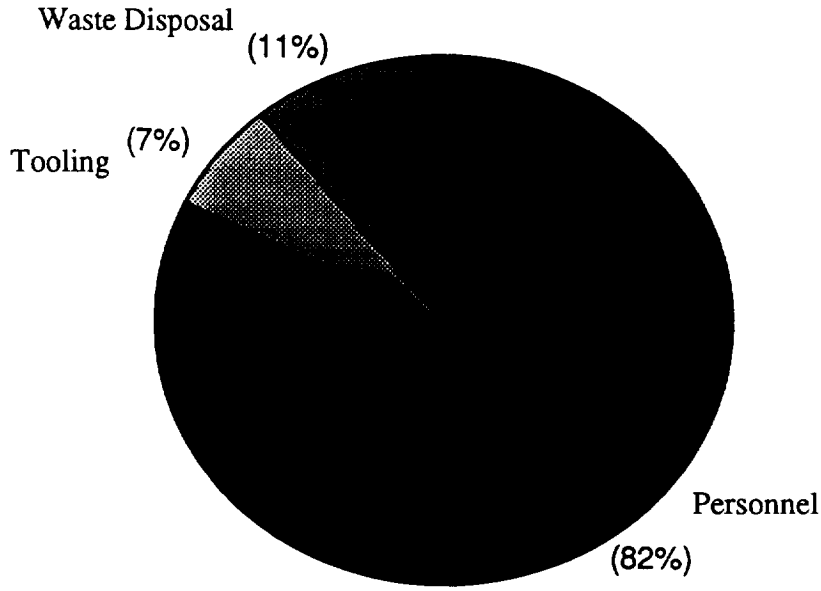

The effects of a slight decrease in either the estimated number of man-hours or the amount of waste disposal on the total cost of the aircraft is illustrated in Figure 10.2.3. A

decrease of 20 man-hours decreases the total aircraft cost by approximately $314. Thus for every man-hour, the total aircraft cost increases by $15.68. Note that this number was greater than the $10/hr rate pay because of the overhead factor and the profit allowance.

The effects of decreasing the amount of waste disposal was not as pronounced. A 1 lb decrease in waste disposal decreases the total cost of the aircraft by $250. A decrease any less than 1 lb is improbable because the initial waste disposal estimate was only 1.5 lbs.

Figure 10.2.3: Influence of Waste Disposal and Production Hours on Cost

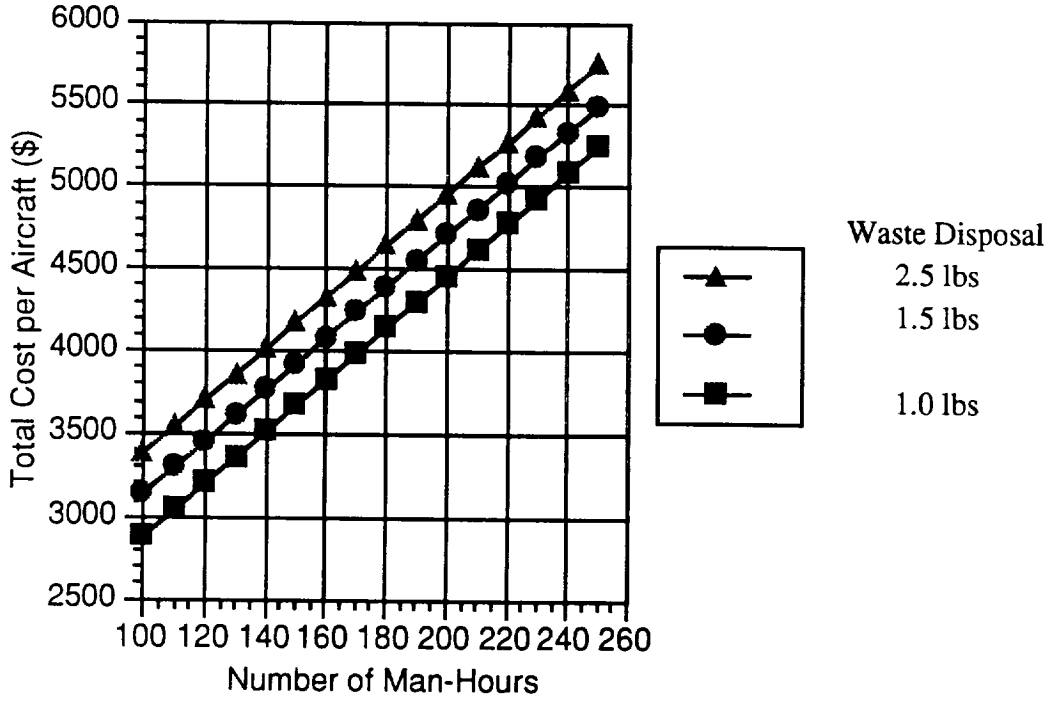

10.3 Economic Performance

Some cost measures of merit were also calculated for *The Elite*. They can be found in Table 10.3.1. These merit factors were based on depreciation costs, maintenance-insurance costs, and fuel costs. Depreciation costs recognize that the flight hardware has a limited life. Current technology in Aeroworld permits a total lifetime of 100 flight hours. Also, depreciation costs increase with range and decrease with cruise speed. The depreciation costs for *The Elite* were $5.10/flight. The Maintenance-Insurance costs increase with the design speed (60 ft/sec) and the maximum takeoff weight (4.88 lbs) and for *The Elite* were $0.20/flight. The fuel costs per flight depend on the current draw, the flight time (0.1157 hour), and the fuel cost ($3.08/amphour) and for *The Elite* were equal to $4.65/flight.

Table 10.3.1: Economic Figures of Merit for *The Elite*

Depreciation Cost/flight	$ 5.10
Maintenance-Insurance Cost/flight	$ 0.20
Fuel Cost/flight	$ 4.65
Cost per Flight (CPF)	$ 9.95
Cost per Flight Minute (CPFM)	$ 1.43
Cost per 1000 feet (CP1000)	$ 0.335

The cost per flight (CPF) is the sum of the depreciation costs, the maintenance-insurance costs, and the fuel costs. The depreciation costs are high because they are directly related to the total cost per aircraft, which for *The Elite* is fairly high. However, if the total cost per aircraft proves to be high even after manufacturing is completed, the depreciation costs could still be decreased by decreasing the flight time. The other major contributor to the CPF is the fuel costs which also could be decreased by decreasing the flight time. For instance, keeping the cruise speed at 60 ft/s but flying only 15000 ft instead of the entire range of 25000 ft would decrease the CPF by 62% to only $6.12/flight.

The cost per flight minute (CPFM) is directly proportional to the CPF and inversely proportional to the flight time. Moreover, since the CPF is directly proportional to the flight time, the CPFM is actually independent of the flight time. Similarly, the cost per 1000 feet (CP1000) is directly proportional to the CPF and inversely proportional to the range. These dependencies correspond to the CP1000 being inversely proportional to the cruise speed. Thus, a decrease in flight time by decreasing the cruise speed would decrease the cost per flight, increase the cost per 1000 feet, and keep the cost per flight minute the same. Thus, if the pilot desires to minimize the cost per flight, he could do so by decreasing the distance of the flight, keeping the cruise speed and thus the CPFM and CP1000 the same. To minimize the cost per 1000 feet (thereby increasing the cruise speed), a trade off must be made between the cost per flight and the cost per 1000 feet.

APPENDIX A

Critical Design Summary:

Parameter	Initials of RI:	2-10-94	2-17-94	2-24-94	3-3-94	Final Design
*[all distances relative						
to aircraft nose						
and in common units]*						
DESIGN GOALS:						
V cruise	Tuan	60 ft/sec	65 ft/sec	65 ft/sec	65 ft/sec	60 ft/sec
No. of passengers/crew	Doug	6	6	6	6	6
Max Range at Wmax	Tuan	30,500 ft	30,500 ft	30,500 ft	30,500 ft	32336 ft
Max R/C at SL	Steve					16.1 ft/s
Altitude cruise	Doug				50 (ft)	50 ft
Minimum turn radius	Doug					20 ft
Max Range at Wmin	Tuan					33000 ft
Maximum TO Weight-WMTO (lb)	Doug/Dan	4.25	4.25	4.25	4.88	4.88 lb
Minimum TO Weight - Wmin (lb)	Doug/Dan	4.1	4.1	4.1	4.83	4.83 lb
BASIC CONFIG.						
Wing Area	Amy	6.5 ft^2		6.5 ft^2	6.5	6.5 ft^2
Maximum TO Weight - WMTO (lb)	Doug/Dan	4.22 lb		4.22 lb	4.88	4.88 lb
Empty Flight Weight	Doug/Dan	4.17 lb		4.17 lb	4.83	4.83 lb
Wing loading(WMTO) lb/ft^2	Jonathan	.65 lb/sq.ft.		10.3 oz/ft^2	0.75	0.75 lb/ft^2
max length (in)	Jonathan	38 inches		38 inches		38 inches
max span (ft)	Amy	7.21 ft		8 ft		7.66 ft
max height	Jonathan					1.5 ft
Total Wetted Area	Jonathan				17.0 sq ft	17.0 sq ft
WING						
Aspect Ratio	Amy	8		9		9
Span (incuding fuselage)	Amy	7.21ft		8 ft		7.66 ft
Area (ft^2)	Amy	6.5		6.5	6.5	6.5 ft^2
Root Chord	Amy	0.9 ft		10 3/16 inches		10 3/16 inches
Tip Chord	Amy	0.9 ft		10 3/16 inches		10 3/16 inches
taper Ratio	Amy	1				1
C mac - MAC	Jonathan			-0.0582		-0.0582
leading edge Sweep	Jonathan	0				0
1/4 chord Sweep *	Jonathan	0				0
Dihedral	Jonathan			8 degrees		5 degrees
Twist (washout)	Amy	0				0
Airfoil section	Jonathan			DF101		DF101
Design Reynolds number	Jonathan			350,000		350,000
t/c	Jonathan			0.11		0.11
Incidence angle (root)	Jonathan			0.72 degrees		1.2 degrees
Hor. pos of 1/4 MAC	Jonathan			13.03 inches		13.03 inches
Ver. pos of 1/4 MAC	Jonathan					
e- Oswald efficiency	Amy			0.949		0.949
CDo -wing	Amy	0.056		0.008		0.008
CLo - wing	Amy			0.0995		0.0095
CLalpha -wing	Amy			0.083 /degree		.083 /degree
FUSELAGE						
Length	Amy	38 inches	38 inches	38 inches		38 inches
Cross section shape	Amy	circular	5 in dia			circular - 5 in diam.
NominalCrossSectionArea (in^2)	Amy	(average diameter = 4 in)		12.57		0.0873 ft^2
Finess ratio	Amy			7.6		7.6
Payload volume (cubic in.)	Amy	25 in^3	25 in^3	25 in^3		25 in^3
Planform area	Amy				1.04	1.06 ft^2
Frontal area (sq. ft.)	Steve	0.155	0.155	0.155	0.3595	0.155 sq. ft.
CDo - fuselage	Steve	0.0194		0.0194	0.00608385	0.00608385
CLalpha - fuselage	Jonathan				0.00673 /deg	0.00673 /degree
EMPENNAGE						
Horizontal tail						

Area (ft^2)	Dan		1.2	1.6	0.9	0.9 ft^2
span	Dan		1.8	2.4	1.8	1.8 ft
aspect ratio	Dan		9	3.6	3.6	3.6
root chord	Dan			8 inches	0.5 ft	0.5 ft
tip chord	Dan			8 inches	0.5 ft	0.5 ft
average chord	Dan			8 inches	0.5 ft	0.5 ft
taper ratio	Dan	1				1
l.e. sweep	Dan	0		15 degrees	15 degrees	15 degrees
1/4 chord sweep	Dan	0		15 degrees	15 degrees	15 degrees
incidence angle	Dan	0			-1.32 degrees	-2 degrees
hor. pos. of 1/4 MAC	Dan				34.0 inches	34.5 inches
ver. pos. of 1/4 MAC	Dan					10.4 in. above ground
Airfoil section	Jonathan			SD8020		SD8020
e - Oswald efficiency	Jonathan				0.956	0.956
CDo -horizontal	Steve	0.0014			0.00110769	0.00110769
CLo-horizontal	Jonathan			0	0	0
CLalpha - horizontal	Dan			3.803		3.803
CM mac - horizontal	Jonathan				0	0
Vertical Tail						
Area (ft^2)	Amy				0.55	0.3 ft^2
Aspect Ratio	Amy				2.2	1.2
root chord	Dan				0.5 ft	0.5 ft
tip chord	Dan				0.5 ft	0.5 ft
average chord	Dan				0.5 ft	0.5 ft
taper ratio	Dan					1
l.e. sweep	Dan					45 degrees
1/4 chord sweep	Dan					49 degrees
hor. pos. of 1/4 MAC	Dan				34	34.5 in
vert. pos. of 1/4 MAC	Dan					14.875 degrees
Airfoil section	Jonathan	flat plate		flat plate	flat plate	flat plate
SUMMARY AERODYNAMICS						
Cl max (airfoil)	Jonathan			1.14		1.14
Cmo (airfoil)	Jonathan			-0.0582		-0.0582
CL max (aircraft)	Jonathan			1.03		1.03
lift curve slope (aircraft)	Jonathan			0.083 deg-1		0.083 /degree
CDo (aircraft)	Steve	0.1282	0.0289	0.035		0.0325
efficiency - e (aircraft)	Steve	0.733		0.89		0.89
Alpha stall (aircraft)	Jonathan			12.333°		12.333 degrees
Alpha zero lift (aircraft) °	Jonathan			-0.23		-0.23
L/D max (aircraft)	Jonathan			14.8		14.8
Alpha L/D max (aircraft)	Jonathan			9.0 °		9.0 degrees
WEIGHTS (pounds)						
Weight total (empty)	Doug/Dan	4.17 lb		4.173	4.834	4.834
C.G. most forward-x&y	Doug				13.36	13.36
C.G. most aft- x&y	Doug				13.471	13.471
Avionics (lb)	Doug				0.31	0.31
Control Linkages (lb)	Doug				0.14	0.14
Payload-Pass.&lugg.-max (lb)	Doug/Dan	0.74 oz		0.74 oz	0.0463	0.0463
Engine & Engine Controls (lb)	Doug		12 oz	12 oz	0.657	0.657
Propeller (lb)	Tuan			0.074 lbs	0.097	0.097
Fuel (battery) (lb)	Tuan			1.38 lbs	1.38	1.38
Structure						
Wing (lb)	Jonathan				1.05	1.05
Fuselage (lb)	Jonathan				0.5	0.5
Main Landing gear (lb)	Dan				0.256	0.256
Nose gear (lb)	Dan				0.173	0.173
empenage weight (lb)	Dan				0.15625	0.15625
PROPULSION						
Type of engines	Steve			Astro 15		Astro15
number	Tuan	1				1
placement	Steve	nose (tractor)				nose (tractor)
Pavail max at cruise (60 ft/s)	Steve/Tuan		170 watts		170 watts	132 watts
Preq cruise	Steve/Tuan		65 watts		65 watts	77.6 watts
max. current draw at TO	Tuan			16 amps	14.292 A	4.2 amps

cruise current draw	Steve		17.78 A	10 amps	13.5 A	10.357 amps
Propeller type	Tuan	Zinger 11-7	Zinger 10-7	John Brothers11-8	Zingali 10-8	Zingali 10-8
Propeller diameter	Tuan		10"		10"	10 in
Propeller pitch	Tuan		7	8	8	8 in
Number of blades	Tuan		3		3	3
max. prop. rpm	Steve/Tuan					16310 rpm
cruise prop. rpm	Steve/Tuan					13687 rpm
max. thrust	Steve/Tuan				4.653 lb	4.3 lbs
cruise thrust	Steve/Tuan					1.05 lb
battery type	Steve/Tuan			P-130SCR	P-130SCR	P-130SCR
number	Steve/Tuan			13	13	13
individual capacity	Steve/Tuan			1300 mah	1300 mah	1300 mah
individual voltage	Steve/Tuan			1.2	1.2	1.2
pack capacity	Steve/Tuan			1300 mah	1300mah	1300mah
pack voltage	Steve/Tuan			15.6	15.6	15.6
STAB AND CONTROL						
Neutral point	Dan					41% MAC
Static margin %MAC	Dan					11% MAC
Hor. tail volume ratio	Dan		0.359		0.359	0.35
Vert. tail volume ratio	Amy					0.0105
Stabilator area (ft^2)	Dan				0.9	0.9 ft^2
Stabilator max deflection	Dan			20 deg (tail)	12°	12 degrees
Rudder Area	Dan				0.9	0.3 ft^2
Rudder max deflection	Dan				15°	15 degrees
Aileron Area (ft^2)	Dan				0.75	0.75 ft^2
Aileron max deflection	Dan			15°	15°	15 degrees
Cm alpha	Dan			0.655	0.655	-0.45
Cn beta	Dan			-1.1	-1.1	0.025
Cl alpha tail	Dan				0.0663	0.0663
Cl delta e tail	Dan				0.0663	0.0663
PERFORMANCE						
Vmin at WMTO	Tuan					24.8 ft/s
Vmax at WMTO	Steve			77.5	77.5	71.71 ft/s
Vstall at WMTO	Jonathan			23.44	23.44	24.8 ft/s
Range max at WMTO	Tuan					32919.3 feet
Endurance @ Rmax	Tuan					14.86 min
Endurance Max at WMTO	Tuan					18.62 min
Range at @Emax	Tuan					27933ft
Range max at Wmin	Tuan					33790 ft @ V = 35
ROC max at WMTO	Steve					16 ft/s @ V = 36.5 ft/s
Abs. Ceiling	Steve					194306 ft
Min Glide angle	Steve					3.87°
T/O distance at WMTO	Steve					26.0 ft
Route Percent Servicable at Cruise	Steve					94.30%
SYSTEMS						
Landing gear type	Doug	tricycle				tricycle
Main gear position	Doug	4				15.5 in
Main gear length	Doug					5 in
Main gear tire size	Doug	2" diameter				2 in diameter
nose/tail gear position	Doug	4.375" beh prop				4.375 in behind prop
n/t gear length	Doug					5 in
n/t gear tire size	Doug					2 in diameter
engine speed control	Doug	TEKIN				TEKIN speed control
Control surfaces	Doug	stabilator,rudder				rudder, stabilator
TECH DEMO - Final						
Max Take-Off Weight	Doug					
Empty Operating Weight	Doug					
Wing Area	Jonathan				6.5 ft^2	
Hor. Tail Area	Dan					
Vert Tail Area	Dan					
C.G. position at WMTO	Doug					
1/4 MAC position	Jonathan				13.03 in	
Static margin %MAC	Dan					

V takeoff	Steve				24.8 ft/s	24.8 ft/s
Range max	Tuan					
Airframe struct. weight	Doug					
Propulsion sys. weight (lb)	Tuan				2.134	2.134 lb
Avionics weight	Doug					
Landing gear weight	Doug					
ECONOMICS:						
raw materials cost	Amy		$150		$150	$160.00
propulsion system cost	Amy		150		150	$172.58
avionics system cost	Amy		150		150	$280.00
production manhours	Amy		180		180	180 hours
personnel costs	Amy		1800		1800	$1,800.00
tooling costs	Amy		500		500	$150.00
total cost per aircraft	Amy		4312		4312	$4,394.45
current draw at cruise WMTO	Amy		17.78 A	10 amps	13.5 A	10.233 amps
CPF at Vcruise and Rmax	Amy					$8.37
CPFM	Amy					$1.21
CP1000	Amy					$0.34

APPENDIX B

Initial Weight Data Base

Airplane	#of passengers	Weight (lbs)	Cruise Vel (ft/sec)	Endurance (sec)	Range (ft)	Fuselage Vol (cubic inches)	Fusel Length (inches)	Wing Area (square ft)	Wing Span (ft)	Aspect Ratio (deg)	Dihedral (ft)	HTail Area (ft)	VTail Area (Volts)	Battery
Initial Guess		3.81	28	240	5500	549.504	51	7	7	7	7	1.3	0.6	51
El Toro	51	5	28	978	25000	691.2	40	6.94	8.33	10	9	1.25	0.49	40
Pale Horse	30	4.98	30	646.8	20000	1416.96	51.2	7	8	9.14	20.6 (P)	0.97	0.46	51.2
???	50	3.81	32	510	8000	1537.92	44	5.81	5	4.3	10	1.1	0.347	44
FX-90		2.75	24	479.4	12210	238.464	17	4.38	5.84	7.79	/	0.482	0.35	17
Arrow 227		5	27	558	15990	1587	58.2	9.51	10	10.52	13	1.57	0.72	58.2
Drag-n-Fly		2.73	25	193	4831	670.464	41	6.02	8.5	12	8	1.05	0.5	41
Screem-J4D		3	23	234	5500	25.92	37	5.46	8	11.72	12 (P)	0.63	0.38	37
Penguin		3.125	25	105.3	2609	259.2	42	4.67	7	10.5	10	1.04	0.42	42
Bunny	100	5.3	30	478	14728	1957.5	58	10	9.22	8.5	6 (P)	2.98	0.97	15.6
Hot Box	40	4.29	30	858	20606	862.13	57	7.33	8	8.72	7	1.01	0.42	10.8
RTL-46	100	5.1	35	811.2	19430	2376	66	9.93	9.17	8.46	10	1.92	0.73	14.4
Blue Emu	60	4.79	20	788.4	23600	1255.38	58.8	10	10	10	8	1.61	0.68	13.2

Airplane	WEIGHTS (oz)													
	Engine	Mount	Servos	Prop	Speed Control	Batteries	Receiver	Wing	Fuselage	Empenage	Landing Gear	Total (lb)		
Initial Guess	/	/	/	/	/	/	/	/	/	/	/	/		
El Toro	9.05	/	/	0.5	7.5	21.3	/	14	15	3	7.1	4.84		
Pale Horse	9.12	1.12	1.28	0.8	1.76	24.16	0.96	17.6	13.28	1.92	5.12	4.82		
???	/	/	/	/	/	/	/	/	/	/	/	/		
FX-90	5.5	1	1.2	2	3.23	7.46	0.95	10.5	10	3.5	/	2.83		
Arrow 227	8.9	1.91	1.2	0.54	2.66	20.55	0.95	15.5	11	3.4	5	4.48		
Drag-n-Fly	8		1.2	/	3.23	8.24	0.95	12.1	1	2.64	2	2.46		
Screem-J4D	6.5	/	1.2	1	3.23	8	0.95	10.36	5.22	1.18	2.4	2.5		
Penguin	10.3	4	1.8	2	3	7	1	12.5	10	1.7	2.9	3.51		
Bunny	7.5	1.12	1.8	0.69	3.25	18	0.95	14.4	11.68	6.3	6	3		
Hot Box	13.71	/	6.84	/	/	17.8	/	13.2	7.83	/	3	4.28		
RTL-46	11.5	/	7.44	0.87	/	14.75	/	21	8.9 (w/emp)	3.6	5.1			
Blue Emu	24.28	/	5.92	5	/	13.53	/	14.74	14.5 (w/emp)	3.5	4.79			
												AVE WEIGHT =	3.87363636	lbs.

APPENDIX C:
Computer Codes

```
C
C     ******************************************************
C     Computer code to determine the horizontal tail areas
C     and locations needed to rotate at take-off at certain
C     tail deflection angles.
C     ******************************************************

      REAL dLift,dtail,Lift,W,ltt,lt
 33   FORMAT(8x,f8.4,8x,f5.3,3x,f5.3,5x,f6.2,8x,f6.3,4x,f8.4)
C     OPEN (UNIT=2, FILE='f1')
C     OPEN (UNIT=3, FILE='f2')
      OPEN (UNIT=4, FILE='f3')
C     OPEN (UNIT=5, FILE='f4')
      Pi = 4.0*ATAN(1.0)

      W = 4.8
      rho = 0.002378
      Vto = 25.0

      cw = .84896
      bw = 7.646
      Sw = 6.49
      ARw = bw**2/Sw
      alplo = 2.0*Pi/180.
      Clalpw = 5.73
      CbLalpw = Clalpw/(1.+Clalpw/(Pi*Arw))
      CLo = .0995
      WRITE(6,*)  Clalpw,CbLalpw, CLo

      Lift = 0.5*rho*CLo*Sw*Vto**2

      dWeight = 2.25/12.0
      dLift = 4.0228/12.0

      ct = 6.0/12.
C     St = 2.0
C     alpt = -15.*Pi/180.
      lt = 21./12.

      WRITE(6,*) '    alpha tail (deg)   ct    St      lt        tLift     mom'

      DO 20 alptt = 8.,20.,2
      WRITE(4,*) ' '
      WRITE(6,*) ' '
```

```
      alpt = -alptt * Pi/180.
C     DO 5 ctt = 5.0,8.5,.2
C     ct = ctt/12.
      DO 10 St = .5,2.5,.01
      DO 30 ltt = 16.,24.,.01
      lt = ltt/12.

      bt = St/ct
      ARt = bt**2/St
C     ARt = 3.6

      dtail = lt - dWeight
      Clalpt = 5.73
      CbLalpt = Clalpt/(1.+Clalpt/(Pi*ARt))

      tLift = 0.5*rho*CbLalpt*alpt*St*Vto**2

      rmom = Lift*dLift - W*dWeight + ABS(tLift)*dtail

C     WRITE(6,33) alpt*180/Pi,ct*12.,St,lt*12.,tLift,rmom

      IF (ABS(rmom) .LT. 6.0E-5) THEN
      WRITE(4,*) ltt, St
C     WRITE(6,*) '*******', alptt,Ltt,St
      ENDIF

C     WRITE(2,*) alptt,rmom
C     WRITE(3,*) ctt, rmom
C     WRITE(4,*) St, rmom
C     WRITE(5,*) ltt, rmom

 30   CONTINUE
 10   CONTINUE
C     WRITE(4,*) ' '
C     WRITE(5,*) ' '
C 5   CONTINUE
 20   CONTINUE

C     CLOSE (UNIT=2)
C     CLOSE (UNIT=3)
      CLOSE (UNIT=4)
C     CLOSE (UNIT=5)

      STOP
      END
```

```
      PROGRAM AE350
C     PROGRAM TO AUTOMATE LIFTING-LINE THEORY
C
C     Declare variables and types
C
      REAL lambda, AR, twist, AROOT, pi
      REAL cam(50), THETAP, mo , Y(50)
      REAL THETAN(50), YDISTN(50), CRDN(50), MON(50)
      REAL D1, D2, M(50,51), A(50)
      REAL CL(50), L(50), COSTH(50)
      REAL SIGMA, CLW, CDI
      INTEGER SPAN, I, J, K, astate, sstate


*************************************************************************
C
C     Prompt user for necessary input and program parameters/open datafiles
C
*************************************************************************

      SPAN = 10

      pi = 4.0*atan(1.0)

      lambda = 1.0

      write(0,*) 'Enter the Aspect Ratio'
      Read(5,*) AR

      twist = 0.0
      twist = twist*pi/180.0

      Do 4 I = 1, SPAN
            THETAN(I) = pi*I/(2.*SPAN)
 4          YDISTN(I) = COS(THETAN(I))

            write(6,*) 'Enter the max camber at the root.'
            read(5,*) cam(1)
            cam(1) = cam(1)*3.1415926/180.0
            Do 6 I= 1, SPAN
 6                cam(I) = cam(1)


            AROOT = 0*3.14159/180.0

            mo = 5.73
            do 43 I = 1, SPAN
                 MON(I) = mo
 43         continue

            rho = 0.00238
            visnu = 0.00015723
            Write(6,*) 'Enter the flight velocity'
            Read(5,*) vinf
            Write(6,*) 'Enter the planform area'
            Read(5,*) Sarea
            Write(6,*) 'Enter the CLmax of the airfoil'
            Read(5,*) CLmax
            Sstep = 0.01
            Astep = 1.0*3.1415926/180.0
            sstate = 0
            astate = 0
            CLsum1 = 0.0

C
*************************************************************************
```

```
C
C       Begin program routines for calculating coefficient matrices
C
*****************************************************************
C
  109   Continue

        do 7 I = 1, SPAN
                CRDN(I) = 1.0 - (1.0-lambda)*COS(THETAN(I))
    7   continue


        do 30 I = 1,SPAN
                D1 = MON(SPAN)/(CRDN(I)*MON(I))
                D2 = MON(SPAN)/(2.0*AR*(1.+ lambda)*SIN(THETAN(I)))
                        do 10 J = 1,SPAN
                                K = 2*J - 1
                                M(I,J) = (D1 + D2*K)*SIN(K*THETAN(I))
   10                   continue
   30           continue

*****************************************************************
C
C       Find absolute angles of attack (left side of the equations)
C
*****************************************************************
        do 110 I = 1, 50
                A(I) = 0.0
  110           CL(I) = 0.0
        Tlift = 0.0
        SIGMA = 0.0
        CLsum = 0.0

        do 69 I = 1,SPAN
                M(I,SPAN+1) = AROOT - twist*COS(THETAN(I))
     *                          + cam(I)*(1.0-COS(THETAN(I)))
C               WRITE(6,*) M(I,N+1)
   69   continue
C
C
C*****************************************************************
C
C       Send augmented matrix M(SPAN,SPAN+1) to subroutine to solve
C       for the coefficients Ai through Aspan by gaussian elimination
C
*****************************************************************

        CALL SIMEQN(M, A, SPAN)

C
*****************************************************************
C
C       Open data files to prepare for output and plotting of results
C
*****************************************************************
C
        OPEN(UNIT=69, FILE = 'CLout')
        OPEN(UNIT=79, FILE = 'Lout')

                dimen = 0.5*rho*vinf*vinf*Sqrt(Sarea/AR)
                b = Sqrt(AR*Sarea)
                c = b/AR

        do 16 I  = 1, 50
                MON(I) = mo
                THETAP = 3.141592*I/(2.0*50.0)
```

```
                do 12 J = 1, SPAN
                        K = 2*J - 1
                        CL(I) = CL(I) + A(J)*SIN(K*THETAP)
   12           continue
C
C*****************************************************************
C
C       Calculate sectional lift coefficient (CL) and Lift per Span
C
C*****************************************************************

                CL(I) = CL(I)*MON(SPAN)/(1.0 - (1.0-lambda)*COS(THETAP))
                If (CL(I) .GT. CLmax) CL(I) = 2.0*CLmax - CL(I)
                L(I) = CL(I)*(1.0 - (1.0-lambda)*COS(THETAP))*dimen
                Y(I) = COS(THETAP)*b/2.0
                write(69,*) Y(I), CL(I)
                COSTH(I) = COS(THETAP)
   16   continue

C
C       Lift at center line is equal to Cls*SIN(pi/2) -> Cls
C
                do 3 I = 1, 49
                        CLsum = CLsum + (CL(I)+CL(I+1))/2.0*(Y(I)-Y(I+1))
  3                     Tlift = Tlift + (L(I) + L(I+1))*(Y(I)-Y(I+1))

        do 57 J = 1,50
                write(79,*) Y(J), L(J)
   57   continue
C
*****************************************************
C
C       Determination of Oswald efficiency factor (SIGMA)
C
*****************************************************
C
        do 85 I = 2,SPAN
                K = 2*I - 1
                SIGMA = SIGMA + K*A(I)**2/(A(1)**2)
   85   continue
        write(6,*) 'Correction factor (sigma)=',SIGMA
        write(6,*) 'Oswald efficiency factor for the wing:', 1.0/(1.0 + SIGMA)
C
*************************************************************************
C
C       Calculation of wing lift coefficient (CLW) and induced drag coeff. (CDI)
C
*************************************************************************
C
                CLW = MON(SPAN)*pi*A(1)/(2.0 + 2.0*lambda)
                CDI = (CLW**2/(pi*AR)) * (1. + SIGMA)

        Write(6,*) 'Wing Lift Coefficient at AOA:',AROOT*180/pi,'(deg)',CLW
        Write(6,*) 'Necessary Wing area', Sarea
        write(6,*) ' '
        write(6,*) 'Induced drag coeff for the wing:', CDI
        write(6,*) ' '
        write(6,*) 'Total Integrated Wing lift', Tlift
        write(6,*) ' '
        write(6,*) 'Center Line Section CL', CL(50)
        write(6,*) ' '
        write(6,*) 'Reynolds number =', c*vinf/visnu

        weight = 3*4.76
        write(6,*) ' '
        write(6,*) 'weight', weight
```

```
      write(6,*) 'span', b
      write(6,*) 'cord', c
      write(6,*) 'vinf', vinf
      write(6,*) 'CLsum', CLsum

      CLOSE(69)
      CLOSE(79)

      IF ((ABS(weight-Tlift) .GT. 0.0001) .OR.
     *  (ABS(CLsum-CLsum1) .GT. 0.0001)) Then
            IF (weight .GT. Tlift) Then
                  IF (sstate .EQ. 1) Sstep = -Sstep/2.0
                  sstate = 0
            Else
                  IF (sstate .EQ. 0) Sstep = -Sstep/2.0
                  sstate = 1
            Endif
            vinf = vinf + Sstep
            IF (CLsum .GT. CLsum1) Then
                  IF (astate .EQ. 1) Astep = -Astep/2.0
                  astate = 0
            Else
                  IF (astate .EQ. 0) Astep = -Astep/2.0
               astate = 1
            Endif
            AROOT = AROOT + Astep
            CLsum1 = CLsum
            GOTO 109
      Endif
      stop
      end

      SUBROUTINE SIMEQN(A, X, N)

C     This program solves a set of simultaneous equations by Gaussian
C     elmination to create an upper triangular system, followed by
C     back-substitution to abtain the solution.
C
C     Maximum number of equations in set.
C
      INTEGER MAXEQN
      PARAMETER (MAXEQN=50,MAX2=MAXEQN*(MAXEQN+1))
C
C     Local variabiiles
C
      REAL A(MAXEQN, MAXEQN+1), X(MAXEQN), DET,LARGE
      INTEGER N, I, J
      LARGE = 0.0
      DET = 1.0
C
C
C     Read in number of equations
C
C     Check to see if maximum equations is exceeded.
C
      DO 10  I = 1, N
            DO 13 J = 1,N+1
   13 CONTINUE
   10 CONTINUE
      IF (N .GT. MAXEQN) THEN
            WRITE (0,*) 'Maximum number of equations is exceeded.'
            WRITE (0,*) '(Maximum number=',MAXEQN,')'
            STOP
      END IF
C
C     Read in coefficients and constant into the arrays and find
```

```
C       largest value
C
C
C
        DO 99  I = 1,N
                DO 88  J = 1,N+1
        IF (ABS(A(I,J)) .GT. LARGE) LARGE=ABS(A(I,J))
   88   CONTINUE
   99   CONTINUE
C
C       Use Gaussian elimination to triangulate the equations
C
        CALL GAUSS(A,MAXEQN,N,LARGE)
C       WRITE(6,*) 'LARGE:', LARGE
C
C       Solve new set by back-substitution
C
        CALL BACK(A,MAXEQN,N,X,DET)
C       WRITE(6,*) 'DET:', DET
C
C       Calculate and print answer confidence ratio
C
        IF (ABS(DET/LARGE) .LT. 2E-7) THEN
                WRITE(6,*) 'WARNING DETERMINANT RATIO IS SMALL!'
        END IF
C
C       Print results
C
C       WRITE (6,101) ABS(DET/LARGE),DATSET,(I, X(I), I=1,N)
C  101  FORMAT(/,'Determinant Ratio=',F10.5,//,'The solutions to the data
C     + set,',X,A12, 'is:',//,3('A(',I2,') = ',E13.5,TR5),/,)
C
        RETURN
        END
C
C       Subroutines Gauss and Back follow below
C
C
        SUBROUTINE GAUSS(A,MAX,N,LARGE)
C
C       This subroutine triangulates a set of N equations Ax=B
C       using Gaussian elimination.
C
C       Dummy arguments (temporary since actual arguments are in MAIN
C
        INTEGER MAX,N
        REAL A(MAX,MAX+1),LARGE
C
C       Local variables
C
        REAL PIVOT,ABSP,MULT,TEMP
        INTEGER PROW,I,J,K
C
C       Eliminate one element from each row in turn
C
        DO 40 I=1,N
C
C       Set initial values for PIVOT and PROW
C
        PIVOT=A(I,I)
        ABSP=ABS(PIVOT)
        PROW=I
C
C       Look for a larger potential pivot
C
        DO 10, J=I+1,N
          IF (ABS(A(J,I)).GT.ABSP) THEN
```

```
            PIVOT=A(J,I)
            ABSP=ABS(PIVOT)
            PROW=J
          END IF
   10   CONTINUE
C
C       Check to see if pivotal element is "zero"
C
        IF (ABS(PIVOT/LARGE) .LT. 2E-7) THEN
              WRITE(0,*) 'Ill-conditioned system! Process aborted!'
              STOP
        END IF
C
C       Was a larger pivot row found?
C
        IF (PROW.GT.I) THEN
          DO 20, J=I,N+1
            TEMP=A(I,J)
            A(I,J)=A(PROW,J)
            A(PROW,J)=TEMP
   20     CONTINUE
        END IF
C
C       Eliminate coefficients of X(I) from rows I+1 to N
C
        DO 30 J=I+1,N
          MULT=A(J,I)/PIVOT
          A(J,I)=0.0
          DO 25 K=I+1,N+1
            A(J,K)=A(J,K)-MULT*A(I,K)
   25     CONTINUE
   30   CONTINUE
   40   CONTINUE

C
C       Gaussian elimination is completed
C
        RETURN
        END

        SUBROUTINE BACK(A,MAX,N,X,DET)
C
C       This subroutine solves an upper triangular system of simultaneous
C       equations through back-substitution.
C
C       Temporary arguments
C
        INTEGER MAX,N
        REAL A(MAX,MAX+1),X(N),DET
C
C       Local variables
C
        REAL QUOT
        INTEGER I,J
        DO 77  I= 1,N
        DO 66  J= 1,N+1
C       WRITE(6,*) A(I,J)
   66   CONTINUE
   77   CONTINUE
C
C       Calculate X(N)
C
        X(N)=A(N,N+1)/A(N,N)
C
C       Now calculate remaining values in reverse order
C
```

```
      DO 20 I=N-1,1,-1
        QUOT=A(I,N+1)
        DO 10 J=I+1,N
          QUOT=QUOT-A(I,J)*X(J)
10    CONTINUE
      X(I)=QUOT/A(I,I)
20    CONTINUE
C
C     Evaluate the determinant
C
      DO 50 I=1,N
      DET=DET*A(I,I)
C     WRITE(6,*) 'A(',I,I,'):', A(I,I)
C     WRITE(6,*) 'DET*:  ',DET
50    CONTINUE
C
C     Solution by back-substitution method complete
C
      RETURN
      END
```

```
C       RPV Propulsion Program
C             by Tuan A. Le
C             March 24, 1994
C       Design Program to calculate the power available, power required,
C       current draw, motor rpm, range, and endurance for a propulsion system.

        REAL n,Ia,Kt,Kv,Nm,Np,Ng,J,Mah,Wgt(3),Volt(5)

        OPEN(UNIT=10,FILE='POWER',STATUS='UNKNOWN')
        OPEN(UNIT=11,FILE='CURRENT',STATUS='UNKNOWN')
        open(12,file='PAV')
        write(11,*) 'Velocity Range Endurance Ia Vact J Preq Pavail Nm etap'

        Mah = 1400.
        batcap = Mah/1000.
        PI = 4.*atan(1.)
        rho = 0.002378
        CDo = 0.0325
        Clmax = 1.03
        AR  = 9.0
        S = 6.5
        b = sqrt(AR*S)
        c = b/AR
        e   = 0.89
        n   = 1.0

        Wgt(1) = 4.83-.55
        Wgt(2) = 4.83+.05
      Wgt(3) = 4.83+.55
        Volt(1) = 1.4
        Volt(2) = 8.0
        Volt(3) = 10.5
        Volt(4) = 12.8
        Volt(5) = 15.6

        Kv   = 7.8568E-4
        Kt   = 1.097846
        Tloss= 1.372935
c       Tloss = 0.
      Ra   = 0.120
        Rbat = 0.08
      Ng    = 0.95
c       Ng = 1.
        Dprop = 10./12.
        GR    = 31./14.
```

```
C       Code to calculate Pavail and Preq
        do 2000 ii = 2,2
                W = Wgt(ii)
      VINIT=sqrt(2.*W/(RHO*S*CLMAX))
        do 1000 Vact = 6.0,15.7,.1
c       do 1000 iii = 1,5
                idone = 0
c               Vact = Volt(iii)
      do 30 V=Vinit,75.,0.01
                delta = 500.
                Nm = 6000.
                Q  = .5*rho*V**2
                CL = n*W/(Q*S)
                CD = CDo+CL**2/(PI*e*AR)
                Treq  = 1.356*CD*Q*S
                Preq  = 1.356*0.5*rho*V**3*S*CD
20     CONTINUE
      Ia=(Vact-Kv*Nm)/(Ra+Rbat)
      PmoA=7.397E-4*(Kt*Ia-Tloss)*Nm
      Np=Nm/GR
      J=V*60./(Np*Dprop)
C       Zingali Cp and eta curve fits
        Cp=-3.460082E-1*J**3+4.064685E-1*J**2-2.062646E-1*J + 1.305385E-1
        etap= -6.734308E+0*J**3+1.143146E+1*J**2-5.931978*J+1.662525
C       Graupner Cp and eta curve fits
c       Cp=-2.253302E-1*J**2+1.181663E-1*J + 8.265346E-2
c       etap=-5.002783*J**3+5.884037*J**2-1.799132*J+7.734548E-1
        PmoB=1.356*Cp*rho*(Np/60.)**3*Dprop**5/Ng
      if(PmoA .LT. 0.) then
                print *, 'PmoA negative'
                goto 999
        endif
        if(PmoB .GT. PmoA)  then
                delta = delta/2.
                Nm = Nm-delta
                goto 20
        endif
      if(abs(PmoA-PmoB).GT.1.E-3) THEN
          Nm=Nm+delta
        goto 20
      endif
        if(J .GT. .75) then
                print *, 'Advanvce Ratio too high'
                goto 999
        endif
```

```
      Pavail=7.397E-4*(Kt*Ia-Tloss)*Nm*Ng*ETAp
      if(Pavail .LT. 0.) then
            print *, 'Pavail Negative'
            goto 999
      endif
c     write(10,*) V,Preq,Pavail,Vact,J,Nm,Np
C     Calculate Range and Endurance
      ENDURANCE = (batcap)/Ia*60.
      RANGE       = ENDURANCE*V*60.
      if((idone .EQ. 0) .AND. Pavail .LT. Preq) then
      print *, 'file:
V,RANGE,ENDURANCE,Ia,Vact,W',V,RANGE,ENDURANCE,Ia,Vact,W
      write(11,4444) V,RANGE,ENDURANCE,Ia,Vact,J,Preq,Pavail,Nm,W
      print *,'V,J,Preq,Pavail',V,J,Preq,Pavail
      idone = 1
      goto 30
      endif
30    continue
999   continue
    idone = 0
      print *
    write(10,*)
1000  continue
    print *
    write(11,*)
2000  continue
4444  FORMAT(F6.2,F10.2,F8.3,F8.3,F7.3,F9.5,F8.3,F7.2,F10.2,F6.3)
      STOP
      END
```

APPENDIX D

Zingali 10-8 Propeller Data

INPUT TO PROP123

A.) Propeller Designation: Zingali10-8

B.) Number of Blades: 3 Diameter: 10.00000

C.) Airfoil section selected:
NACA44XX Low RE

D.) Blade thickness entered as:
INCHES

E.) Blade data entered at radial locations specified as:
INCHES

F.) Radius at which blade setting is measured: 4.00000

G.) Blade setting (i.e. ref angle for whole blade): 17.6570

H.) Number of radial data positions (3-9): 9

I.)

Data Point	Radius*	Chord	Thickness*	Angle
1	1.000	0.723	0.337	51.854
2	1.500	0.802	0.271	40.325
3	2.000	0.861	0.230	32.482
4	2.500	0.889	0.206	26.990
5	3.000	0.862	0.171	22.997
6	3.500	0.785	0.147	19.991
7	4.000	0.686	0.113	17.657
8	4.500	0.577	0.096	15.798
9	5.000	0.429	0.081	14.287

J.) Refinement Analysis:
ANALYSIS INCLUDING INDUCED VELOCITY AND TIP LOSSES

K.) Cl/Cd coefficient adjustments:
MACH AND REYNOLDS NUMBER ADJUSTMENTS

L.) Altitude: 0. feet
Rho: 2.37690E-03

M.) Airspeed FIXED at: 40.9000

N.) Range of Advance Ratio to be used in calculations:
Jmin: 0.340000 Jmax: 0.800000

OUTPUT FROM PROP123 FOR ZINGALI 10-8 PROPELLER

PERFORMANCE ESTIMATE for **zingali 10-8**

Analysis options: RA= 3 and LDA = 4

Fractional rad, X: 0.30 0.45 0.60 0.70 0.75 0.80 0.85 0.90 0.95
Radial position, r: 1.50 2.25 3.00 3.50 3.75 4.00 4.25 4.50 4.75
Blade chord, C: 0.80 0.88 0.86 0.79 0.74 0.69 0.63 0.58 0.51
Thickness, In: 0.12 0.13 0.13 0.12 0.11 0.10 0.10 0.09 0.08
Thickness ratio, T: 0.15 0.15 0.15 0.15 0.15 0.15 0.15 0.15 0.15
Blade Angle, Beta: 40.33 29.52 23.00 19.99 18.75 17.66 16.67 15.80 15.02
Geometric Pitch,GP: 8.00 8.01 8.00 8.00 8.00 8.00 8.00 8.00 8.01
Solidity, S: 0.153 0.168 0.165 0.150 0.141 0.131 0.121 0.110 0.097

THRUST, POWER, EFFICIENCY, AND VELOCITIES

J: 0.400 0.430 0.460 0.490 0.520 0.550 0.580 0.610 0.640 0.670 0.700
Ct: 0.149 0.139 0.132 0.127 0.120 0.114 0.107 0.101 0.094 0.087 0.078
Cp: 0.089 0.088 0.087 0.086 0.084 0.083 0.080 0.078 0.075 0.072 0.067
eta: 0.667 0.676 0.697 0.720 0.738 0.756 0.773 0.788 0.800 0.809 0.813
Mt: 0.462 0.430 0.403 0.378 0.357 0.338 0.321 0.306 0.292 0.280 0.269
RPM: 11700 10884 10174 9551 9000 8509 8069 7672 7312 6985 6685

Thrust Distribution: (dCt/dX vs. X and J)

X	J: 0.40	0.43	0.46	0.49	0.52	0.55	0.58	0.61	0.64	0.67	0.70
0.30	0.07	0.07	0.06	0.06	0.05	0.05	0.05	0.05	0.04	0.04	0.04
0.45	0.17	0.13	0.12	0.12	0.11	0.11	0.10	0.10	0.09	0.08	0.07
0.60	0.21	0.21	0.19	0.19	0.18	0.17	0.16	0.15	0.14	0.13	0.11
0.70	0.25	0.24	0.23	0.22	0.21	0.20	0.19	0.17	0.17	0.15	0.14
0.75	0.26	0.25	0.24	0.24	0.22	0.21	0.20	0.18	0.18	0.16	0.14
0.80	0.27	0.26	0.26	0.24	0.23	0.22	0.20	0.20	0.18	0.17	0.15
0.85	0.27	0.26	0.26	0.25	0.23	0.22	0.21	0.20	0.18	0.17	0.15
0.90	0.27	0.27	0.26	0.24	0.23	0.22	0.21	0.20	0.18	0.17	0.15
0.95	0.37	0.35	0.33	0.31	0.30	0.28	0.27	0.25	0.23	0.22	0.20

Torque Distribution: (dCq/dX vs. X and J)

X	J: 0.40	0.43	0.46	0.49	0.52	0.55	0.58	0.61	0.64	0.67	0.70
0.30	0.006	0.006	0.006	0.006	0.006	0.006	0.005	0.005	0.005	0.005	0.004
0.45	0.014	0.013	0.013	0.013	0.012	0.012	0.012	0.011	0.011	0.010	0.010
0.60	0.021	0.021	0.021	0.020	0.020	0.020	0.019	0.018	0.017	0.017	0.016
0.70	0.025	0.025	0.025	0.024	0.024	0.024	0.023	0.022	0.021	0.020	0.019
0.75	0.027	0.027	0.026	0.026	0.026	0.025	0.024	0.023	0.023	0.022	0.020
0.80	0.028	0.028	0.028	0.027	0.027	0.026	0.025	0.025	0.024	0.023	0.021
0.85	0.029	0.029	0.029	0.028	0.028	0.027	0.026	0.026	0.025	0.023	0.022
0.90	0.029	0.029	0.029	0.028	0.028	0.027	0.026	0.026	0.025	0.023	0.022
0.95	0.030	0.030	0.030	0.030	0.029	0.029	0.029	0.028	0.028	0.027	0.026

Angles of Attack (Degrees)

X	J: 0.40	0.43	0.46	0.49	0.52	0.55	0.58	0.61	0.64	0.67	0.70

0.30	15.50	14.42	8.60	8.12	6.87	6.14	5.05	4.09	3.35	2.50	1.68
0.45	12.30	7.62	6.75	6.31	5.43	4.65	4.20	3.34	2.66	1.95	1.29
0.60	6.39	6.12	5.35	4.76	4.18	3.73	3.16	2.58	2.07	1.49	0.92
0.70	5.69	5.15	4.64	4.14	3.75	3.25	2.74	2.25	1.77	1.25	0.75
0.75	5.31	4.83	4.37	4.13	3.54	3.04	2.58	2.07	1.64	1.16	0.65
0.80	4.97	4.52	4.33	3.74	3.29	2.84	2.40	1.94	1.51	1.05	0.58
0.85	4.63	4.21	4.05	3.51	3.06	2.63	2.19	1.81	1.38	0.94	0.49
0.90	4.26	4.16	3.64	3.20	2.80	2.39	2.05	1.61	1.23	0.82	0.39
0.95	7.38	6.82	6.25	5.69	5.13	4.58	4.02	3.47	2.91	2.36	1.82

Reynolds Number (millions)

X	J: 0.40	0.43	0.46	0.49	0.52	0.55	0.58	0.61	0.64	0.67	0.70
0.30	0.066	0.064	0.053	0.052	0.050	0.049	0.048	0.047	0.046	0.045	0.044
0.45	0.103	0.082	0.079	0.077	0.075	0.073	0.071	0.069	0.067	0.066	0.064
0.60	0.104	0.103	0.098	0.095	0.093	0.090	0.088	0.086	0.084	0.081	0.079
0.70	0.110	0.106	0.103	0.100	0.097	0.094	0.092	0.089	0.087	0.085	0.082
0.75	0.110	0.106	0.103	0.101	0.097	0.094	0.092	0.089	0.087	0.084	0.082
0.80	0.108	0.105	0.103	0.099	0.096	0.093	0.090	0.088	0.085	0.083	0.081
0.85	0.105	0.102	0.101	0.097	0.093	0.091	0.088	0.086	0.083	0.081	0.079
0.90	0.100	0.099	0.095	0.092	0.089	0.086	0.084	0.082	0.079	0.077	0.075
0.95	0.132	0.123	0.115	0.108	0.102	0.097	0.092	0.088	0.084	0.080	0.077

* Thickness values limited by available Cl and Cd data
for the selected airfoil section.

Appendix E - Manufacturing Plan

Introduction and General Manufacturing Concerns

This appendix details the construction phase of the design project. It presents the assembly breakdown, the major concerns associated with each component, the individual construction responsibilities, the macro schedule for construction, and a brief run through the assembly procedure.

There are a two major concerns that will carry though all phases of the construction process. First, everything must be done to prevent the weight of the aircraft from growing. Through careful planning, the Elite design team has tried to anticipate most of the parts necessary to build the aircraft. Additional pieces will only be added if they are deemed absolutely vital to the success of the technology demonstrator. Secondly, the center of gravity of the aircraft will be checked throughout the building process. This will help to ensure that the center of gravity ends up in the design location once the construction is complete.

Assembly Breakdown and Major Component Concerns

The assembly of the Elite technology demonstrator is divided into component sections. These components are in turn divided into their substructure components. The breakdown of components is shown below. Also shown in the table are the critical assembly areas or concerns associated with each section.

Structural Components	Critical Areas/Issues
Fuselage - Aircraft frame - Engine mounts - Servo tray - Nose gear mounts - Engine nacelle - Tail cone	Main wing/fuselage mating Connection with horizontal stabilator Firewall Mating of vertical tail Stiffness of servo tray to avoid flexure under control activation Engine vibrations Sturdy nose gear attachment

Main Wing - Wing frame - Landing gear mounts - Ailerons	Maintaining airfoil shape Mating of two wing halves Connection to fuselage Sturdy landing gear mounts that resist splitting and tearing of wood
Horizontal Stabilator - Stabilator frame - Fuselage mounts - Control horn placement	Maintain airfoil shape Solid connection to fuselage that still allows for easy control activation Avoid structural flexure during activation
Vertical Tail - Tail frame - Rudder - Control horn placement	Perpendicular alignment with fuselage Avoid structural flexure during rudder activation
Miscellaneous Subsystems - Landing gear - Control Rods and Links	Stiffness of control rods Smooth and easy control activation

As one can see for the above table, a major area for concern is the mating of the main aircraft components. In these areas, very detailed instructions and tolerances must be laid out to insure that all the components will fit once they have been assembled separately. In addition, the different component assembly team must keep in constant communication if any structural modifications are made.

Another concern is the structural response to a control surface deflection. The structure must be carefully constructed to prevent significant structural deformations under the loads associated with the surface deflection.

Assembly Teams and Macro Fabrication Schedule

The Elite design team was divided into divisions responsible for the fabrication of the individual major components of the aircraft. Doug Staudmeister and Steve Stem are in charge of the fuselage construction. Jonathan Fay and Dan Avis are heading up the wing and stabilator fabrication. Amy Rueter and Tuan Le are building the vertical tail as well as the engine nacelle and tail cone. Below is a macro time schedule for the

fabrication process.

April 8-10

Cutting of Raw Materials/Part Construction

- Bulkheads
- Ribs
- Spars and Longerons
- Firewall

Composite Beam Construction (graphite tape enforced beams discussed in Section 9.0)

April 11-15

Fuselage Construction

Wing Construction (two wings made consecutively)

Empennage Construction and Integration into Fuselage

April 16-17

Monokoting Aircraft

Initial Major Component Mating

April 18

Day to meet pressing and/or unforeseen manufacturing difficulties

April 19

Aircraft Rollout

Brief Manufacturing Assembly Procedure

Fuselage: The airframe assembly begins with the shaping of the top and bottom longerons. Since the Elite incorporates a curved fuselage, the longerons will have to be pre-soaked in water and then pinned into the desired shape on the full scale plans. These longerons will then have to be allowed to dry, thus forming a permanent curve into the longeron. Once the top longeron has been formed, the bulkheads will be placed along its length except for the rear-most bulkhead. Next the pre-formed bottom longeron will be laid into the bulkheads along with the two side longerons. At this time, the firewall will be added to the airframe and the servo tray can be integrated into the fuselage. With the servo tray complete, the servos can be installed and the control linkages and rods can be laid out inside the aircraft frame. In the area above the wing, a sheet of balsa will extend down along the sides of the fuselage to the wing surface, thus providing a

smooth saddle mating to the wing. The hardwood blocks for the main wing mating can be added along with the engine and nose gear mounts. This completes the fuselage construction until other major components have been completed.

Main Wing: The main wing construction begins with spacing out the ribs in the wing jig one half of the wing at a time. The top, bottom and leading edge spars can be glued into place. The leading edge spar is then sanded into a smooth round shape. The partial wing frame is then removed from wing jig and the trailing edge spar is added to the frame. Next the trailing edge is added to the rear spar at the non-aileron spanwise positions. With half of the wing frame complete, the aileron assembly can be added to the wing with the control wire running along the hinge line. The above steps are repeated to form the opposite side of the wing. With two completed wing halves, the wing is locked into the desired dihedral angle while the spars from each wing half are cemented together with fiberglass. At this time the front-bottom-center section of the wing is sheeted with balsa to provide a resting place for the batteries. Now the fuselage mating blocks and the main gear blocks can be incorporated into the wing along with the soft balsa rounded wing tips. At this time the wing may be covered. Lastly the main gear are added.

Horizontal Stabilator: The horizontal stabilator frame is constructed just like a miniature wing except that extra care must be taken to build in the desired sweep back angle. Three hardwood blocks are slid into the middle of the graphite rod but not glued to it (the middle hardwood block has the control horn screwed to it). These blocks are the stabilator connection to the fuselage. Hardwood blocks are then glued to the appropriate rib and spar locations in the stabilator frame as the attachment cowlings for the graphite rod. Each half of the stabilator then slides onto the graphite rod and securely glued to it. At this time the stabilator can be covered with monokote. Once the horizontal stabilator has been constructed the outer two hardwood blocks in the middle of the graphite shaft will be glued to the second to last fuselage bulkhead. Now the rear-most bulkhead will be glued to fuselage in effect sandwiching the hardwood blocks between the bulkheads. Then the middle hardwood block is glued to the shaft and the control horn linked to the control rod. Thus the fuselage-horizontal stabilator assembly is complete.

Vertical Tail: The vertical tail and rudder are simple truss structures with rounded leading edges. Once these trusses are complete, they can be covered. After covering, the two parts can be hinged together. The vertical tail assembly is glued to the top longeron of the fuselage. In addition, the trailing edge spar of the vertical tail extends into the fuselage and connects to the rear bulkhead of the aircraft. The leading edge of the rudder also extends into the fuselage where the control horn is attached.

Engine Nacelle and Tail Cone: These are light-non load carrying coverings that are constructed to complete the sleek fuselage curves at the nose and tail respectively. They are fabricated in the same fashion as the fuselage frame.

Miscellaneous Construction Information:

- The glue used in construction is the fast drying cyanoacrylate glue.

Cost Accounting and Control: Each member of the team is responsible for logging his own hours and machine use on the "Tooling Time Sheet" and "Construction Time Sheet." On the following two pages are samples of these two sheets.

CONSTRUCTION TIME

NAME	DATE	# HOURS	TASK

TOOLING TIME SHEET

NAME	TOOL	TURN ON? (Y/N)	TIME USED	COST

Appendix F

Flight Validation, Component Test and Manufacturing Hours

Flight Validation Testing Review
April 21-27, 1994
The Elite

Summary:
The technology demonstrator was completed and aircraft was noteworthy for the extreme attention to detail in the manufacturing and its attractive "style." It successfully completed its initial taxi tests and it handled very well. The flight tests were rather dramatic. The first takeoff was successful but after completing a single 180° left-hand turn the right wing failed terminating the flight.

Taxi Testing Results: April 21, 1994
Ground handling of the aircraft was excellent. Steering was responsive and all the members of the design team were able to control the aircraft. Acceleration at partial throttle was good but no attempts were made to rotate off the nose gear during the taxi tests.

Flight Testing Results: April 27, 1994
The final data sheet for the technology demonstrator is attached. Preflight inspection revealed that the aileron hinges had loosened and the ailerons were reinforced with plastic tape. The nose gear was realigned. For the first flight the aircraft accelerated to takeoff speed, rotated and lifted-off wings level. Rotation to take-off attitude was easily accomplished and the aircraft climbed to approximately 15' and immediately entered left-hand 180° turn. The bank angle appeared to exceed 60°. Roll response was very good but full aileron and rudder were used in the turn. Immediately upon leaving the turn as the aircraft approached a wings level attitude the right wing (outboard wing in the turn) failed at the root, bent upward approximately 90° and the aircraft crashed.

Post flight inspection of the wing indicated a failure of the upper spar flange (cap) very similar to the component tests. The outboard ribs in bays 1 and 2 were crushed, the "posts" between the spars in the second bay had separated at their connection points, the web in bay 1 (the grain in the web was spanwise) appeared to tear along the grain. The failure was localized to the main spar in bays 1 and 2. The construction team cited the recollection that the balsa used for the upper spar cap was "softer" than that in the component test wing.

Wing Component Static Load Test, April 19, 1994
Spring 1994
The Elite

Summary:
A wing component was tested to failure. The wing was completed (excluding ailerons) and attached to a rigid centerbody in a manner similar to the actual fuselage attachment. The weight of the wing as tested was not provided. The loading was based upon an aircraft weight of 4.84 lb and the wing was designed to a 3g limit load.

This component wing actually was used to conduct two separate tests. An initial load deflection test was conducted in which a 0.5lb load was applied at each wing rib location from the root to the tip. This was done for the left wing without monokote and the right wing after it had been monokoted. The bending moment at the root due to the 0.5lb load were computed and the deflections at the tip were measured. Both are listed on the attached Table and Plot. During this test audible "cracking" was apparent in the left wing but no visible damage was detected and the wing was not repaired.

During the component test to failure, the left wing (the one already subjected to a static load) failed first with failure of the main spar near the root. Due to the manner in which the wing was mounted to the static test support - a four bolt attachment of the carrythrough to a rigid support- the loading was able to be increased until failure was encountered on the right wing. In both cases the failure mechanism was identical. The top spar failed in what appeared to be a buckling collapse. The most inboard wing bay had a balsa sheet for a spar web but the sheet did not extend from rib to rib. In the next outboard bay three small "posts" were used in lieu of a spar web. It appears as if the rib between the two bays was crushed, the spar separated from the balsa sheet in the first bay (either debonded or splintered) then the unsupported length of the top spar was between the root rib and the first post. Failure occurred in the top spar in this region and the wing failed.

3-g Load Distribution:
The approximation to the 3-g ultimate load was applied starting at the root. The load was based upon an assumed aircraft weight of 4.8 lb. The spanwise locations where the loads were applied started 3" from the root and were spaced at 6" intervals. The 3-g load was applied in the increments shown in the table starting at the root.

This processes continued until the left wing failed. The left wing failed when the total load applied to both wings was 7.8 lb. The right wing failed when the load applied to the right wing only was 5.65 lb.

Spanwise location (distance from root in inches)	Load (lb)
3	1.1 (.5, .5, .1)
9	1.1 (.5, .5, .1)
15	1.1 (.5, .5, .1)
21	1. (.5, .5)
27	.95 (.5, .25, .1, .1)
33	.85 (.5,.25,.1)
39	.75 (.5, .25)
45	.35 (.25, .1)

Wing Tip Deflection:

The tip deflection was measured as the load was increased. The tip deflection is presented for left wing only up to the point where the left wing failed.

Total Load (lb) - Both wings	Tip Deflection (in)
4	1.
4.6	1.5
5.6	1.75
6.6	2.25
7.6	3.5
7.8	5.25

Additional Information:

Aircraft Weight = 4.84 lb (estimate at this time)
Wing Weight = not provided

Quantification of Stiffness of Monokote

Rib Location (inches)	Moment @ Root (inch-pounds) 0.5 lb load applied at ribs	Tip Deflection (no Monokote)	Tip Deflection (Monokote)
0	0	0	0
2	0.218181818	0.0625	0.0625
7	0.763636364	0.25	0.125
11.5	1.254545455	0.625	0.375
16	1.745454545	1.125	0.5625
20.8125	2.270454545	1.75	0.6875
25.25	2.754545455	2.25	1
29.9375	3.265909091	2.875	1.3125
34.375	3.75		1.625
38.75	4.227272727		1.9375
43.25	4.718181818		2.375

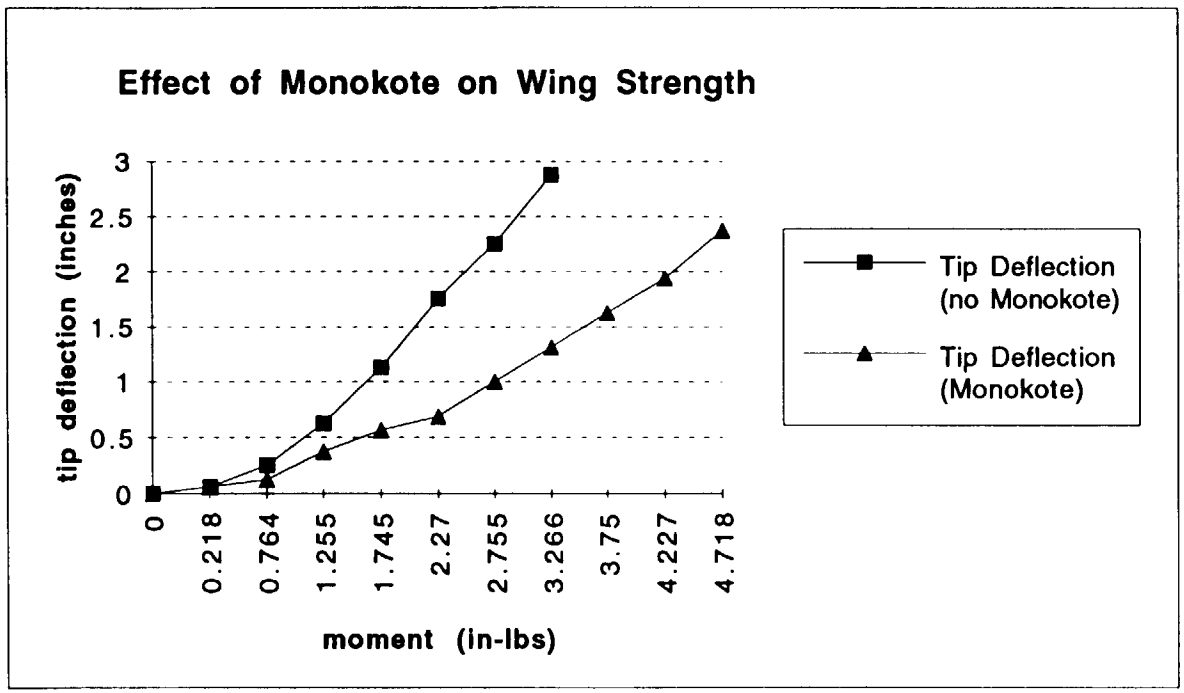

Comparison Between Design and Actual Aircraft Data

	Design Value	Actual Value
Wing Span		
Wing Area		
Vertical Tail Area	0.3 ft²	
Horizontal Tail Area		
Wing Structural Weight (Monokote)		
Wing Structural Weight (no Monokote)		
Fuselage Structural Weight (Monokote)		
Fuselage Structural Weight (no Monokote)		
Vertical Tail Weight (Monokote)		
Vertical Tail Weight (no Monokote)		
Horizontal Tail Weight (Monokote)		
Horizontal Tail Weight (no Monokote)		
Landing Gear Weight		
Propeller Type		
Propeller Weight		
Total Aircraft Weight (post-construction)	4.38 lb	
Total Aircraft Weight (post-flight)	—	
CG Location (post-construction)	13.5625 in.	
CG Location (post-flight)	—	
Weight of Batteries		

AIRPLANE W/O BATTS & NO MONOKOTE ON FUSE 1270 g

Please list any other deviations of the technology demonstrater from the original design.

Wing → Lengthened Landing Gear Mount Bolts Two stations cut on either side; Closed off stations either side of fuselage after structural component test

The Elite

FINAL COST ANALYSIS

TYPE OF COST	ESTIMATED COST	ACTUAL COST
FIXED SUBSYSTEMS	$462.58	$ 462.57
RAW MATERIALS	$160.00	$ 221.00
PERSONNEL	$1800 (180 hrs)	$ [illegible]
TOOLING	$150	$ 241.00
WASTE DISPOSAL	$240	
TOTAL COST PER AIRCRAFT	$4,410.13	

The Elite

CONSTRUCTION BREAKDOWN

CONSTRUCTION ITEM	NO. OF MAN-HOURS	% OF TOTAL HOURS
WING #1 AND WING #2	57	27.50%
MONOKOTE	44	21.20%
FUSELAGE	36.75	17.70%
STABILATOR	25.75	12.40%
MISCELLANEOUS	39	19.20%
VERTICAL TAIL AND RUDDER	4.25	2.00%

Some Notes

1. The total man hours was 207.5 and the total tooling was $315. To take out costs associated with constructing the first wing, 25 man-hours were taken out as well as $75 of tooling costs.
2. Monokoting took more man-hours than expected because of the 2 different colors, stripes, etc.. Also two people usually worked on monokoting at a time, thus increasing man-hours.
3. Monokote does not stick well to 3-ply or reinforcement tape.